NTNU – Trondheim
Norwegian University of
Science and Technology

Numerical Simulation Study on Parameters related to Athabasca Bitumen Recovery with SAGD

Kristin Reka Marianayagam

Earth Sciences and Petroleum Engineering
Submission date: June 2012
Supervisor: Ole Torsæter, IPT

Norwegian University of Science and Technology
Department of Petroleum Engineering and Applied Geophysics

Abstract

The world's total oil reserves are to some extent dominated by heavy oil. The heavy oil reserves are doubled in volume compared to conventional oil reserves. As conventional oil reservoirs are depleting, heavy oil and bitumen possesses a great potential in covering parts of the future energy demand.

The possibility of horizontal drilling has created a pathway for SAGD (Steam Assisted Gravity Drainage), which is the most preferred heavy oil and bitumen recovery method. The mechanism of SAGD involves two parallel horizontal wells, one for production and one for injection. The production well is situated at the bottom of the reservoir and the injection well is placed above. Steam is injected and heats up the oil which is then able to flow to the production well by gravity drainage.

In the present thesis, a numerical study of parameters has been performed in relation to SAGD implementation in the Athabasca field. The thermal simulator utilized is CMG STARS. The Athabasca field is located in Northern Alberta in the Western Canada Sedimentary basin.

Due to the complexity of core extraction in bitumen reservoirs, a comprehensive sensitivity analysis is significant in order to determine the appropriate production approach. The present study confirmed that a decrease in viscosity and increase in porosity yielded higher oil recoveries. All oil recoveries found in 3D simulations were within model uncertainties compared to the 2D result. Increase in horizontal and vertical permeabilities resulted in higher oil recovery up to a certain limit, where exceeding permeabilities provided limited increase in oil recovery. The effect of different vertical well spacing proved to have minor effect on amount of oil produced. Yet, based on cumulative steam oil ratio (CSOR) it was proposed to maintain a vertical well spacing in the range of 3.5 to 7 meters.

Sammendrag

Verdens oljereserver domineres i stor grad av tungolje ettersom reservene av tungolje er dobbelt så store i volum sammenlignet med de tilgjengelige konvensjonelle oljereservene. Derfor er det et stort potensiale i tungolje som kan være med på å dekke fremtidens energi behov.

Muligheten for å bore horisontale brønner gjør at SAGD *(Steam Assisted Gravity Drainage)* er en meget attraktiv metode innenfor utvinning av tungolje. SAGD består av to parallelle horisontale brønner hvor produksjonsbrønnen er plassert på bunnen av reservoaret og injeksjonsbrønnen ovenfor. Damp injiseres og varmer opp oljen slik at den strømmer til produksjonsbrønnen ved hjelp av gravitasjon.

Denne oppgaven er en numerisk studie av reservoarparameterne relatert til SAGD implementering i Athabasca, Canada. Simuleringsverktøyet som er blitt brukt er CMG STARS.

På grunn av kompleksiteten forbundet med utvinning av kjerneprøver i tungolje reservoarer, kan en omfattende sensitivitetsanalyse være med på å gi en god indikasjon på hva som er den best egnede utvinningsmetoden. Det ble bekreftet at en økning i porøsitet og en reduksjon i viskositet ledet til høyere utvinningsgrad av olje. Basert på at alle utvinningsfaktorer var innenfor usikkerheten i simuleringsprogrammet, er det foreslått at en 2D modell vil være tilstrekkelig sammenlignet med en 3D modell. En økning i horisontal og vertikal permeabilitet, leder til høyere utvinningsgrad opp til en bestemt permeabilitetsverdi hvor det ikke lenger forekommer en signifikant økning i utvinningsgrad. Vertikale distanser mellom produksjons- og injeksjonsbrønnen har en begrenset effekt på utvinningsgraden, men basert på det kumulative damp-olje forholdet så var det fortrukket med en vertikal distanse på 3.5 m - 7 m.

Contents

List of figures

List of tables

“Success is moving from failure to failure with no loss of enthusiasm”

Winston Churchill

Preface

This master thesis has been prepared for the degree Master of Science in Earth Sciences and Petroleum Engineering at the Norwegian University of Science and Technology. The present work is a continuation of the project thesis; “Heavy Oil Recovery with Steam Injection”, which was completed in December 2011.

There are several people that have assisted during the work of this thesis. Thanks especially to Souraki, Ashrafi, Karimaie and Torsæter for allowing me to use the data file they have created. In addition I would like to express my gratitude to Yaser Souraki for kindly answering questions related to numerical simulation and SAGD. I will also like to thank Professor Ole Torsæter for valuable insights and discussions.

I wish to thank my fellow students for giving me an unforgettable time whilst completing my university degree.

Finally, I would like to express infinite gratitude to my parents for tremendous support during all these years. Words simply cannot describe.

Trondheim, June 2012

Kristin Marianayagam

1 Introduction

The increasing energy demand is a widely discussed topic in today's society. As the conventional oil reserves are depleting, the need for exploration of unconventional resources are increasing rapidly. Production of heavy oil has for a significant amount of time been limited by technological and economic challenges. However, with today's available advanced technology and the significant increase in oil prices, it is possible to extract oil from unconventional reservoirs with economic feasibility. The world's total oil reserves are to some extent dominated by heavy oil as the heavy oil reserves are *doubled* in volume compared to conventional oil reserves (R. Beall, 2011). Based on this, heavy oil and natural bitumen will most likely become a very substantial contribution to the current conventional oil production.

Heavy oils and natural bitumen are characterized by their high viscosity, high density (low API gravity) and high concentrations of nitrogen, oxygen, sulphur and heavy metals (Attanasi & Meyer, 2007). Amongst the thermal methods available Steam-Assisted Gravity Drainage (SAGD) is the most common method for recovering heavy oil and bitumen. SAGD is basically two parallel horizontal wells, with the production well situated at the bottom of the reservoir and the injection well placed above. Steam is injected and heats up the oil as it propagates through the reservoir. The result is decreased oil viscosity and production of oil by gravity drainage.

The Athabasca oilfield, studied in this thesis, is located in Northern Alberta in the Western Canada Sedimentary basin. The initial oil in place is estimated to be 207 billion m^3, however it is expected that this number will increase as exploratory methods continue to develop (Nasr & Ayodele, 2005).

Core extraction is particularly challenging in bitumen reservoirs, thus *real* data for reservoir parameters are lacking to some extent. Subsequently, the importance of a comprehensive sensitivity analysis is vital. The aim of the thesis is to conduct a simulation study to determine the effects of various reservoir parameters when SAGD is implemented. The software used to complete this task is CMG STARS (Computer Modelling Group; Steam, Thermal and Advanced Processes Reservoir Simulator). The data file was created by; Souraki, Ashrafi,

Karimaie & Torsaeter (2012) and modified by the author to test the various simulation parameters.

In the present thesis, § 2 briefly cover fundamentals of reservoir engineering, which is essential to understand heavy oil recovery. § 3 is a summary of the literature review conducted prior to the numerical simulation performed in this project. It discusses definitions, properties, creation of heavy oil and reserves. In addition it provides a brief explanation of the characteristics related to heavy oil reservoirs. Thereafter it discusses heavy oil recovery in general and gives a brief introduction to the methods available in order to recover heavy oil. A more detailed description of the SAGD process is also included here. Next, § 4 addresses the Athabasca oil field, its location, and geological description. § 5 discusses numerical simulation in general and presents the simulation model. Thereafter a description of the base case and an explanation of the tested variables follow. § 6 displays the results of the parameter study. Finally, a comprehensive discussion of the sensitivity analysis is given in §7 followed by a general conclusion in §8.

2 Fundamentals of reservoir engineering

2.1 Important reservoir parameters

Porosity Φ is the ratio between the pore volume and the total bulk volume of the rock. It defines the fraction of the rock that is able to store reservoir fluids. The *effective porosity* is most often used in all engineering calculations and is an indication of the volume of *recoverable* hydrocarbons that are present in a given reservoir rock.

Permeability k is a rock property that defines the ability of a fluid to flow through a given rock. The unit for permeability is Darcy (D) where one Darcy is equal to 10^{-12} m^2. There is a difference between absolute and effective permeability. Absolute permeability is the permeability when the rock is fully saturated with *one* fluid and is a constant property. When a multi-phase flow is present, for instance if oil and water occupies the same pores in the reservoir, each fluid has its own *effective permeability*, k_{eff}. These permeabilities rely on the fluid saturation of the respective fluid. The sum of these permeabilities is always less than the absolute permeability (Dake, 1978). The *relative permeability* can be defined as the ratio between the effective permeability and the absolute permeability.

Saturation is the ratio between a single fluid in the pores and the total pore volume. Separate saturations exist for oil, gas and water. The sum of these saturations in a given reservoir is equal to one. The residual oil saturation is the saturation of a given oil which is immobile and thus is not recoverable under primary (natural mechanisms) and secondary (i.e. artificial lift and fluid injection) recovery. The irreducible water saturation, S_{wi} is the lowest water saturation that can be achieved in a core plug when the water is displaced by oil or gas. The *connate water saturation* is the lowest water saturation, which is found in situ (reservoir conditions). Connate water is the water, which is trapped in the pores of a rock during formation of the rock (Schlumberger, 2011).

Parameters such as porosity, permeability and pressure determine the behavior of the reservoir. However, when deducing the production approach, oil viscosities and densities become the important parameters. These fluid parameters represent certain production challenges with respect to heavy oil recovery. Viscosity is the most important parameter for the heavy oil producer as this determines the ability of a fluid to flow. Yet, density is the most

important parameter for the oil refiner as this will indicate the yield result after distillation and thus determine the quality of the oil. Despite the importance of the parameters no clear correlation exists between the two. As viscosity varies greatly with temperature and density does not, the latter is commonly used to characterize crude oils.

Dynamic viscosity (μ), is a measure of a fluids resistance to flow. The higher the viscosity the less mobile it is. The unit for viscosity is centipoise (cp = 10^{-3} kg/(m*s)).

Density is defined in terms of API gravity, which is related to specific gravity. *API gravity* is a measure of the lightness or heaviness of petroleum and is related to density (ρ [kg/m^3]) and specific gravity (SG). The lower the API gravity, the denser the oil. The definition of API is (Speight, 2009):

Equation 1: API definition (Speight, 2009)

$$^{\circ}\boldsymbol{API} = \frac{\mathbf{141.5}}{\boldsymbol{SG}(\boldsymbol{at}\ \mathbf{60}^{\circ}\boldsymbol{F}) - \mathbf{131.5}}$$

Specific gravity is the ratio between the density of a given fluid and the density of a reference fluid (Speight, 2009). The specific gravity of a certain oil is given as the ratio between the density of the oil and the density of water

2.2 Basic concepts

2.2.1 Mobility

The mobility λ, of the oil is defined as the ratio between the effective permeability, k_{eff} of the rock to the oil and the viscosity of the oil:

Equation 2: Mobility

$$\lambda = \frac{k_{eff}}{\mu}$$

The *mobility ratio* is the ratio between the mobility of water and the mobility of oil:

Equation 3: Mobility ratio

$$M = \frac{K_{rw} \times \mu_o}{K_{ro} \times \mu_w}$$

Where K_{rw} is the relative permeability to water, K_{ro} is the relative permeability to oil, μ_o and μ_w are the viscosities of oil and water respectively. If *M* is less than one, it illustrates a favourable displacement as oil moves faster than water. If *M* is equal to one this also indicates a favourable displacement as water and oil move at the same speed. However, if *M* is larger than one, it indicates an unfavourable displacement as water moves faster than oil. In general, the higher the mobility ratio, the more probable it is that the injected fluid will bypass the oil (Speight, 2009).

2.2.2 Sweep efficiency

The *displacement efficiency* is defined as the fraction of oil recovered from a zone which is swept by a waterflood or another displacement process (Schlumberger, 2011). The displacement efficiency will by definition lie between 0 and 1. The rate at which the displacement efficiency reaches one depends on the initial conditions, the fluid and rock properties, the type of displacing agent and the amount of displacing agent (Lake, 1989).

Sweep efficiency denotes the volume fraction of rock that is contacted by the injection fluids (Speight, 2009). The sweep efficiency can be subdivided into areal sweep efficiency, vertical sweep efficiency and volumetric sweep efficiency. The *areal sweep efficiency* is the ratio between the area contacted by the displacing agent and the total area. The vertical sweep efficiency is the ratio between the cross-sectional area that is contacted by a displacing agent and the total cross-sectional area. The volumetric sweep efficiency is the ratio between the volumes of oil contacted by a displacing agent and the volume of original oil in place (OOIP) (Lake, 1989).

2.2.3 Viscous fingering

Viscous fingering occurs when a displacing fluid is more mobile than the fluid displaced. In the case of oil and water, water may bypass the oil in the reservoir during a displacement process due to its favourable mobility and thus create an uneven or fingered profile. The result of this is often poor sweep efficiency and may lead to early breakthrough of water (Schlumberger, 2011). A visualization of viscous fingering is shown in Figure 1. The image at the left shows how water displaces the oil initially when it is injected. The image in the middle depicts that when the flood continues, the water swept zone grows but the unfavourable mobility ratio of oil and water together with the heterogeneities in the reservoir causes fingering. The image to the right depicts that a continuous path of water has developed and thus water is being produced. When breakthrough has occurred, unswept oil cannot be produced by continuous water injection.

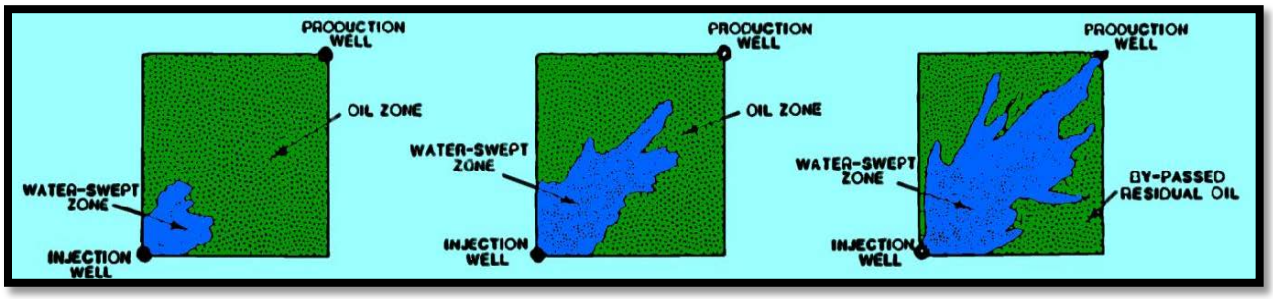

Figure 1: Viscous fingering occurring as water displaces reservoir oil (Pinzewski, 2011)

Additional information and equations corresponding to fundamentals of reservoir engineering may be found in Marianayagam (2011).

3 Heavy oil

3.1 Definition of heavy oil

Various definitions are used amongst petroleum engineers when characterising heavy oil (Speight, 2009). Confusion exists especially within the applications of more viscous materials such as bitumen and asphalt. In different scientific articles, heavy oil can be defined as residual oil fluid, coal tar creosote or viscous crude oil. In the present thesis, the last term will be used.

Heavy oil can be defined as a viscous type of petroleum, with larger fractions of low-volatile and high molecular weight compounds. These compounds vary significantly with respect to chemistry and molecular compositions and do not necessarily consist of only asphaltenes or paraffins. In general, one may say that the heavier components have higher melting points and contribute to the poor fluid properties of heavy oil which in turn leads to low mobility compared to that of conventional oil. Heavy oil typically has lower levels of parafinns, which are straight-chain alkanes, and contains moderate to higher proportions of asphaltenes. It should be underlined that it could be fallible to characterise specific heavy oil properties as various definitions exist. Yet, a definition has been included in the following paragraph in order to give the reader an idea of the magnitude of properties important in heavy oil recovery.

Light oil/conventional oil is denoted as oil that possesses an API gravity of at least 22° and a viscosity that does not exceed 100 cP.

Heavy oil is defined as oil that contains a significant amount of asphaltenes. The oil is very dense with a low API gravity and a high viscosity. Various specific definitions for heavy oil has been proposed, yet a limit has been set to a maximum API of 22° and to a minimum viscosity of 100 cP.

Extra heavy oil is denoted as the heavy oil with an API lower than 10°.

Natural bitumen is also called tar/oil sands and has similar characteristics to that of heavy oil. However, natural bitumen is even more dense and viscous. The viscosity is defined to be larger than 10 000 cP (Meyer & Attanasi, 2003).

3.2 Heavy oil geology and reserves.

3.2.1 Creation of heavy oil

There is a general agreement amongst geochemists that all crude oils initially has an API gravity between 30 ° and 40°. Heavy oils with lower API gravity are created at a later stage, after significant degradation during migration and entrapment (Curtis, et al., 2002). Vast amounts of heavy oil are residuals of formerly light (conventional) oil that has lost its lighter molecular weight components due to degradation of bacteria, water washing and evaporation (Meyer & Attanasi, 2003). Degradation refers to the process that occurs when bacteria and other living organisms feed themselves on organic materials such as hydrocarbons (Speight, 2009). The process of degradation removes the lighter hydrocarbons and thus the remaining oil becomes denser and more viscous i.e. inhabits the characteristics of heavy oil. In addition to the degradation process, the lighter hydrocarbons may have evaporated from the shallow formations. Water washing refers to the process at which formation water removes the lower molecular weight hydrocarbons that are more soluble in water (Curtis, et al., 2002).

3.2.2 Heavy oil reservoirs

Heavy oil reservoirs are often geologically young i.e. from the cretaceous era. Heavy oil is most often found in rather young formations such as the Pleistocene, Pliocene and Miocene (Curtis, et al., 2002). Thus, a common denominator for such reservoirs are that they tend to be rather shallow (as the rock is deposited at a later stage). Shallow in this case refers to depths that are less than 1000 metres below the surface as defined by Speight (2009). As the pressure is less at shallower depths, the seals in heavy oil reservoirs are less effective (Curtis, et al.,

2002). The lower seal pressure allows gas to evaporate and escape and thereby increases the density and viscosity of the oil even further. The shallow conditions also result in relatively low reservoir temperatures; between 40°C to 60°C. In addition the shallow depths result in rather fragile structures where faults may create heterogeneities in the reservoir (Speight, 2009).

3.2.3 Reserves

Oil reserves are the estimated quantities of conventional and unconventional oil reserves that are technically and economically recoverable (Lake, 1989). The total amount of oil in a reservoir is denoted as *oil in place*, however only a fraction of this can by economical and technological feasible methods be brought to the surface. Thus, it is only this fraction, the volume of recoverable oil that is denoted as reserves. The ratio between the reserves and the oil in place is called the *recovery factor (RF)* and this may change over time as technology is developed and recovery techniques become economically feasible. In general, the early estimates of recovery factors of an oil field are rather conservative and will often increase with respect to time (Speight, 2009).

According to Meyer & Attanasi (2003) the estimated volume of technically recoverable heavy oil on a world basis is 434 billion barrels. The similar estimate of bitumen is 651 billion barrels. It should here be noted that the above volumes are based on *known* reserves, hence it should be taken into consideration that the value has most probably increased as this article was submitted in 2003.

3.3 Heavy oil recovery

Gates (2010) argues that there are two requirements of a technically successful bitumen recovery. Firstly the bitumen must become mobile by lowering its viscosity by several orders of magnitude. Secondly, the mobile bitumen must be moved to a production well. There are different ways to lower the bitumen viscosity. Heat, often injected in the form of steam;

solvent dilution which basically is simple mixing of solvent and bitumen resulting in a single oil phase; and compositional changes in the bitumen to yield a lower viscosity by adding solvent.

When determining the recovery method for a specific heavy oil reservoir, it is important to remember that a successful technique for one reservoir may not be applicable to other reservoirs. Each method must be tailored in order to fit the specific fluid and reservoir properties. Essential properties are amongst others; the geological setting (i.e. the depth, areal extent, and thickness of the reservoir), oil composition (i.e. density, viscosity and gas content), the presence of bottom water or top gas zones, petrophysical and geomechanical properties (i.e. porosity, permeability, and rock strength), the presence of shale layers and the variation of these properties across the reservoir (Speight, 2009).

3.3.1 General methods

When producing from heavy oil reservoirs operators tend to produce with primary recovery methods as long as possible. Cold production is the most common form of primary production in heavy oil reservoirs. However, cold production gives a recovery factor of only 1-10 % in heavy oil reservoirs. Accordingly, there is a rapid need for secondary recovery methods. Cold production with artificial lift, including injection of a light oil, or diluent, to decrease the viscosity might be a valid option. When cold production is no longer economically feasible, tertiary methods in the form of thermal recovery are usually implemented. (Curtis, et al., 2002)

Gates (2010) argues that cold production is typically feasible in heavy oil reservoirs with high solution gas and in situ viscosities less than 50 000 cP. The viscosity of Athabasca bitumen often exceeds 1 million cP, thus thermal recovery methods are required.

3.3.2 Thermal recovery methods

In *hot water flooding*, heated water is injected into the reservoir in order to displace the in place oil immiscibly (Farouq Ali, 1974). Immiscibility is the process at which two fluids interact but do not mix. Hot water flooding is similar to conventional water flooding; the only difference is the temperature increase with respect to the injected water and hence *hot* water flooding is more applicable to heavy oil reservoirs.

However, this method has demonstrated limited success due to the occurrence of viscous fingering. Viscous fingering occurs frequently in hot water flooding due to the higher mobility of the injected water compared to that of the in place oil. This results in a poor volumetric sweep efficiency resulting in early breakthrough of water and a relatively low recovery of oil. Based on this Farouq Ali (1974) argues that whenever possible steam-based methods should be preferred.

In the general process of *In situ combustion* a fire front is created in the reservoir with the aid of air injection. The fire front moves in the reservoir and consumes or displaces the fluids ahead of it towards the production wells. Significant heat loss does occur to the surroundings. Yet, the heat generation rate in the combustion zone must exceed the minimum ignition temperature of the oil in the reservoir (Farouq Ali, 1974).

With *wellbore heating* the objective is to heat the immediate surroundings close to the wellbore, the radial distance may be as short as a few feet. The resulting decrease in flow resistance will increase the oil recovery (Farouq Ali, 1974).

3.3.3 Steam injection

Steam based methods have been implemented for several decades as it was commercialized in the early 1960´s (Speight, 2009). Steam injection involves injecting high pressure and high temperature steam into the reservoir. Water is converted to steam by the use of heaters and insulated pipelines transport the steam to the injection wells (Khan & Islam, 2007).

Steam oil ratio (SOR) is defined by Gates (2010) as; *"the volume of steam needed, in cold water equivalent (CWE) per unit volume of produced bitumen"*. Basically, the SOR is the amount of steam injected per barrel of oil produced (Speight, 2009). This is an indication of the efficiency of the bitumen/heavy oil recovery (Carlson, 2003). The cumulative steam oil ratio (CSOR) does to a large extent reveal whether or not a steam-based project is economically feasible. Consequently if the cost of steam exceeds the amount generated by the following oil recovery the project may be unfeasible.

Cyclic steam injection was first implemented in the early 1960´s (Speight, 2009). In this method steam is injected into the formation for a certain period of time. Thereafter the well is shut in for a period. When production is started up again there will preferably be a dramatic increase in oil production. The production rate will most likely decline with time, yet the production may still exceed the rate prior to stimulation (Farouq Ali, 1974). The application of cyclic steam stimulation is widely known, however the major limitation concerning this method is the rather low recovery factors achieved. With steam-oil ratios ranging from 3-5, typically 20-35 % may be recovered (Speight, 2009).

Steam flooding is also named continuous steam injection or steam drive. It is a thermal recovery method where steam generated at the surface is injected into the reservoir through specially distributed injection wells (Schlumberger, 2011). In this method steam is used as the displacing agent. The injected steam increases the temperature of the crude oil. Farouq Ali (1974), states that the most significant effect of steam flooding is the decrease in viscosity and the thermal expansion. A sufficient effective permeability is required in order to conduct a successful steam drive. This to ensure injection rates high enough to increase the reservoir temperature sufficiently to mobilize the oil. The heat generated also distilles the light oil components that condense at the oil bank (the portion of a reservoir, which has increased oil saturation), move ahead of the steam front and hence reduce the viscosity further (Schlumberger, 2011). The hot water that condenses from the steam and the steam itself, create an artificial drive and increase the sweep efficiency. Subsequently the oil is driven towards the production wells. Another significant factor related to heavy oil recovery with steam flooding is that steam reduces the interfacial tension that binds paraffin's and asphaltenes to the rock surface. This occurs parallel to the steam distillation of the light crude oil. Further the light crude oil creates a small oil bank that can remove residual oil due to its miscibility (Schlumberger, 2011). Once the flow resistance is reduced, other driving forces

present in the reservoir such as gravity, solution gas and natural water drive; effect the improved recovery rates (Speight, 2009).

Figure 2 shows an ideal scenario of what should occur in a reservoir when undergoing steam injection. The injected steam will rise until it reaches an impermeable layer, in this case the overburden. Thereafter it will spread laterally, until it reaches the production well and breakthrough occurs. Steam will preferably, due to the density difference between steam and oil, push the oil downwards so that the oil can be produced by gravity drainage. (Curtis, et al., 2002).

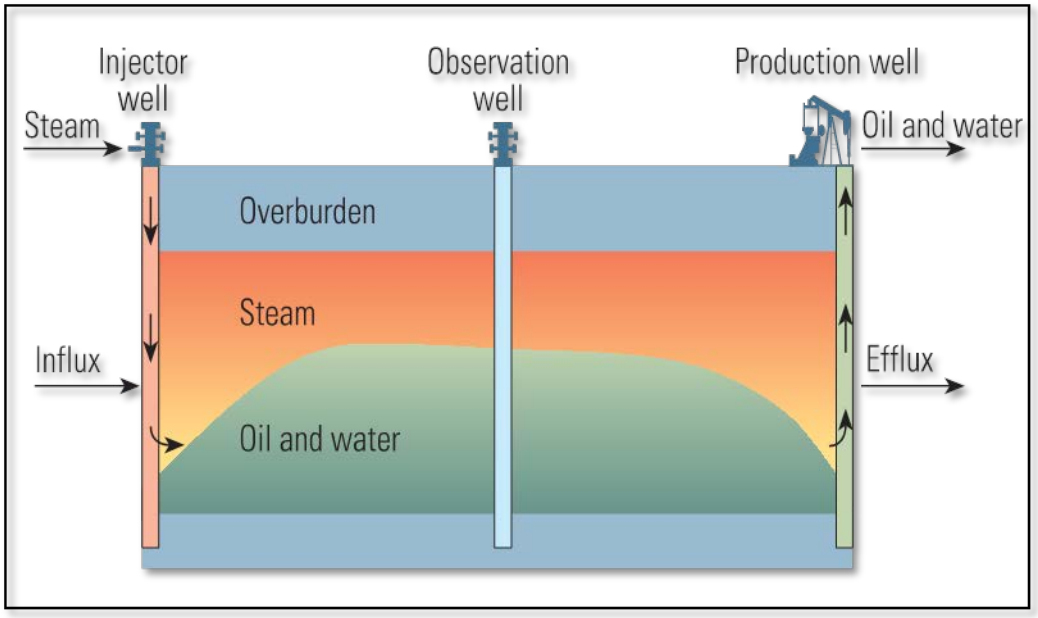

Figure 2: Ideal scenario of steam injection into heavy oil reservoir (Curtis, et al., 2002)

However, due to heterogeneties in the reservoir the injected steam will travel along unknown paths. Despite this, depending on fluid parameters and reservoir properties, steam flooding in a heavy oil reservoir may result in a recovery factor up to 80% (Curtis, et al., 2002).

3.3.4 Steam-Assisted Gravity Drainage

Steam-assisted gravity drainage (SAGD) is a technique that was developed in Canada. Several pilot studies have been carried out in order to test the method. The SAGD method was initially developed to recover bitumen from the Canadian oil sands. In Athabasca bitumen reservoirs, SAGD is the most used commercial steam based process (Gates, 2010).

The basic concept of SAGD is two parallel horizontal wells which have a large contact area with the formation. Prior to the steam injection, a preheating period takes place. Heating is conducted in the injection well and production well to obtain communication between the wells. After the preheating period, as visualized in Figure 3, hot steam is injected in the top horizontal well and introduced to the reservoir. The lower picture demonstrates how the steam heats up the surrounding oil. The heat causes the oil viscosity to decrease and thereby increases its mobility (Curtis, et al., 2002). As the viscosity is reduced the heavy oil thins from the oil sands and separates. A steam chamber develops and the density difference causes the steam chamber (the steam saturated zone) to rise to the top of the reservoir and to expand gradually sideways. After some time it will allow drainage from a very large area. The mobilized oil then drains to the production well situated at the bottom of the reservoir due to gravity. The oil and condensed water are thereafter produced at the production well. The reason why this method relatively new is due to directional drilling as it has only been possible to drill horizontal wells the last 10-15 years.

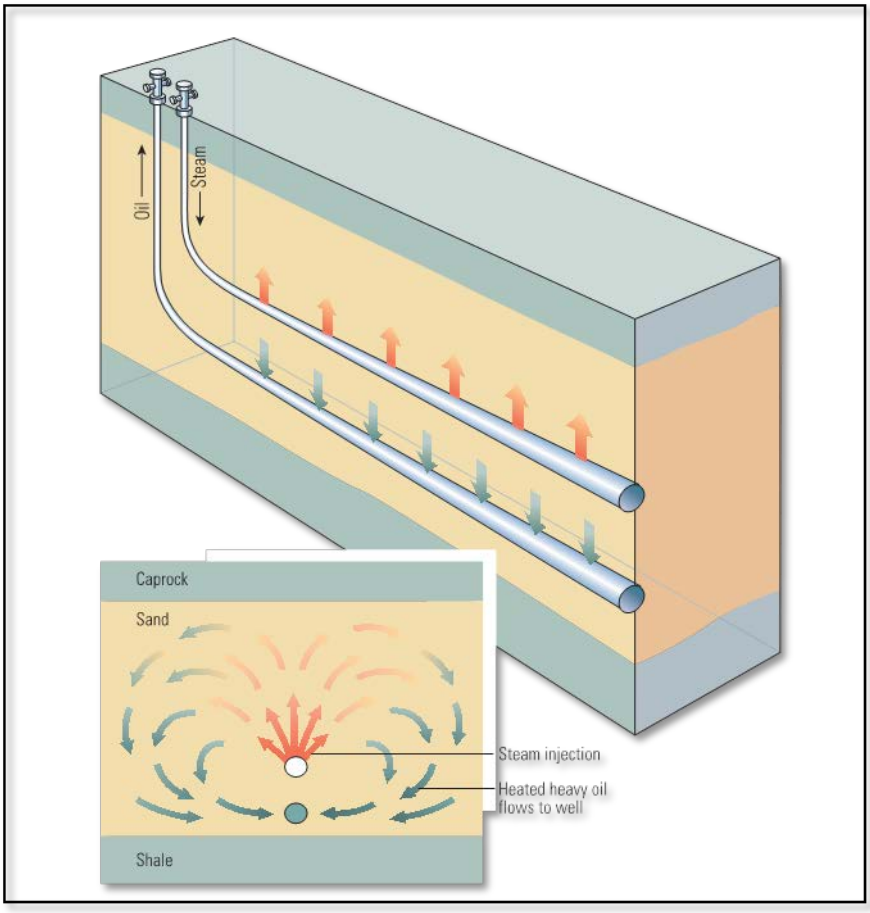

Figure 3: Steam-assisted gravity technique (Curtis, et al., 2002)

The injected steam reduces the oil viscosity down to 1-10 cp, depending on the reservoir conditions such as temperature and fluid properties of the oil. Gases produced during SAGD are normally methane with some carbon dioxide and traces of hydrogen sulphide (Speight, 2009).

The vertical distance between the injector and the producer is normally 5-7 metres (Speight, 2009). This method is very efficient and it is claimed that it will increase the recovery by 60-70 % of the oil in place and is therefore the most efficient thermal recovery method (Speight, 2009). In addition to high ultimate recovery the SAGD method improves steam oil ratio compared to other steam-based methods (Speight, 2009).

Speight (2009) argues that in the SAGD method, the injection pressure is much lower than the fracture pressure to ensure that the steam does not break into a thief zone. A thief zone is as

defined by Speight (2009): *"Any geologic stratum not intended to receive injected fluids in which significant amounts of injected fluids are lost"*. Moreover, the injection pressure and the production pressure should be approximately *identical* in order to prevent viscous fingering, coning processes, and prevent water influx and oil loss to high permeable streaks.

The SAGD process is very stable compared to other methods due to no pressure-driven instabilities such as coning, channelling or fracturing. It is merely a gravity driven process and is therefore extremely stable as the process zone grows only by gravity segregation. Yet, to achieve a successful SAGD production it is important to balance the injected and produced volumes and thus maintain the volume balance. If the steam pressure becomes lower than the pressure in the water zone, this will lead to water influx. In order to avoid this, the pressure in the steam chamber must be increased to suppress the influx. In addition, the pressure in the production well must be decreased. After some time the water influx will terminate and the pressures will balance. It is also of high significance that the system tends to repair itself due to the density differences between the phases. (Speight, 2009).

Another interesting phenomenon related SAGD is when horizontal streaks of shale or other impermeable barriers are present. One would assume that this will create a production problem in SAGD as the steam will not be able to flow through the impermeable layers. However, in the case of a shale layer, the steam heats up the shale. As the shale is heated, the kinetic energy of the water particles in the shale increase until they are released from the shale. Subsequently, dehydration occurs *instead* of thermal expansion. As the water is released from the shale, the fracture pressure in the shale decreases. When the pore pressure *exceeds* the fracture pressure in the shale, vertical fractures are created. Hence, a flow path is developed through the shale where steam and oil may flow. This effect combined with gravity segregation may result in 60-70 % recovery even in reservoirs were many shale streaks are present (Speight, 2009). Yet, it should be noted that the thickness of the shale will be a determining factor, as this phenomenon will not apply to shale above a certain thickness.

Challenges related to SAGD

In all processes where hot fluid is injected there is a problem of heat loss from the injection wells to the overburden formations. If the injection wells are inadequately insulated and the injection rates are rather low it is more likely that a larger fraction of the injected heat is lost. This effect may be strengthening with respect to reservoir depth because this reflects the

distance that the steam has to travel in order to reach the reservoir. An effect of this with respect to steam-based methods is that steam may condense in response to the heat loss. This may result in the steam actually entering the reservoir as hot water, and thereby the effects of hot water flooding will apply. Measures should be taken in advance to ensure that injection wells are completed in such a way that steam condensation is avoided (Speight, 2009).

In the SAGD method however, heat loss is to some extent reduced due to the non-condensable gases. Due to the density difference, the non-condensable gases tend to stay high in the reservoir structure and thus in a way acts as a “heat insulating blanket” to the injection well, resulting in minimizing the vertical heat loss that occurs when the chamber grows laterally (Speight, 2009).

The technical issues related to the SAGD methods are related to low initial oil rate, artificial lifting of bitumen to the surface, horizontal drilling and operation, and the implementation of SAGD where there are very low reservoir permeability, low pressure or bottom water (Speight, 2009).

One of the limitations to SAGD is the short lifespan of the wells, so it is important to ensure that the drilling cost does not exceed the money generated by production. Another limitation related to SAGD is the cost of steam. It is important to keep the steam oil ratio as low as possible in order to maximize the economical outcome.

An extended version, describing the theory of heavy oil and heavy oil recovery, can be found in Marianayagam 2011.

4 Athabasca oil field

4.1 Location

The Athabasca oilfield is located in Northern Alberta in the Western Canada Sedimentary basin (Figure 4). Three major deposits are located in the province of Alberta: Athabasca, Cold Lake and Peace River. Together they contain at least two thirds of the world's discovered bitumen in place, estimated to be 1.7 trillion barrels. The Athabasca deposit is centred on the city of Fort McMurray, the Cold Lake deposit is situated at the North of Lloydminster and the Peace River deposit is situated in northwest Alberta. (Attanasi & Meyer, 2007).

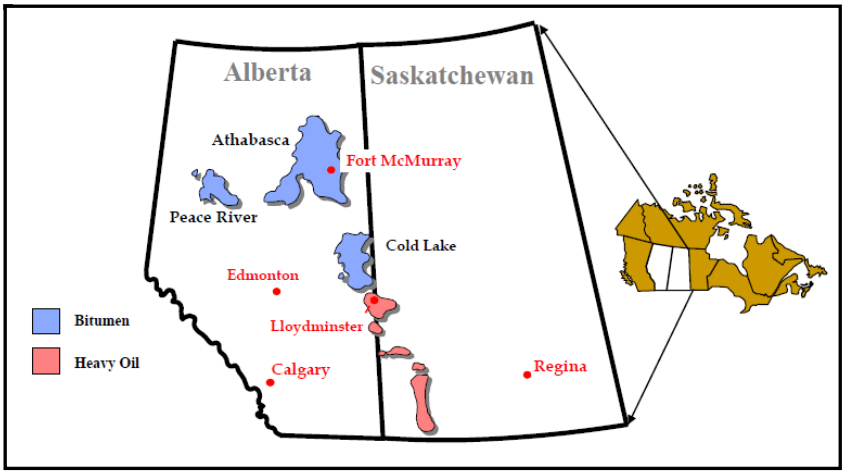

Figure 4: Major oil sand deposits of Canada (Nasr & Ayodele, 2005)

4.2 Geological description

Natural bitumen occurs in clastic and carbonate reservoir rocks (Attanasi & Meyer, 2007). This type of oil is frequently found close to the earth's surface and thus often at shallow depths. The average depths of the deposits in Alberta are; Athabasca: 200 m, Cold Lake: 400 m, Peace River: 500m (Nasr & Ayodele, 2005). Despite the average depth being 200 m, the Athabasca reservoirs may be found at depths 0 – 500 m. The Athabasca oil sand deposit is the largest petroleum accumulation in the world, corresponding to an area of about 46 000 km^2 (Tavallali & Harding, 2011).

In the Athabasca oil sand, most of the bitumen deposits are found within a single contiguous reservoir, the lower cretaceous McMurray formation (Tavallali & Harding, 2011). The areal extent of the McMurray deposit is in the order of 300 km north-south and 100 km east-west (McCormack, 2001). The thickness of the total McMurray formation is approximately 40-100 m and the average is approximately 30 metres of clean bitumen saturated sands. In the Athabasca oil sand the bitumen bearing zone is the McMurray-Wabiscaw interval (Tavallali & Harding, 2011).

Both stratigraphic and structural elements are involved in the trapping mechanisms of Athabasca deposit. Yet, the majority of geologists divide the McMurray formation into lower, middle and upper members. The McMurray formation is situated over the Devonian formation which consists of limestone. As depicted in Figure 5 the Wabiscaw member of the Clearwater formation is overlying the McMurray formation. This formation provides the shale cap rock to the bitumen reservoir.

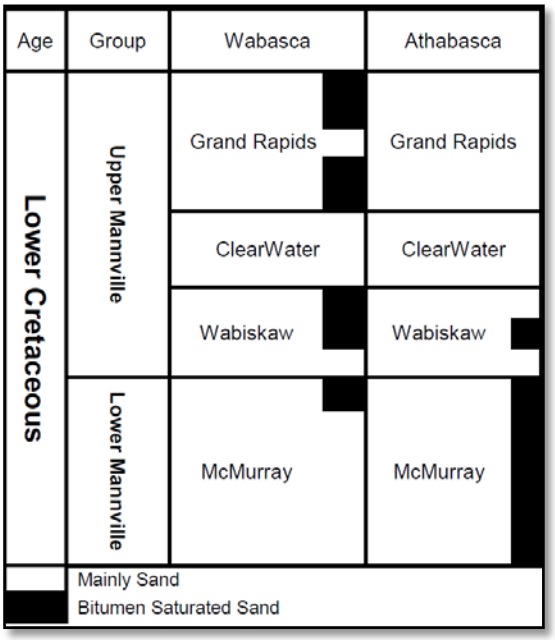

Figure 5: Correlation chart of lower bitumen deposits at Athabasca oil sand: (Tavallali & Harding, 2011)

Over the Clearwater formation a formation consisting merely of sandstone (Grand Rapids) is deposited. The McMurray formation is separated by shaly layers, which can be up to two metres thick (Tavallali & Harding, 2011).

Moreover, the Athabasca oil sands deposits are very heterogeneous when considering physical reservoir properties such as the geometry, distribution of components, porosity and permeability. The properties of the reservoir and bitumen vary both vertically and laterally. An example is that the viscosity distribution over a 50 m vertical interval or 1 km lateral distance may vary in an order of magnitude (Tavallali & Harding, 2011). The average composition of Alberta bitumen is 84 % Carbon, 10 % Hydrogen, 0.9 % Oxygen, 0.4 % Nitrogen and 4.7 % Sulphur (Nasr & Ayodele, 2005). The density of the bitumen may vary from 6° to 11° API gravity. The porosity and permeability are very high in the McMurray formation and can be up to 25-35% and 6-12 D respectively. As for all bitumen reservoirs the oil is highly viscous. The average reservoir temperature in Athabasca is 11°C and at these conditions the oil is immobile (Tavallali & Harding, 2011). A much advantaged characteristic of the deposit is that the grains are dominantly water wet and that the bitumen is not in direct contact with the sand grains (Nasr & Ayodele, 2005).

4.3 Reserves

In Canada, bitumen recovery from the Alberta natural bitumen deposits, constitute one third of the crude oil produced (Attanasi & Meyer, 2007). The reserves are of the same magnitude as that of the conventional reserves in Saudi Arabia (Nasr & Ayodele, 2005). Figure 6 displays the initial volume of bitumen in place for the three deposits in Northern Alberta in comparison to other major oil countries.

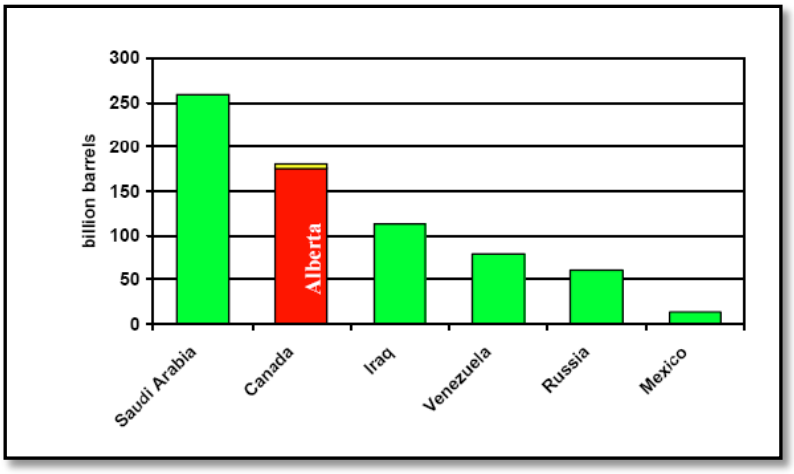

Figure 6: Comparison of Alberta and world proven oil reserves (Nasr & Ayodele, 2005)

As seen in Table 1, the Alberta Energy and Utilities Board (AEUB) estimates the total initial volume in place of bitumen for the three deposits to be 259.1 billion cubic meters. Yet, as the exploratory methods continue develop it is estimated that this number could reach 400 billion cubic meters of bitumen (Nasr & Ayodele, 2005). Thus one may conclude that Canada holds the world largest bitumen deposits. In addition, Athabasca holds the largest bitumen deposit in Alberta.

Table 1: Initial volumes of bitumen in place for Athabasca, Cold Lake and Peace River (Nasr & Ayodele, 2005)

Deposit	Initial volume in Place (10^9 m^3)
Athabasca	*206.7*
Cold Lake	31.9
Peace River	20.5
Total	**259.1**

The Alberta oil sands are the only bitumen deposits that are exploited commercially today (Attanasi & Meyer, 2007). The McMurray formation in north-eastern Alberta constitutes a significant amount of the world's currently identified oil resources. It has been estimated that over 40 million barrels ($6.35 \times 10^9 m^3$) may be recovered by SAGD. This volume is in addition to the oil recoverable by surface mining in the areas with minimal overburden (McCormack, 2001).

5 Numerical reservoir simulation

5.1 Basic concepts of thermal reservoir simulation

Production of a reservoir may only occur once. If a mistake in the production approach is made, there is a high probability that it will be there during the whole life of the wells involved and this may occur at an extensive cost. Therefore, it is of high importance to evaluate the reservoir thoroughly before conducting and deciding on production approach. Study carried out by a numerical simulation model may be conducted several times. Thus various alternatives may be examined and the best possible production approach may be determined (Chow, 1993). The optimum method of depletion may be deduced based on the reservoir model's performance under different conditions. Hence, these numerical models *improve* the physical understanding of the reservoir to a great extent. However, it is essential to be aware of the uncertainties related to numerical models and gain knowledge about which areas the models are applicable for. Therefore, a physical analysis, such as a laboratory experiment, should be evaluated together with the reservoir model in order to accomplish a thorough understanding of the reservoir.

In general, reservoir simulation is used to predict fluid flow in a porous medium. Unlike other aspects of nature the reservoir is not visible to us. It is therefore the reservoir engineer's job to predict and understand those conditions despite the lack of visibility. The simulation tool is used to investigate these abstract conditions. It is important to remember that the simulator may solve complex problems, and is capable to evaluate input, but it is *not* capable of determining *input that should have been entered* (Carlson, 2003). Thus, it is very important for the reservoir engineer to evaluate all inputs and outputs and compare them to other data in order to deduce if the results are reasonable or not.

Moving over to *Thermal reservoir simulation,* one observes an additional complexity compared to that of conventional reservoir simulation. As Mike Carlson (2003) states in his book; "Thermal simulation is probably the most challenging aspect of reservoir simulation at present". Black oil simulators are based on volumetric material balance and Darcy's Law. In addition, a thermal reservoir model has to include conservation of energy (Carlson, 2003).

Accordingly, more input data is required in a thermal simulator compared to that of a black oil simulator, as for instance thermal properties, must be added to the input stream.

The simulation software used in this thesis is CMG (Computer Modelling Group) STARS (Steam, Thermal and Advanced Processes Reservoir Simulator. CMG STARS is a thermal simulator created especially to simulate heavy oil and bitumen reservoirs.

5.2 Model description & base case data

The grid cells in the directions of length, width and height are denoted by the letters *i, j, and k,* respectively. The reservoir grid consists of 101 blocks in *i* direction, 1 block in *j* direction and 15 blocks in *k* direction. An image of the reservoir grid is shown in Figure 7 and the model definitions are presented in Table 2.

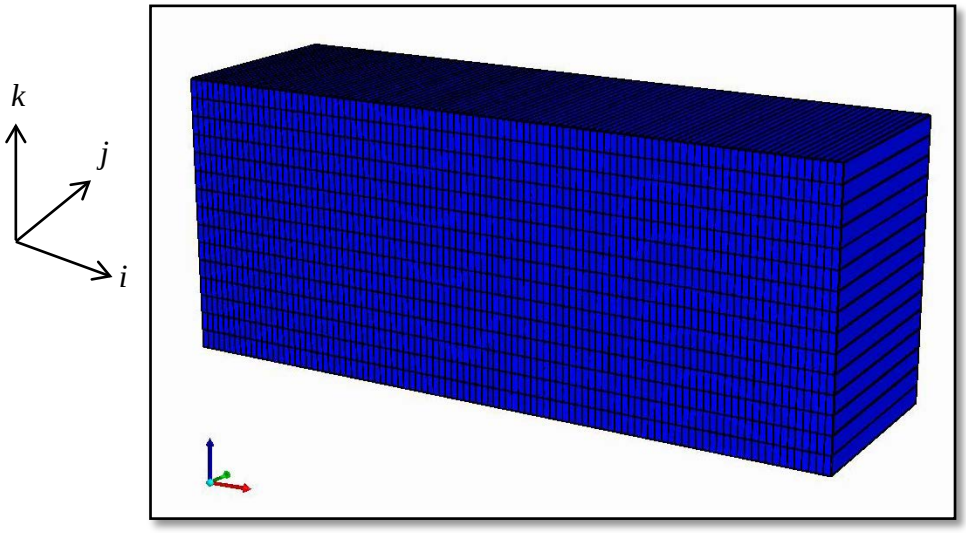

Figure 7: Reservoir grid

Table 2: Model definitions (Souraki, Ashrafi, Karimaie & Torsaeter, 2012)

Model definitions	
Model	Cartesian model
Length of model	101.4 m
Width	30.28 m
Height (thickness)	13.72 m
Initial oil in place	14443.5 Sm^3

The reservoir model base case re-created in this thesis is simulating a section with length, width and height equal to101.4 m x 30.28 x 13.72 m, respectively. When defining the size of the grid blocks the *i* blocks where defined to be 3.3 feet (≈1 m) for the first 50 blocks, then 2.8 (≈ 0.9m) feet for the middle block and then 3.3 feet (≈1 m) for the next 50 blocks. The j block was defined to be 100 feet (30.48 m). The k blocks where to be 3 feet (≈0.9 m) each. The injection well and the production well are placed in the middle of the reservoir grid in *one* grid block. The length of both the injection well and the production well is equivalent to the j block, namely 100 feet (30,48 m).

The base case data file and the initial input data for the present thesis is based on work performed by Souraki, Ashrafi, Karimaie & Torsaeter (2012). The study conducted by the above authors involved laboratory work on oil samples from the Athabasca field in order to determine essential properties. Additionally, a parameter study by numerical simulation was conducted. The data file initially created (Souraki, Ashrafi, Karimaie & Torsaeter, 2012) have been included in Appendix C.

Table 3 displays the initial reservoir properties used for reservoir characterization in the base case:

Table 3: Reservoir characterization (Souraki, Ashrafi, Karimaie & Torsaeter, 2012)

Reservoir Characterization	
Porosity	38 %
Horizontal permeability	7000 mD
Vertical permeability	2100 mD
Initial temperature	10 °C
Initial pressure	2068 kPa
Initial water saturation	0.20
Initial oil saturation	0.80

Table 4 displays the rock and fluid properties in the base case:

Table 4: Rock and fluid properties (Souraki, Ashrafi, Karimaie & Torsaeter, 2012)

Rock and Fluid Properties	
Rock thermal conductivity	106 Btu/(ft*day*F)
Rock heat capacity	35 Btu/(ft^3*F)
Density of bitumen	1013.3 Kg/m^3
Thermal expansion coefficient of bitumen	7.2 E4/°C
Molecular weight	534 Kg/Kgmole
Rock compressibility	5E-4/psi

Input parameters with respect to steam injection are included in Table 5:

Table 5: Steam injection conditions (Souraki, Ashrafi, Karimaie & Torsaeter, 2012)

Steam injection conditions	
Steam injection rate	200 STB/d
Steam quality	90 %
Preheating period	100 days
Steam temperature	215.5 °C (420 °F)

Figure 8 depicts a 2D view (*i*,*k*) of the well placement. The injection well is placed in layer *k* = 10 and the production well is placed in layer *k* = 15. Note that the wells go into the plane (100 feet).

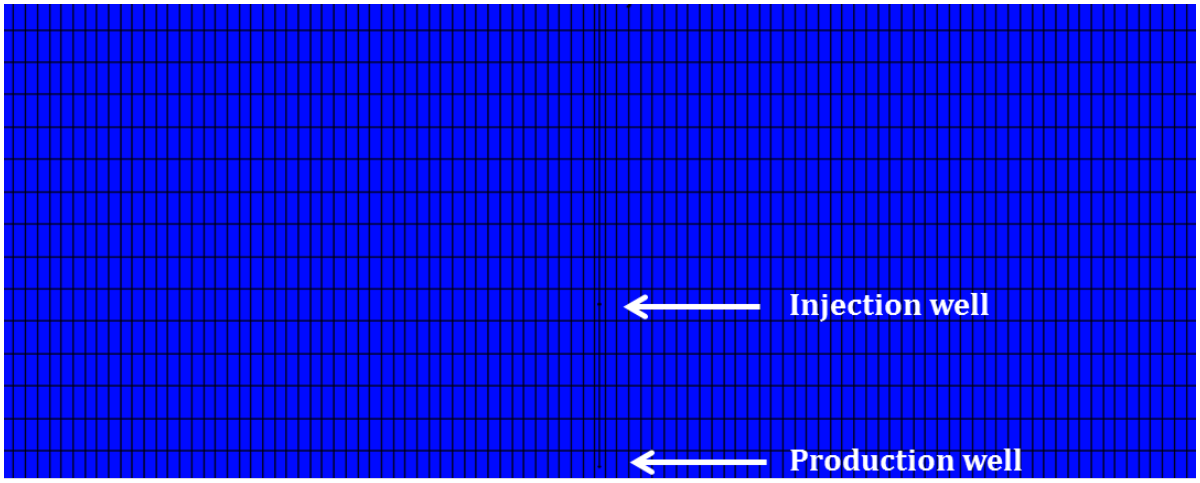

Figure 8: 2D view displaying the layer of production and Injection

One of the most important input variables for numerical reservoir simulation is the relative permeability. The relative permeability curves and residual fluid saturations are required in order to estimate the oil production rate and ultimate recovery (Pollkar, Farouq Ali, & Puttagunta, 1990). Sensitivity analysis with respect to relative permeability data is out of the scope for this thesis, yet it can be mentioned that Pollkar, Farouq Ali, & Puttagunta (1990) deduced that a comparison of relative permeability curves for the Alberta heavy oils indicated that wide variations exist amongst the reported data. Moreover, the authors argue that a range of relative permeability curves may be required to describe the varios recovery mechanisms of heavy oils. The relative permeability input data is given in Appendix A.3. The corresponding figures are given in Figure 9 and Figure 10.

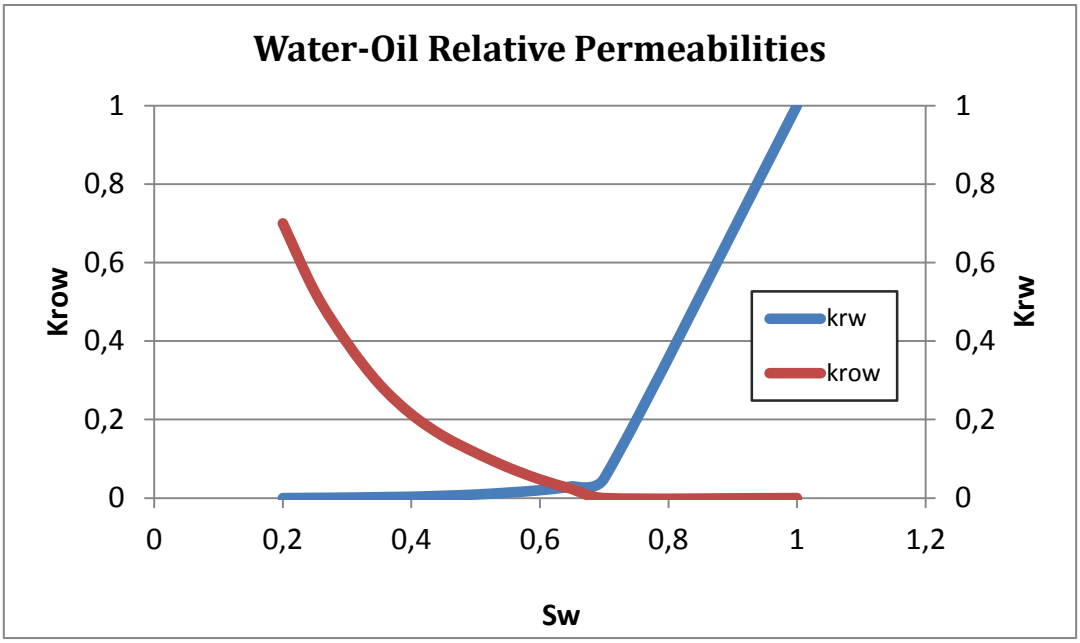

Figure 9: Water-oil relative permeabilities (Souraki, Ashrafi, Karimaie & Torsaeter, 2012)

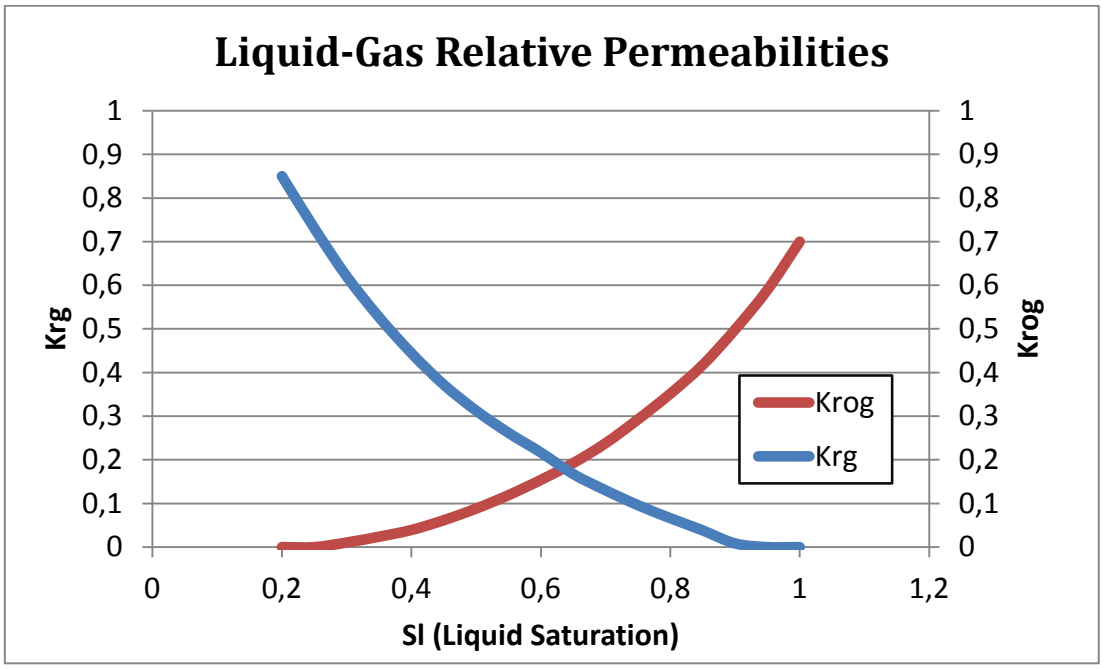

Figure 10: Liquid-gas relative permeabilities (Souraki, Ashrafi, Karimaie & Torsaeter, 2012)

Figure 11 displays the oil rate versus time for the base case. As commented in the figure, the preheating period lasts for 100 days. At this point the connection between the injection well

and the production well is obtained. At first the production well is controlled by a minimum bottom hole pressure at 250 psi.

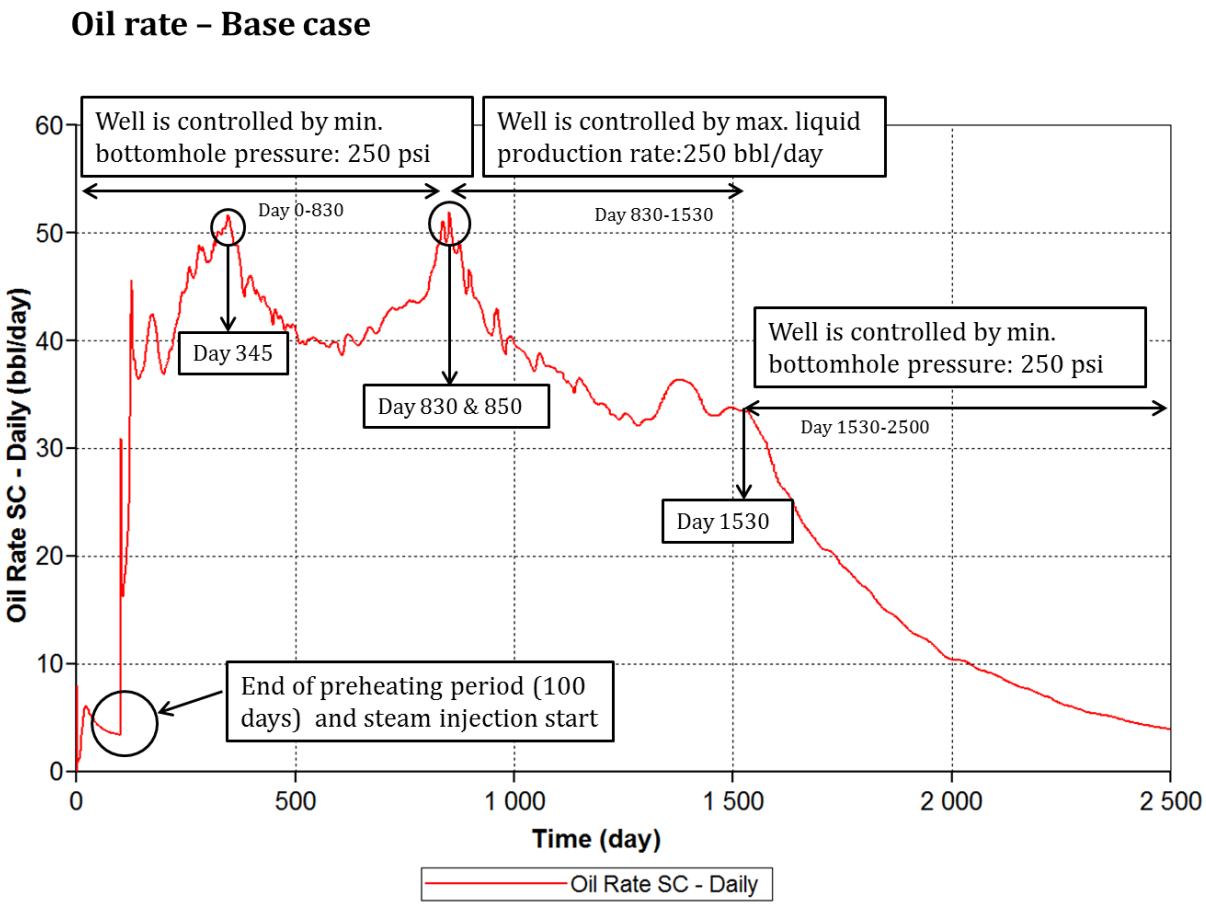

Figure 11: Oil rate - base case

When the base case is simulated the temperature distribution indicates how the steam spreads in the reservoir. Figure 12 displays the spreading of steam. The injection well is placed at the centre of the reservoir due to the spherical expansion of the steam, and thus the placement ensures that the injected steam covers the whole reservoir.

As steam is injected and the production well is opened, oil is produced. At day 345 the first peak can be observed from Figure 11. A possible reason for this can be seen from Figure 12, as this is the time where the steam hits the top of the reservoir and starts to spread laterally. Thereafter a decrease in oil rate is observed as the steam continues to spread laterally. This might be due to the area of increased temperature being further away from the production well. Hence the oil needs longer time to reach the production well, resulting in a decreased

production rate. As a larger area is heated, a larger amount of oil arrives at the production well. Consequently, the oil rate increases until it reaches defined maximum liquid production rate of 250 bbl/d (liquid production rate is total liquid rate, referring to oil phase plus water phase). When the rate has declined sufficiently it is again controlled by the minimum bottom hole pressure at 250 psi. The rate thereafter follows a steady decline until it reaches end of simulation at 2500 days. The turning point at which steam hits the outer reservoir walls take place around day 1530 (Figure 12). At this point in time the entire reservoir is heated and yet the oil rate is declining, probably due to the decline in oil saturation.

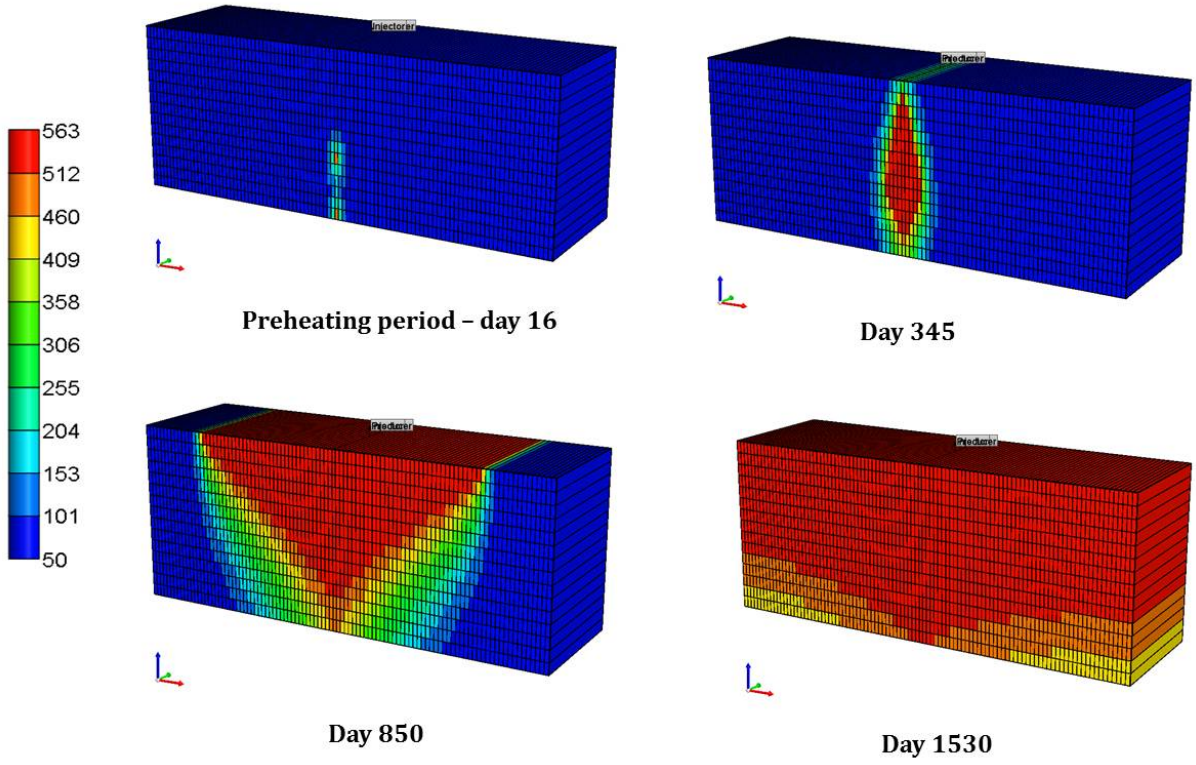

Figure 12: Temperature distribution (°F) - base case

5.3 Simulation variables

In this thesis, different parameters were altered and simulations were ran for various cases. A presentation of the parameter studies is provided next. The overall simulation matrix can be found in Table 15, Appendix A.1.

Viscosity

It can be deduced that the Athabasca bitumen differs to some extent from normal crude oils both in structure and in molecular size. Subsequently the Athabasca bitumen differs in physical properties. It has been proven at several occasions that the Athabasca bitumen has a much higher viscosity and density compared to that of conventional crude oils. Due to the different viscosity-temperature relationship compared to that of conventional oils, the correlations used to predict the viscosities of conventional oil does not deduce an adequate estimation of bitumen viscosity (Khan, Mehrotra, & Svrcek, 1984).

Khan, Mehrotra & Svrecek (1984) developed an empirical model for the correlation and prediction of the bitumen viscosity. According to Khan, Mehrotra & Svrecek (1984) the linear viscosity model predicts the bitumen viscosity well with an average deviance of 4 to 10%. The linear viscosity model is described by the following equation:

Equation 4: Linear viscosity model (Khan, Mehrotra, & Svrcek, 1984)

$$lnln(\mu) = C_1 lnT + C_2$$

where μ is given as the dynamic viscosity in *cp* at atmospheric temperature and pressure. The temperature (*T*) is given in *K*. The empirical constants C_1 and C_2 can be established for each sample and are determined by the least square parameter estimation technique. Khan, Mehrotra & Svrecek (1984) have presented these constants for four different bitumen samples in their paper. This data is displayed in Table 6.

Table 6: Viscosity parameter values (Khan, Mehrotra, & Svrcek, 1984)

Sample no.	C_1	C_2
1	-3.62722	23.2200
2	-3.57379	22.8379
3	-3.73360	23.8162
4	-3.56718	22.7823

Equation 4 was solved for μ with coefficients from sample no. 1 and sample no. 3 in Table 6 and for the average of the four samples. The corresponding temperatures where set to the same as for the base case. Table 16, Appendix A.2 shows the calculated viscosities for the simulated cases.

Grid Refinement

Due to the two dimensional model implemented in the base case it was essential to investigate the possible effects of a three dimensional model. The computer capacity did not allow for more than 10000 grid blocks. Consequently, this is the upper limit in the present analysis. For the three-dimensional model the cases examined are presented in Table 7. It was ensured that the total length of the well was equal to the base case (100 feet) but now consisting of several grid blocks.

Table 7: Simulated cases for grid refinement

Simulation no.	*i*	*j*	*k*
Base case	101	**1**	15
4	101	**2**	15
5	101	**3**	15
6	101	**4**	15
7	101	**5**	15
8	101	**6**	15

Variation in horizontal permeability

The horizontal permeability in the base case is 7000 mD. Due to the complexity of core extraction in heavy oil reservoirs, the permeability calculated may often vary and it is very difficult to measure an exact permeability for a given reservoir containing bitumen (Deutsch, 2010). Thus, different values for horizontal permeability exist amongst different researchers when pursuing their analysis. Based on this, it was essential to test for a wide range of horizontal permeabilities. All the other parameters in the base case where kept constant in order to analyse the effect of variation in horizontal permeability only. The simulated cases are displayed in Table 8.

Table 8: Simulated cases for variation in horizontal permeability

Simulation no.	Horizontal Permeability, k_h (mD)
Base case	7000
9	1750
10	3500
11	4000
12	5000
13	6000
14	8000
15	9000

Variation in vertical permeability

As the base case vertical permeability was 2100 mD, it was essential to test for a range of vertical permeabilities whilst keeping the horizontal permeability constant. Table 9 displays the simulated cases.

Table 9: Simulated cases for variation in vertical permeability

Simulation no.	Vertical Permeability, k_v (mD)
Base Case	2100
16	1050
17	525
18	3000
19	3300

Variation in horizontal and vertical permeability simultaneously

As the sensitivity was tested for horizontal and vertical permeability separately, it was also interesting to test variation in both of them simultaneously. The cases tested for are shown in Table 10.

Table 10: Simulated Cases for Simultaneous Alteration of Horizontal and Vertical Permeability

Simulation no.	Horizontal Permeability, k_h (mD)	Vertical Permeability, k_v (mD)
Base Case	7000	2100
20	1750	525
21	7800	2900
22	5000	4000

Injection Well Location

In the base case, the injection well is placed in layer 10 and the production well is situated in layer 15 i.e. at the bottom of the reservoir. Thus, the vertical distance between the wells is 15 feet (approximately 4, 5 meters). The diagram showing the vertical distance to each layer from the production well can be found in Table 17, Appendix B.3. It was determined to test for injection well placement in layer 7 and 9 in order to test for the preferred range put forward by Speight (2009). In addition, it was tested with the injection well at the top of the reservoir, i.e. layer 1. To test the effects of placing the injection well even closer, it was tested

with injection well in layer 12, 13 & 14. The simulated cases and the corresponding distance between injector and producer can be found in Table 11.

Table 11: Simulated Cases for Injector Well Location

Simulation no.	Injection layer	Distance between injector and Producer (m)
Base case	10	4.54
23	1	12.72
24	7	7.27
25	9	5.45
26	11	3.63
27	12	2.73
28	13	1.82
29	14	0.91

Porosity

Cores from the Athabasca oil sands are relatively easy to obtain due to limited or even absence of overburden (Collins, 1976). Yet, Dusseault (1980) states that reported properties for Athabasca oil sands have historically been fallible as the result of core expansion. Core expansion occurs when gas dissolved in the pore liquid expands and is released. The porosities that were determined despite this phenomenon were very high and resulted in underestimation of material weights and volumes.

Figure 13: Bulk densities and porosity determinations on McMurray Formation oil sands (Dusseault, 1980) summarizes several bulk density and porosity determinations on McMurray Formation oil sands in the time period from 1914 to 1977. Though Dusseault (1980) claims these data to be fallible, it can still give an indication of the scale of porosity that may exist in the McMurray formation. Moreover, (Woodhouse, 1976) argues that the significant expansion of the Athabasca cores occurs as overburden pressure is removed.

The base case porosity is already very high, 38 %, so based on Figure 13, one deduces that it is to some extent unrealistic to increase the porosity higher than 40 %. Therefore the porosity for the highest case in this sensitivity analysis was determined to be 40 %.

TABLE 1. Bulk density and porosity determinations on McMurray Formation oil sands

Bulk Density or Porosity (%)	Source	Comments
1.75 Mg/m³	Ells, 1914	Porosity >40%
1.96 Mg/m³	Blair, 1950	Porosity = 39.2%, Sat. = 89%
2.03-2.08 Mg/m³	Blair, 1950	Reported Porosities: 34% - 46%
35% - 44%	Hardy and Hemstock, 1963	Reported Void Ratios: 0.55 - 0.80
38% - 42%	Doscher *et al.*, 1963	
1.86-2.36 Mg/m³	Carrigy, 1967	Density Log Interpretation
1.98-2.08 Mg/m³	Carrigy, 1967	Density Log: 60 m deep
2.10-2.19 Mg/m³	Carrigy, 1967	Density Log: 300 m deep
35%	Camp, 1970	Average Porosity
35%	Carrigy and Kramers, 1974	Maximum Porosity
20% - 36%	Sah *et al.*, 1974	Geophysical Data
2.1-2.3 Mg/m³	Brooker, 1975	Geophysical Data
2.04-2.40 Mg/m³	Dusseault, 1977	Laboratory and Geophysical

Characteristic saturated bulk density values (Dusseault, 1977) **and corresponding porosities** (assuming S.G. of bitumen = 1.0 and S.G. of mineral = 2.65)

Saturated Bulk Density	Porosity	Material
2.18-2.05 Mg/m³	28% - 36%	Oil-rich sands, well sorted
2.27-2.15 Mg/m³	23% - 30%	Variable oil content, poorly sorted and silty sands
2.40-2.24 Mg/m³	15% - 25%	Oil-poor and oil-free silty sands, silts and silty clays

Figure 13: Bulk densities and porosity determinations on McMurray Formation oil sands (Dusseault, 1980)

Though the information above was included to discuss the range of porosities and the discrepancies regarding findings from the McMurray formation, it should be underlined that it is not the intention of this thesis to find a realistic value of the porosity in the McMurray formation. Instead, the main aim is to examine how variation in porosities will affect the recovery factor and the cumulative oil produced when SAGD is applied to a reservoir with reservoir data corresponding to that of the Athabasca field. The simulated cases chosen to explore the effect of variation in porosity are displayed in Table 12.

Table 12: Simulated cases for Variation in Porosity

Simulation no.	Porosity (%)
Base case	38
30	15
31	20
32	25
33	30
34	40

Injection rate

The following cases were selected in order to investigate the effect of injection flow rate:

Table 13: Simulated cases for Injection Rate variation

Simulation no.	Injection rate (STB/d)
Base case	200
35	150
36	220

In addition, higher injection rates than listed in Table 13 were tested for. However, convergence was not achieved even though the time step size was altered.

Preheating period

As mentioned earlier an effective preheating period is essential to achieve a successful SAGD operation. The base case shows that contact between the two wells is achieved after 100 days. However, as preheating period may be costly (due to production loss), it was interesting to observe the effect on recovery when halving the preheating period in the base case. In addition, it was of interest to observe if a significant increase in oil rate or recovery factor will occur when doubling the preheating period compared to the base case.

Table 14: Simulated cases for different preheating periods

Simulation no.	Preheating period (days)
Base case	**100**
37	**50**
38	**200**

6 Results

6.1 Viscosity

Figure 14 shows the resulting recovery factors (RF) obtained when varying the viscosity. The viscosity data obtained from sample no. 1 result in the lowest recovery, whereas the viscosity data obtained from sample no. 3 has the highest recovery. The general increase in recovery is consistent and limited discrepancies in RF can be observed between the cases. The maximum difference in RF between the two mentioned cases occurs in 2013 and is only 2 %. At the end of production the difference between the two is 0.5 %. The approximate RF at end of production for all cases is approximately 75 %.

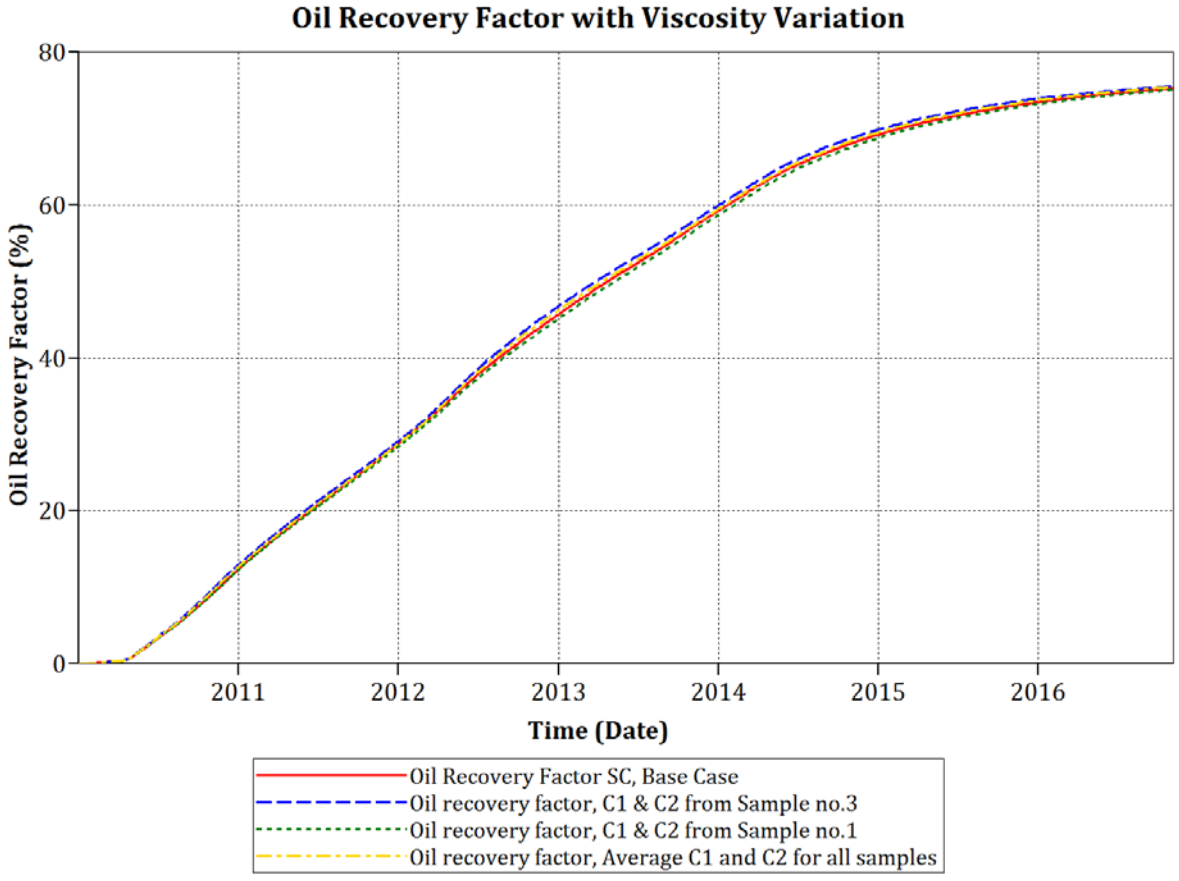

Figure 14: Oil Recovery factor with viscosity variation

Limited discrepancies are also observed when examining cumulative steam oil ratio (CSOR) with viscosity variation (Figure 15). Here it is observed that viscosity data obtained from sample no.1 holds the highest CSOR throughout production, whereas the viscosity data obtained from sample no.3 holds the lowest CSOR. The largest discrepancies between the various tested scenarios can be observed in 2013 where 0.2 bbl/bbl is the difference between the two cases. Yet, at end of production all cases possess approximately the same CSOR of 6.8 bbl/bbl.

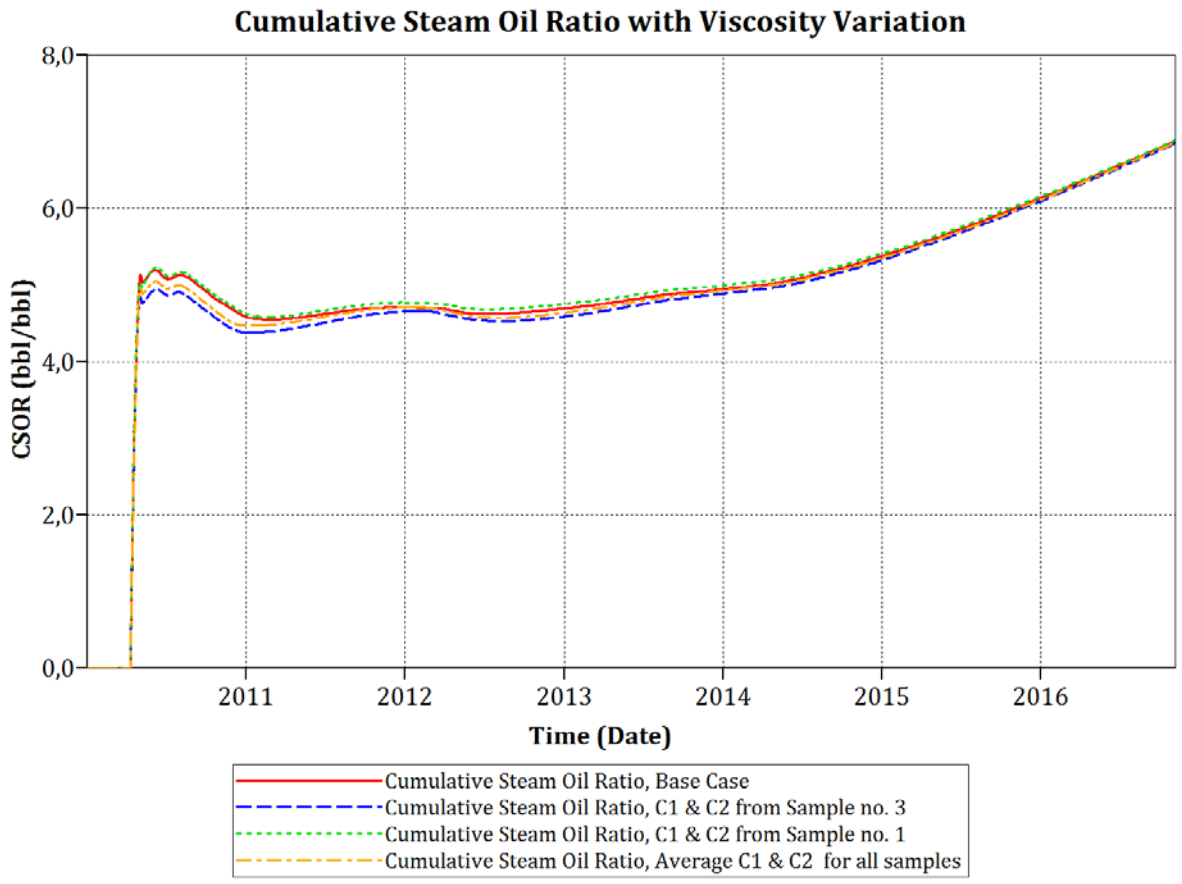

Figure 15: Cumulative steam oil ratio with viscosity variation

Figure 16 shows the oil rate with respect to viscosity variation. The viscosity data obtained from sample no. 3 seemingly has the highest rate until 2013. After 2014 all rates follow the same decline. In this time period the viscosity data obtained from sample no.3 has the lowest rate. Sample no.1 seemingly has the lowest rate until 2013 and thereafter proceeds to possess the highest rate amongst the tested cases.

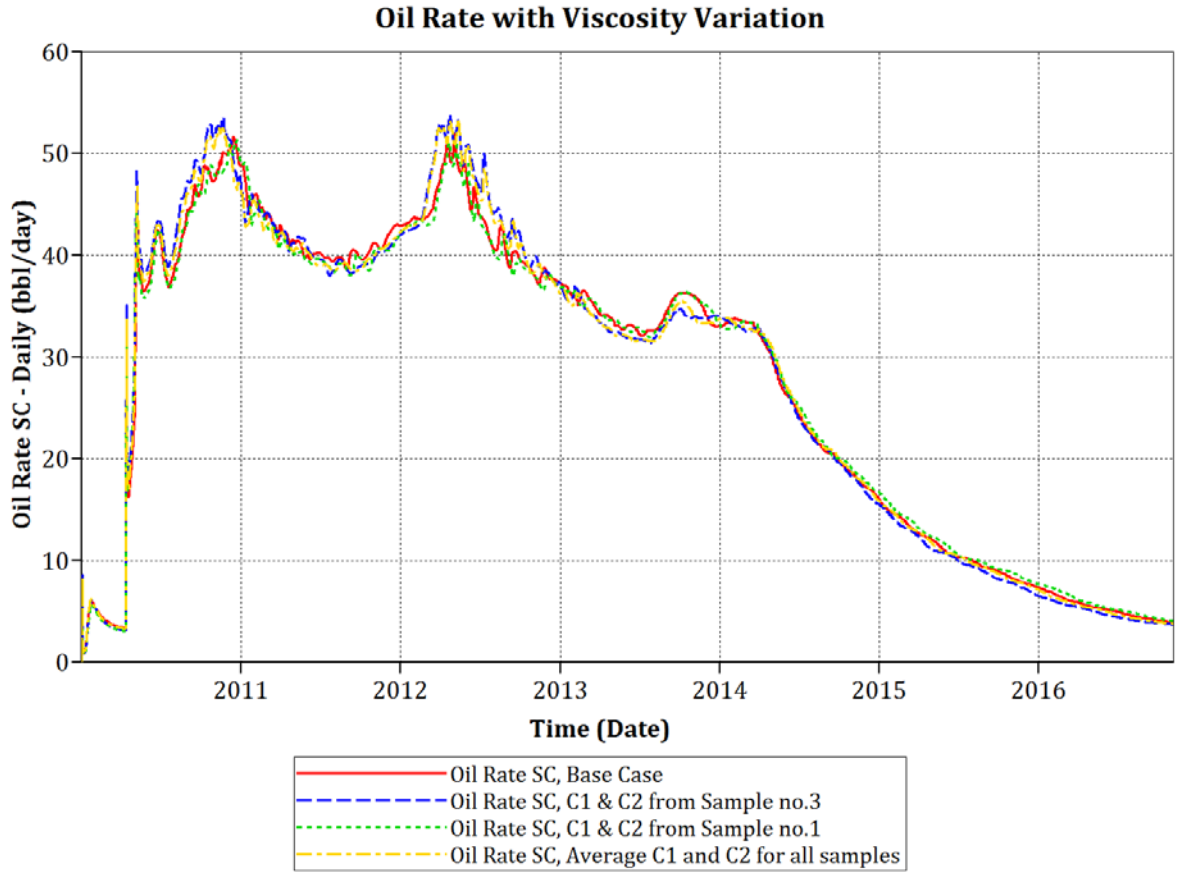

Figure 16: Oil rate with respect to viscosity variation.

6.2 Grid refinement

Figure 17 depicts the recovery factors with respect to grid refinement in the *j*-direction. The results displayed in addition to the base case are the scenarios that created the largest discrepancies. The results of the remaining cases lie in between these curves. Due to clarity all results have not been included here but can be found in Figure 45, Appendix B.1. At the end of year 2016 both *j=2* and *j=6* achieves an RF of 78% whereas the base case achieves a recovery factor of 75%.

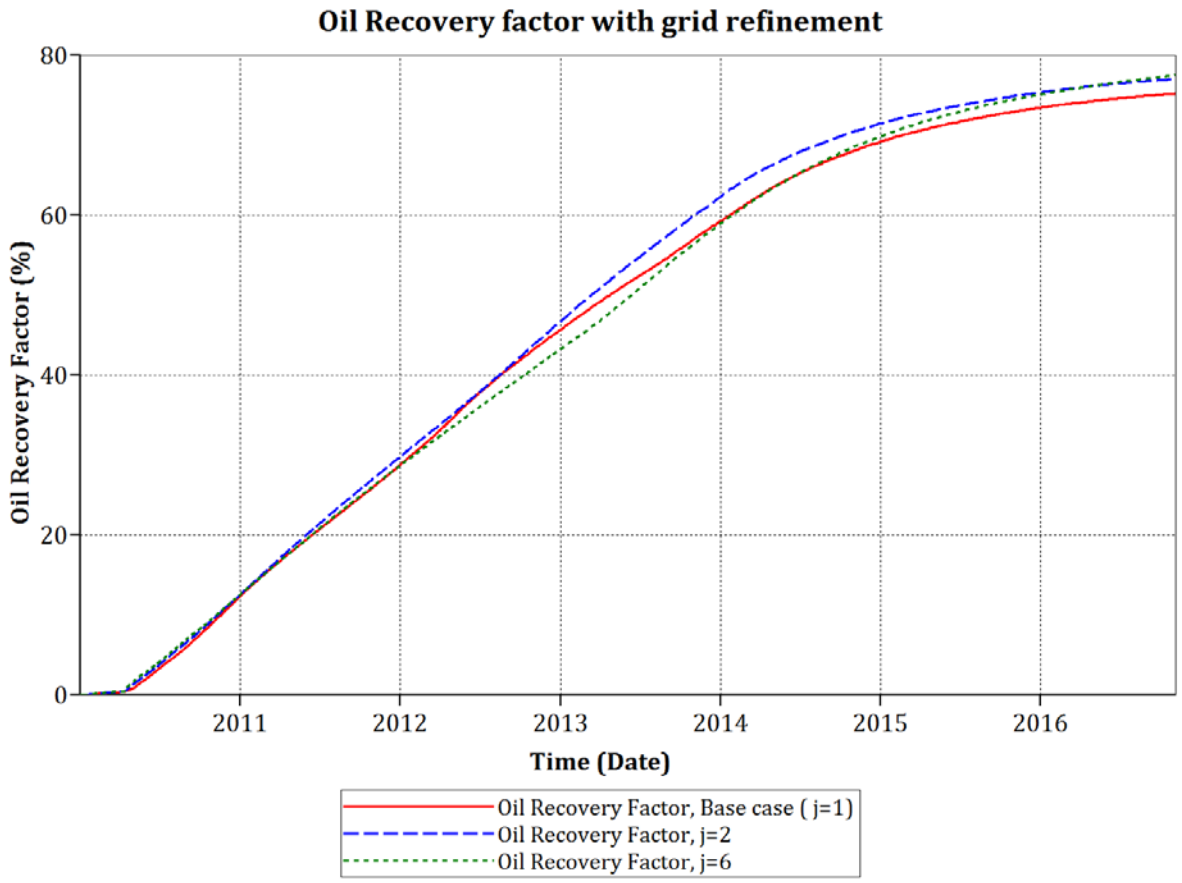

Figure 17: Recovery factor with respect to grid refinement

Figure 18 displays the resulting CSOR with grid refinement. A summary graph displaying all tested scenarios may be obtained from Figure 46, Appendix B.1. It is difficult to define the general trend as the curves seem to overlap each other. However, it may be deduced that *j=2* in general possess the lowest CSOR compared to that of the other cases, whereas the base case *(j=1)* seem to possess the highest CSOR. The end CSOR for the base case is approximately 7 bbl/bbl whereas *j=2 and j=1* yields an end CSOR of approximately 6.7 bbl/bbl.

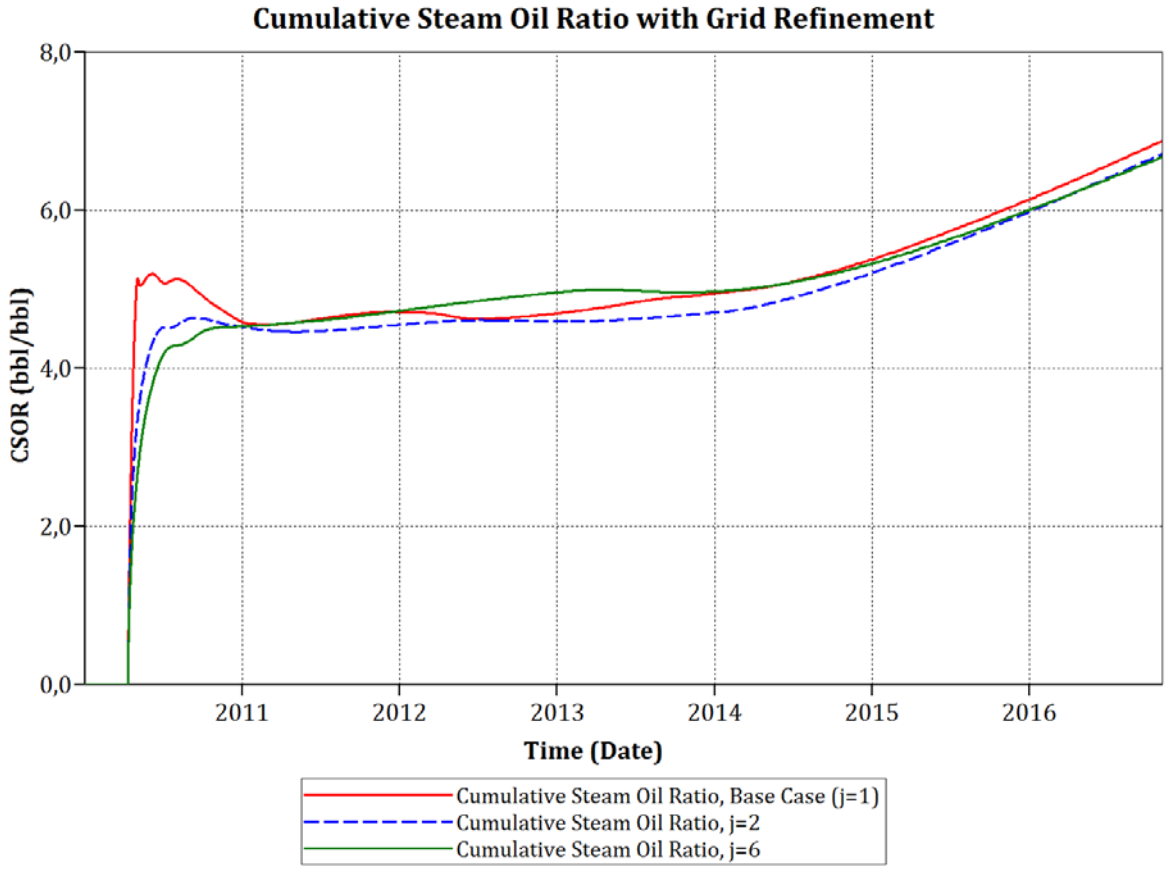

Figure 18: Cumulative steam oil ratio with grid refinement

Figure 19 shows the different oil rates that occur as a result of grid refinement. For clarity, only a selection of the results are depicted here, a summary plot with all simulated cases displaying oil rate with respect to grid refinement can be found in Figure 47, Appendix B.1. As mentioned previously, the oil rate is first monitored by the bottom hole pressure and thereafter limited by total liquid production rate. Despite the fact that the oil rates of the tested cases are not exactly similar, the same number of peaks occurs in the lifetime of the well. Thus one may deduce that in general, they possess the same trend as the base case. From the start of 2014 and onwards to the end of life of the well, all cases follow the same rate of decline.

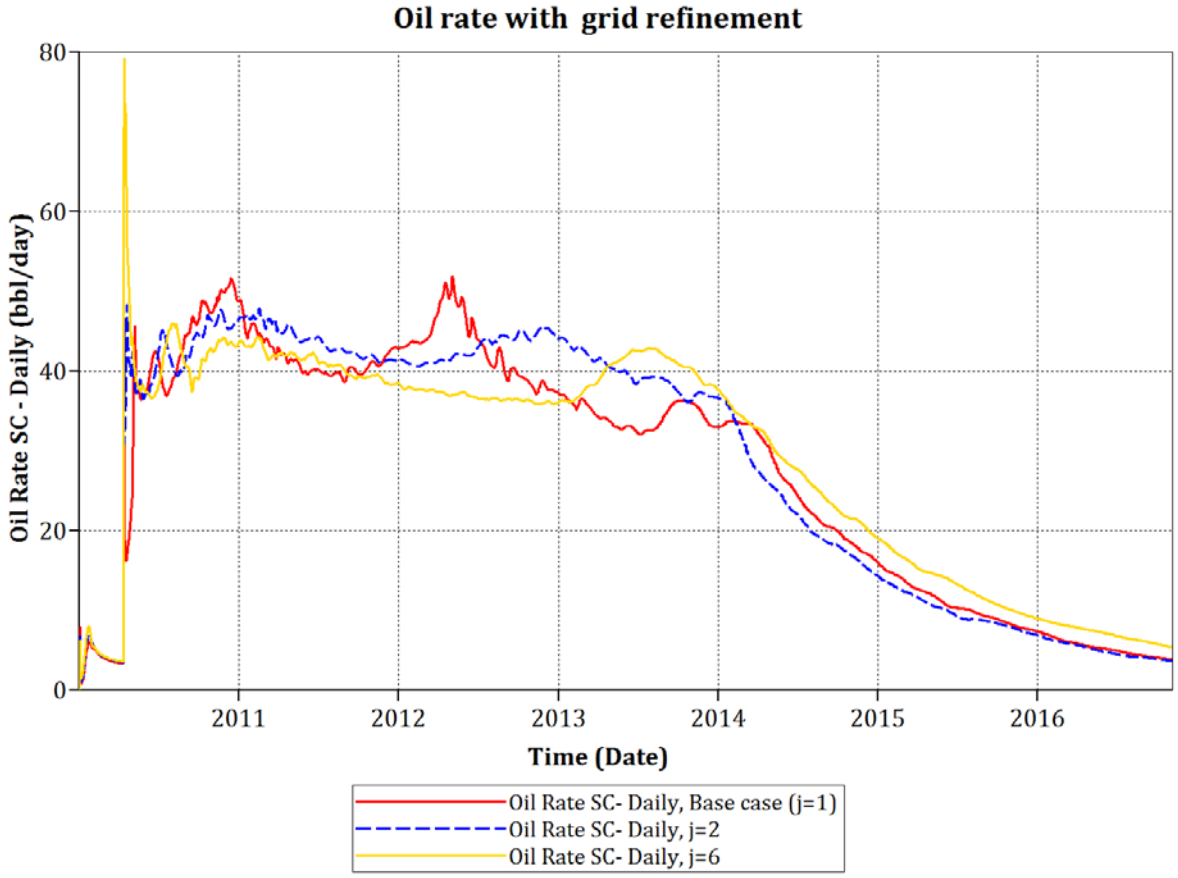

Figure 19: Oil rate with grid refinement

6.3 Variation in horizontal permeability

Figure 20 depicts the recovery factors obtained when the horizontal permeability is altered. For clarification all the results are not included here, RF of the other simulated cases has been included in Figure 48, Appendix B.2. The results indicate that oil recovery increases significantly with increased permeability. However, this increase is only consistent until a horizontal permeability of 7000 mD (base case) is reached. *Exceeding* this horizontal permeability creates a rather limited increase in oil recovery, and the curves seem to overlap each other. At end of simulation (year 2016) the difference in RF between the lowest tested case (k_h=1750) and the highest tested case (k_h=7000 mD) is 19 %. Yet, the difference in end RF between base case (k_h=7000 mD) and highest tested case (k_h=9000 mD) is only 1%.

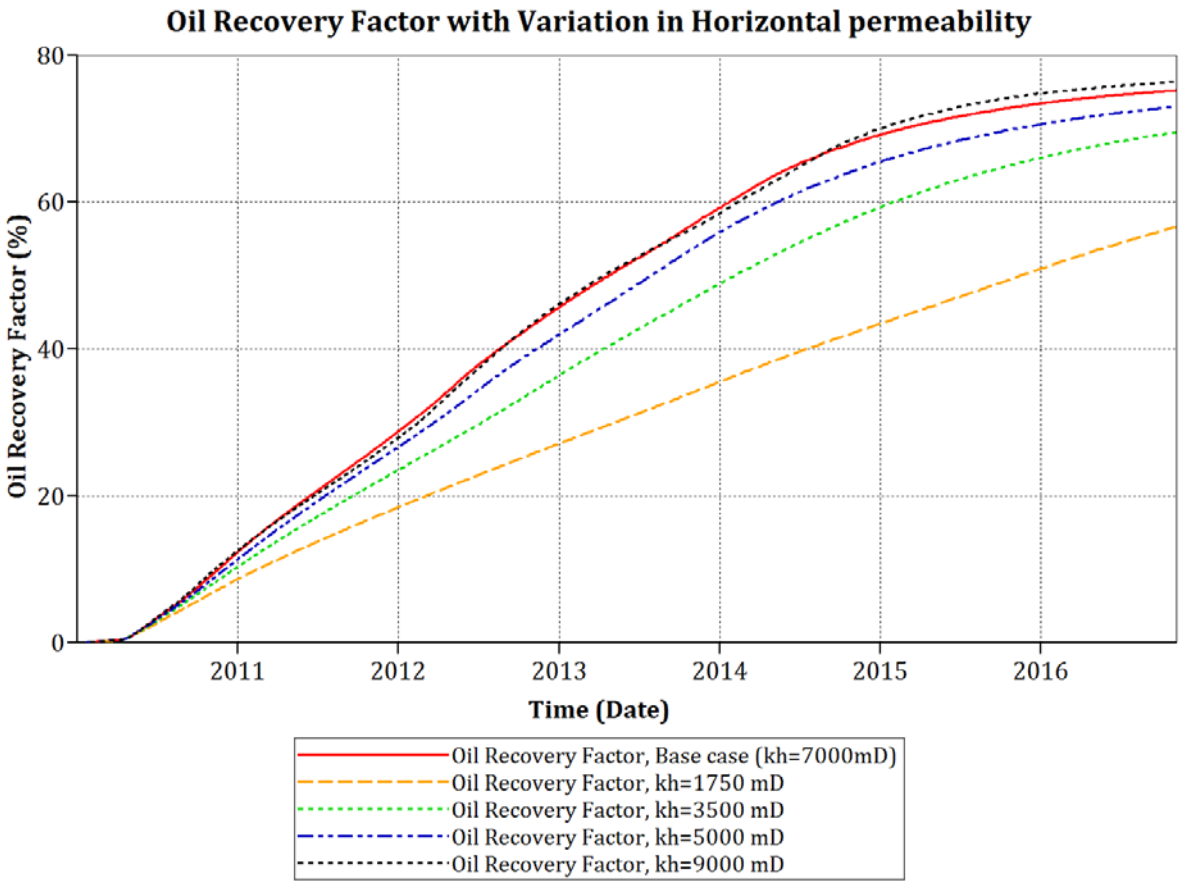

Figure 20: Oil recovery factor with variation in horizontal permeability

Figure 21 depicts CSOR with variation in horizontal permeability. A comparison of all the simulated cases can be obtained from Figure 49, Appendix B.2. The results in general indicate that the CSOR *decreases* with *increasing* horizontal permeability. However, after the tested horizontal permeability reaches base case (k_h=7000 mD) the CSOR is rather similar to all proceeding cases where the horizontal permeability is increased further. The difference in CSOR between the highest tested case (k_h=9000 mD) and the lowest tested case (k_h=1750 mD) is 2.3 bbl/bbl. Yet, the difference in CSOR between the highest tested case (k_h=9000 mD) and the base case (k_h=7000 mD) at the end of simulation (2016) is only 0.06 bbl/bbl.

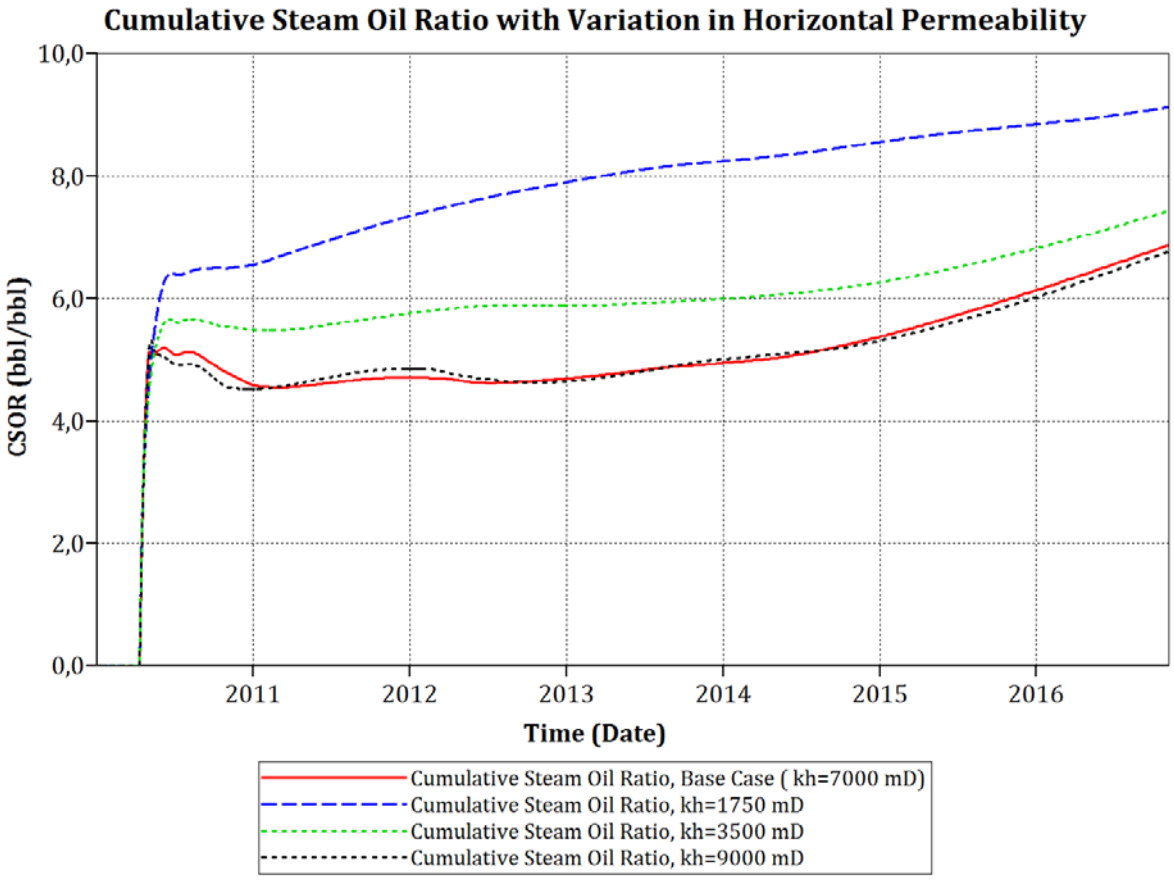

Figure 21: Cumulative steam oil ratio with variation in horizontal permeability

Figure 22 shows the results from the oil rate analysis with respect to variation in horizontal permeability. For clarification all the results have not been included in this section, oil rates for the other simulated cases may be obtained from Figure 50, Appendix B.2. From Figure 22 it can be seen that in general, the oil rate increases with increased horizontal permeability. As it was seen for both the oil recovery and the CSOR, increasing the horizontal permeability further than 7000 mD does not yield significant discrepancies in the result. It is also observed that k_h=*1750* has a very stable decline without any peak production.

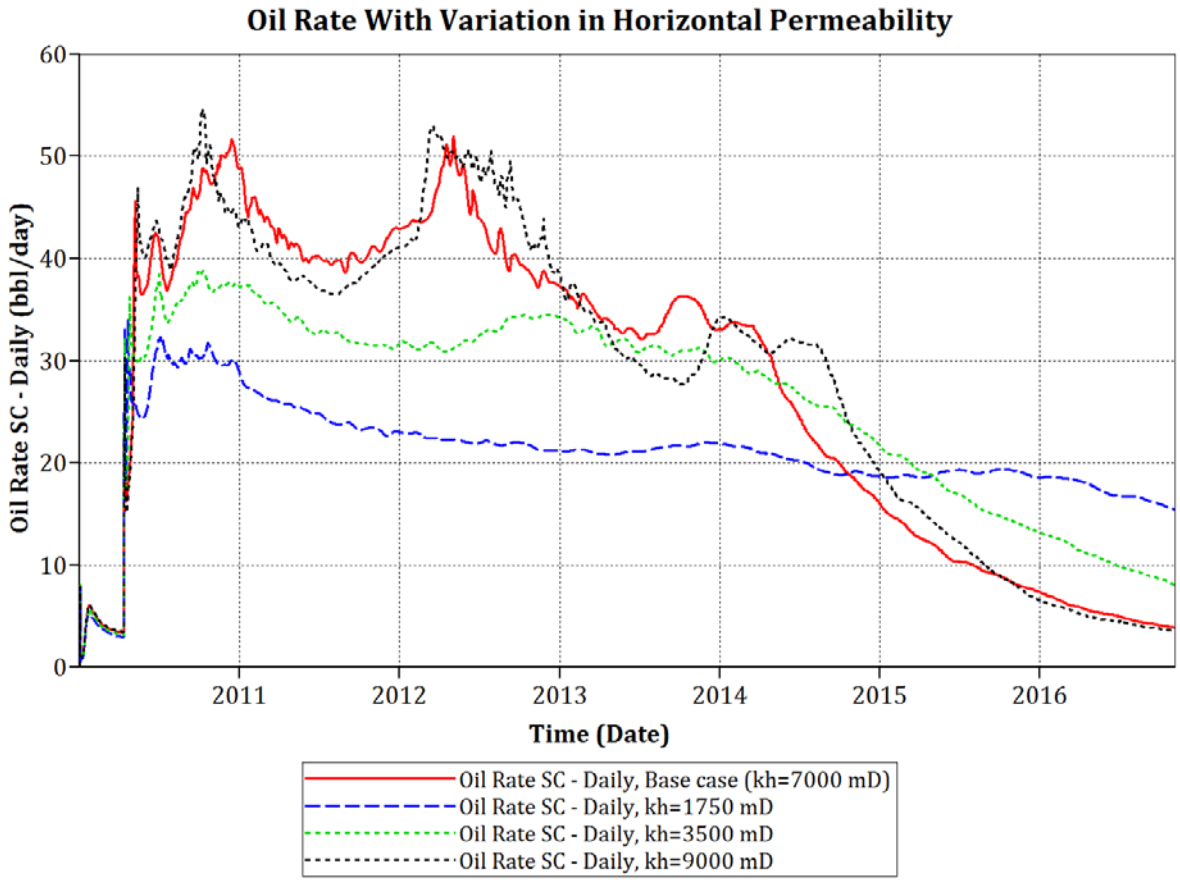

Figure 22: Oil rate with variation in horizontal permeability

6.4 Variation in vertical permeability

Figure 23 depicts the recovery factors obtained with different vertical permeabilties. A general observation is that the oil recovery increases with increasing vertical permeability. However as can be observed from Figure 23, larger discrepancies exist for vertical permeabilities below the base case, whereas increasing the vertical permeability further beyond the base case (k_v=2100 mD) yields similar recoveries. For the case of k_v=*3000 mD* and k_v=*3300 mD*, the resulting recovery factors are the same. At end of production (year 2016) the difference in RF between the highest tested case (k_v=3300 mD) and the lowest tested case (k_v=525 mD) is 20 % whereas the difference between the highest tested case (k_v=3300 mD) and the base case (k_v=2100 mD) is 2.7%.

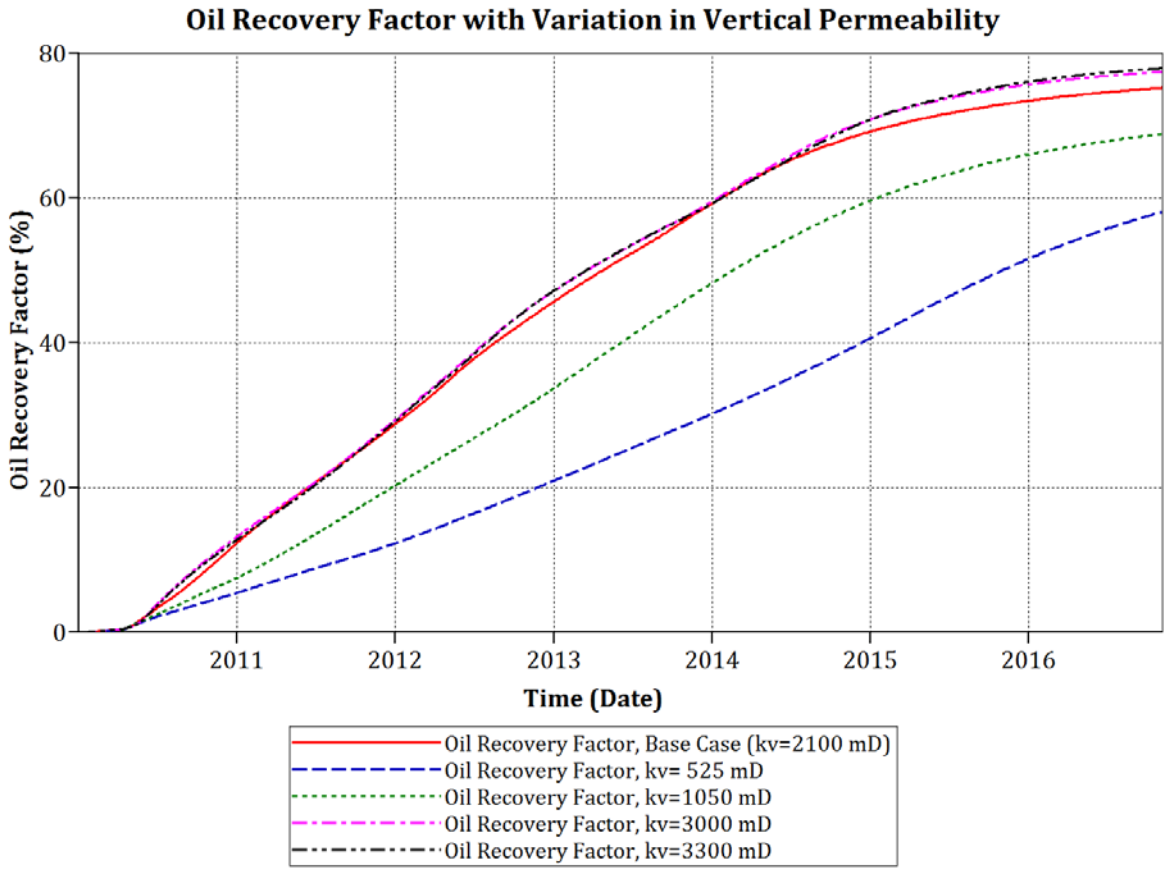

Figure 23: Oil recovery factor with variation in vertical permeability

Figure 24 depicts CSOR with variation in vertical permeability. The general observation from the graph is that the CSOR decreases with increasing vertical permeability. Yet, the differences in CSOR between the various cases decrease towards end of production. It is also observed that increasing the vertical permeability above the base case (k_v=2100 mD) yields limited differences in CSOR. Yet, a peak, higher compared to the base case (k_v=2100 mD) may be observed for k_v=*3000 mD* and k_v=*3300 mD* in mid-2010. The largest difference in CSOR between the highest tested case (k_v=3300) and the lowest tested case (k_v=525mD) occurs in October 2012 and is 4.6 bbl/bbl. Yet, the difference in CSOR at end of simulation time (year 2016) between the highest tested case and the lowest tested case is 2.3 bbl/bbl.

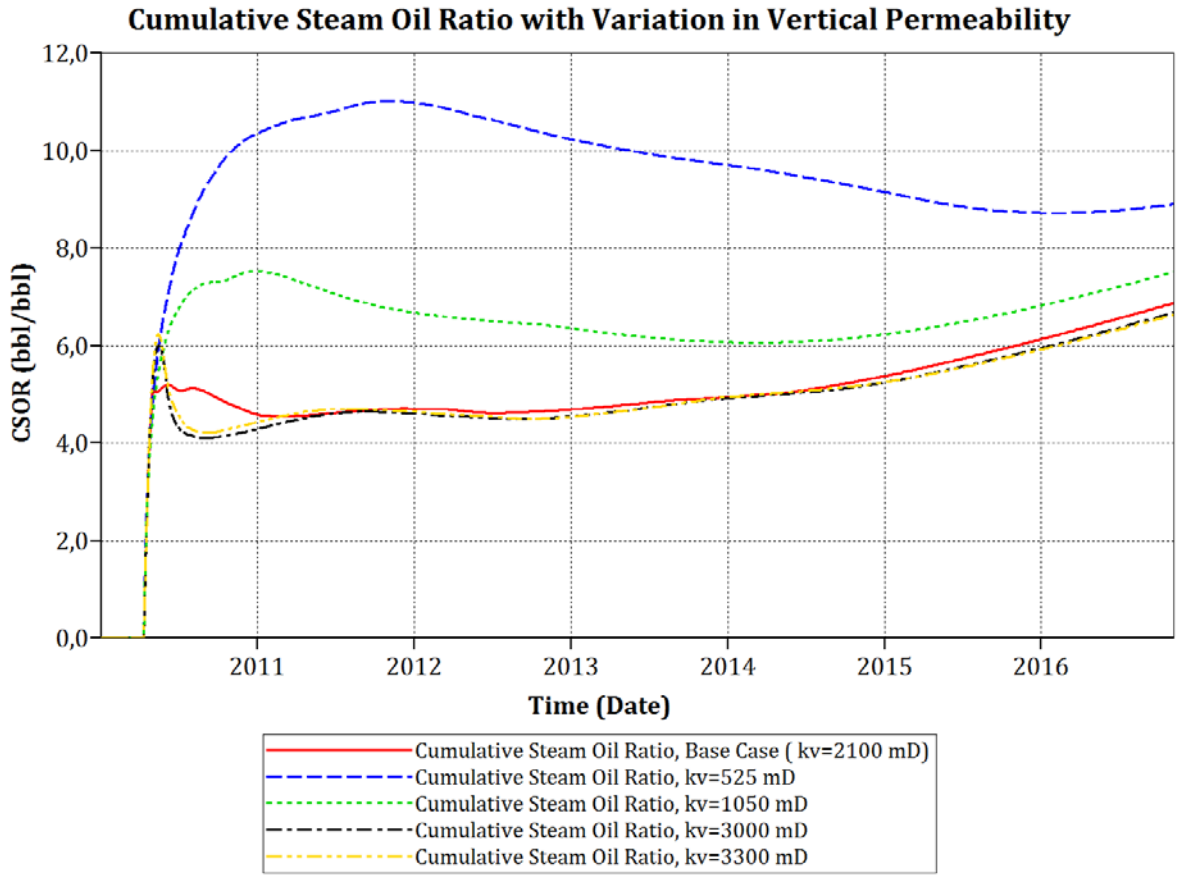

Figure 24: Cumulative steam oil ratio with variation in vertical permeability

Figure 25 depicts the oil rate with vertical permeability variation. Limited consistency may be observed from the graph. At end of production (Year 2016) the lowest tested vertical permeability (k_v=525) possesses the highest rate whereas the *base case (k_v=2100 md), k_v=3000* mD and *k_v=3300 mD* possess the lowest rates. All cases except for the lowest tested case have a consistent decline after end of 2014.

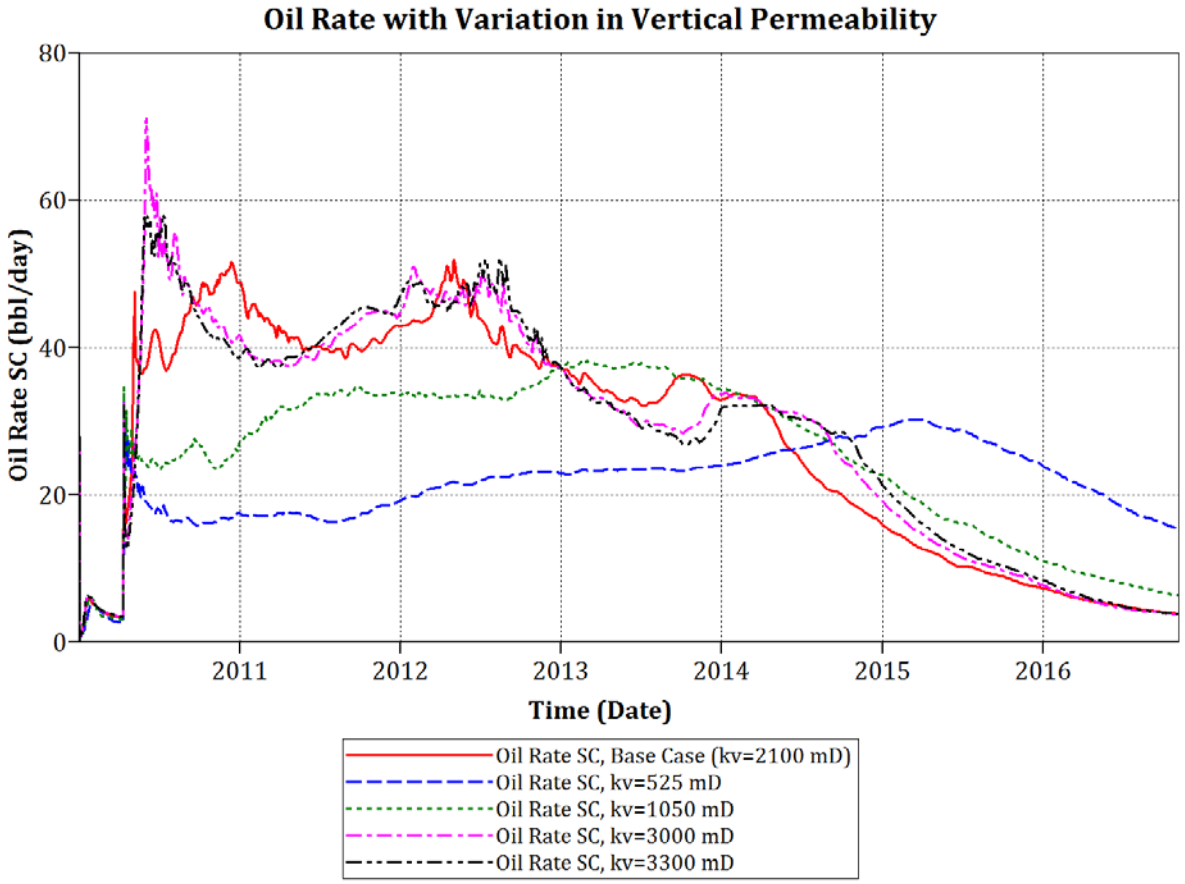

Figure 25: Oil rate with variation in vertical permeability

6.5 Simultaneous variation in k_h & k_v

Figure 26 displays the oil recovery factor with simultaneous variation in horizontal and vertical permeability. In general, the RF increases with increasing k_h & k_v. As also observed when examining the variation in k_h & k_v separately, increasing the permeability over a certain value limits the discrepancies between the simulated cases. The difference between the highest and lowest RF obtained is 42 %, which occurs for the highest (k_h=7800 mD & k_h=2900 mD) and the lowest (k_h=1750 mD & 525 mD) tested cases. However, it should here be noticed that though *k_h=5000 mD & k_v=4000 mD*, has a *lower* RF at ended simulation time compared to that of the highest tested case, it actually possess the highest RF most of the production time in comparison to the other simulated cases.

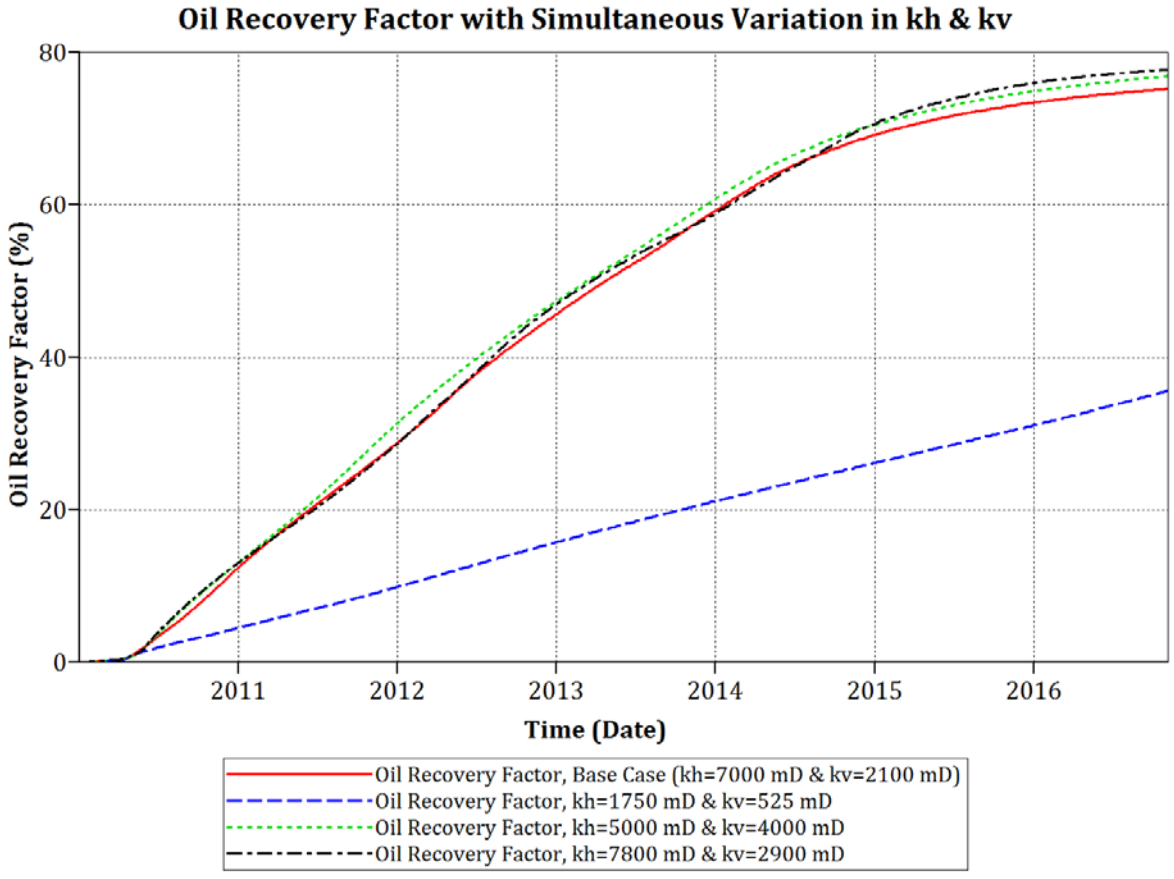

Figure 26: Oil recovery factor with simultaneous variation in k_h & k_v

Figure 27 displays the resulting cumulative steam oil ratio with simultaneous variation in horizontal and vertical permeability. Very low horizontal and vertical permeability (k_h = 1750 mD and k_v = 2100 mD) yield very high CSOR. At end of simulation time (year 2016) the CSOR value is 14.5 bbl/bbl for this case. The other cases got a CSOR value of approximately 6.8 bbl/bbl.

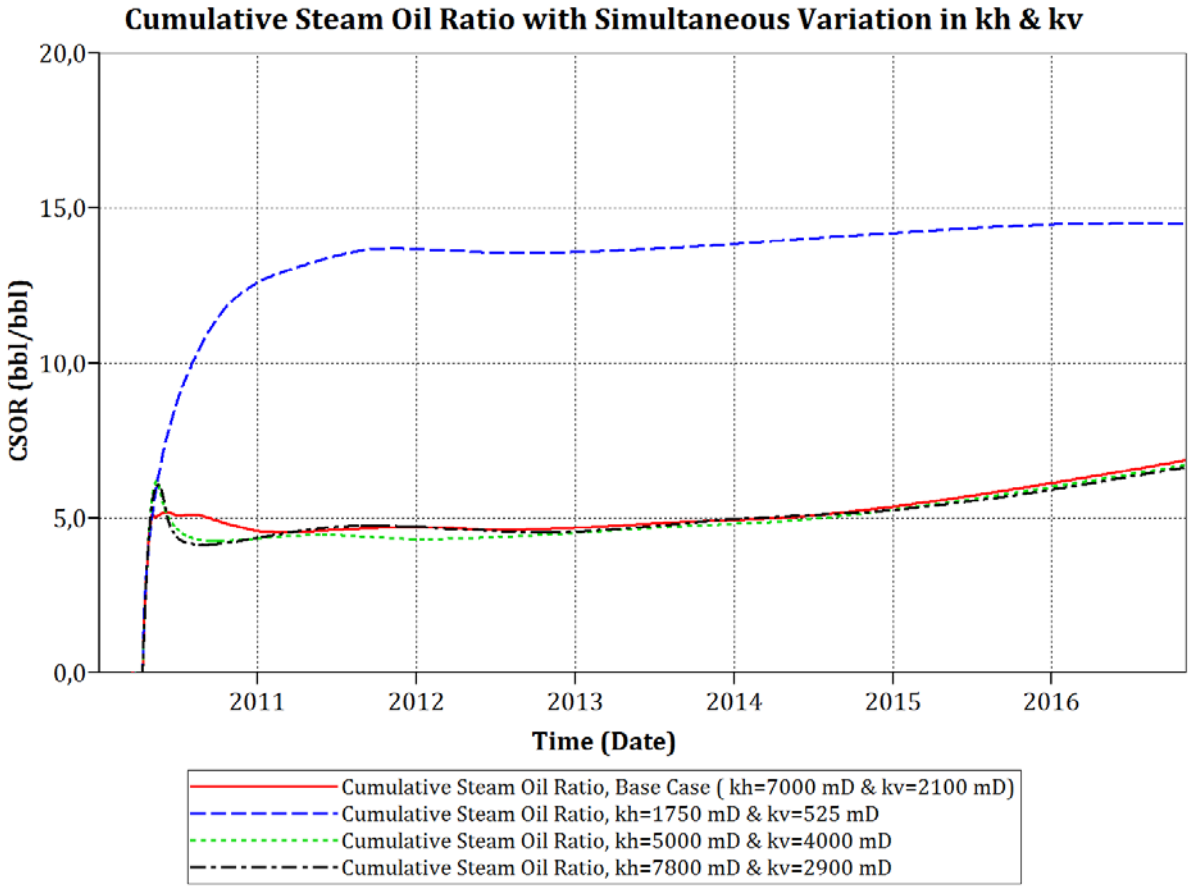

Figure 27: Cumulative steam oil ratio with simultaneous variation in k_h & k_v

Figure 28 displays the oil rate with simultaneous variation in k_h & k_v. At first it seems obvious that the highest test case (k_h=7800 mD & k_v=2900 mD) has the highest rate, though it must be noted that it only have the highest peaks compared to the other cases. The lowest rate is found for the lowest permeability case (k_h=1750 mD and k_v=525 mD). This rate is rather constant and lies around a value of 13 bbl/d.

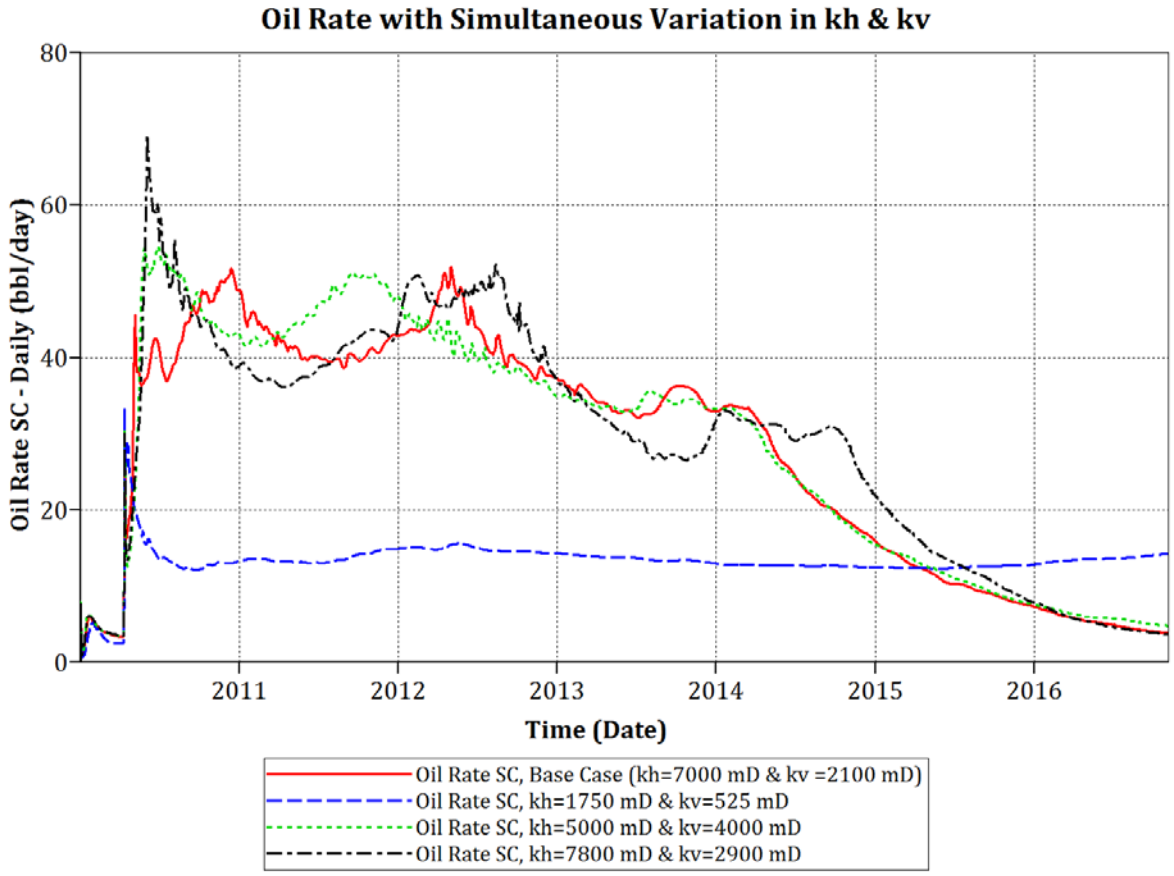

Figure 28: Oil rate with simultaneous variation in k_h & k_v

6.6 Injection well location

Figure 29 depicts a selection of the results when analysing oil recovery with respect to layer of injection. A plot of all the simulated cases can be found in Figure 51, Appendix B.3. In general, the results indicate that placing the injector well in layer 1, 7 and 9 will overlap the trend of the base case (injection in layer 10) and thus approximately the same amount of oil will be produced in these cases. Placing the injection well in layer 12 leads to a slight decrease in cumulative oil produced, during the production period. An equal but more profound trend is seen for injection well placement in layer 13. However, at the end of production RF becomes approximately equal to the base case. Accordingly, all the well placements except injection well in layer 14 yield an approximate end RF of 75 % (year 2016). Placing the injection well in layer 14 leads to a significant decrease in oil recovery and results in an ultimate recovery of 60 %.

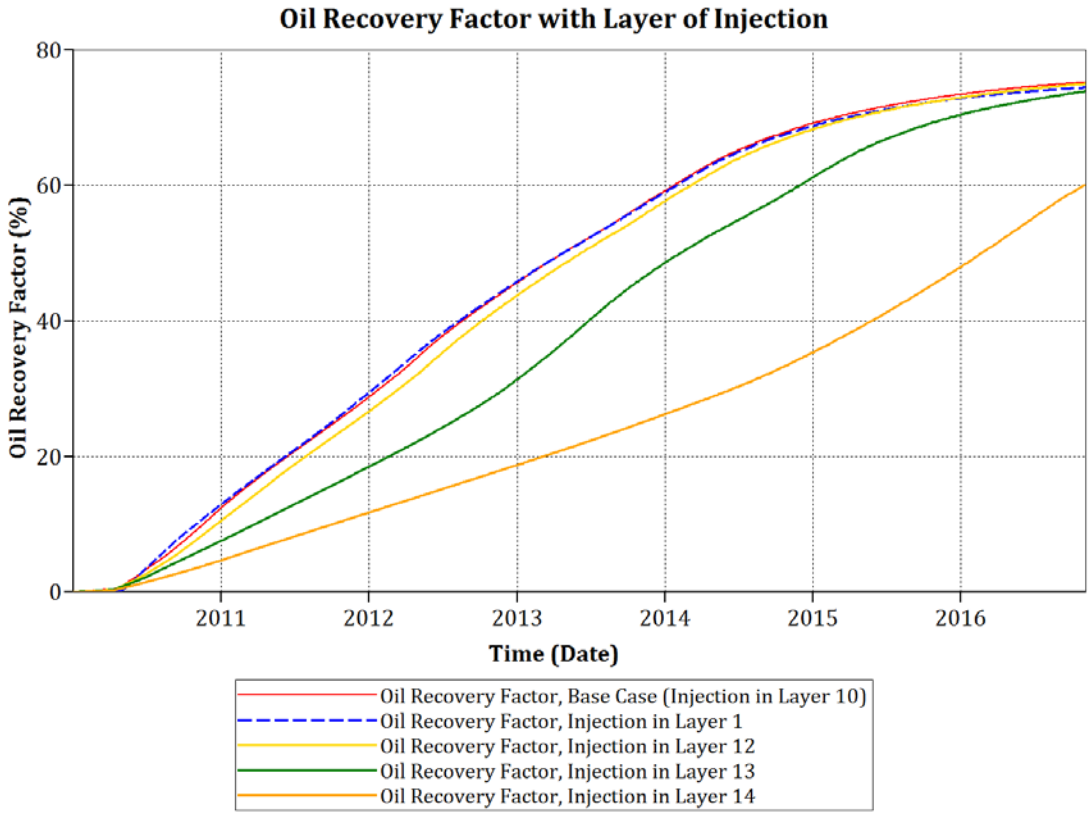

Figure 29: Oil recovery factor with layer of injection

Figure 30 shows the cumulative steam oil ratio with respect to layer of injection. All the simulation results have not been included here due to clarity, however a plot with all the results can be found in Figure 52, Appendix B.3. The general trend indicates that placing the injection well close to the production well yields high CSOR. Placing the injection well in Layer 14 results in an CSOR of 8.5 bbl/bbl at end of production (year 2016). Whereas all other tested cases, despite the variation throughout production, yields an end CSOR of approximately 7 (+/- 0.2) bbl/bbl. It should also be noticed that the peak CSOR that occurs at start of production in the case of placing the injection well in layer 1 is 12 bbl/bbl.

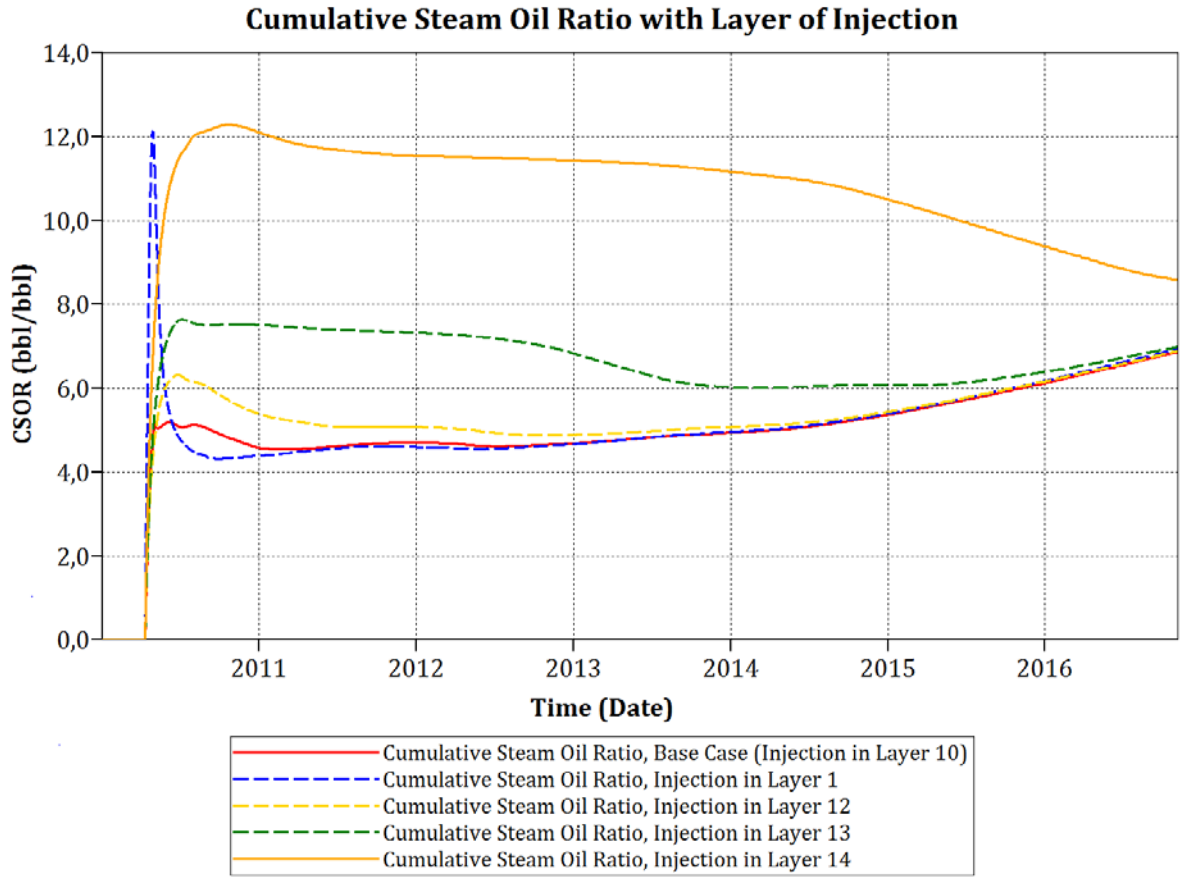

Figure 30: Cumulative steam oil ratio with layer of injection

Figure 31 shows the oil rate for a selection of the results when altering layer of injection. A comprehensive plot with all simulated results can be found in Figure 51, Appendix B.3. Placing the injection well in layer 13 & 14 yields the lowest oil production rates in the start of the production period and the highest towards the end. The other simulated cases follow the same trend but varies to some extent during the first period of production. The cases that achieved higher rates at the start achieve lower rates after 2012.

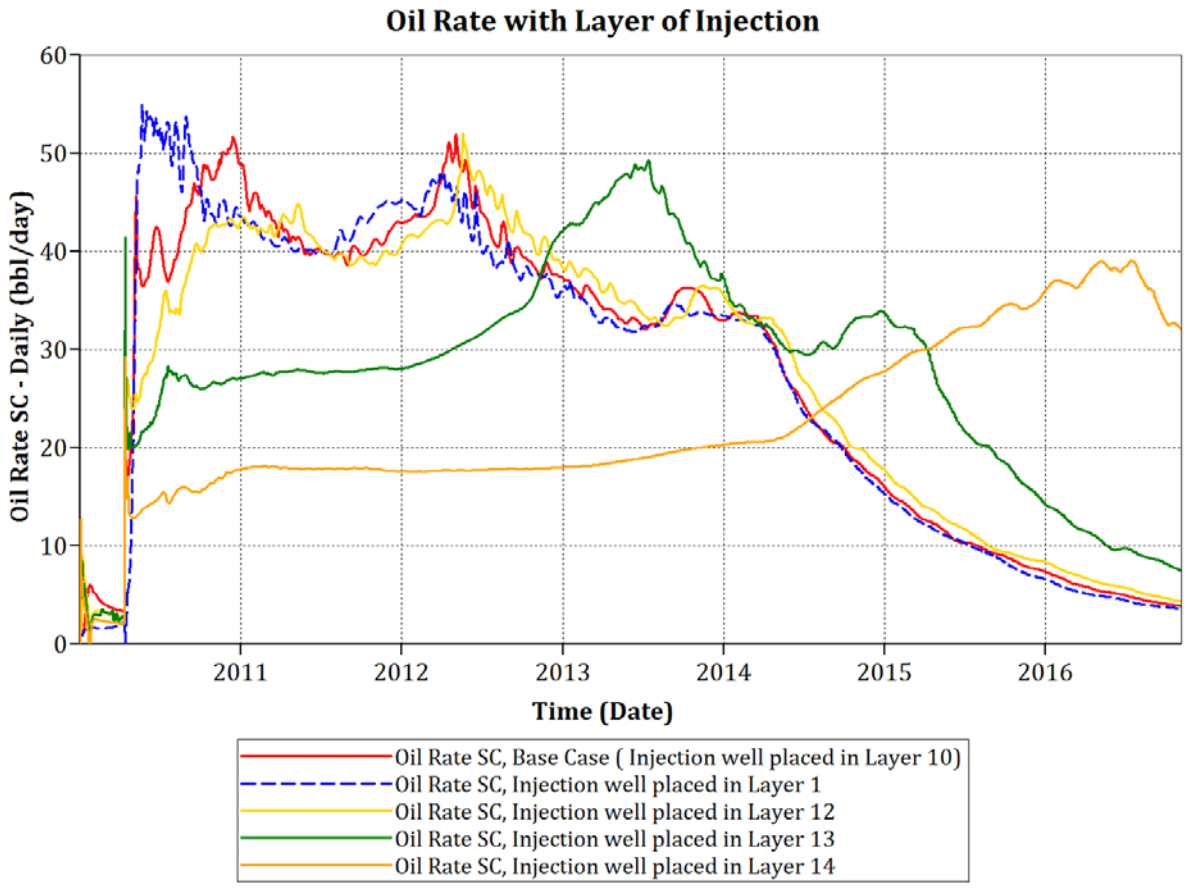

Figure 31: Oil rate with layer of injection

6.7 Porosity variation

Figure 32 displays the results obtained when examining cumulative oil produced with respect to porosity variation. The results show high levels of consistency. An increase in porosity leads to higher cumulative oil production. Subsequently the lowest tested porosity (15%) yields lowest cumulative oil produced i.e. 28314 bbl at end of year 2016, whereas the highest tested porosity (40 %) yields the highest cumulative oil produced i.e. 73154 bbl at end of year 2016.

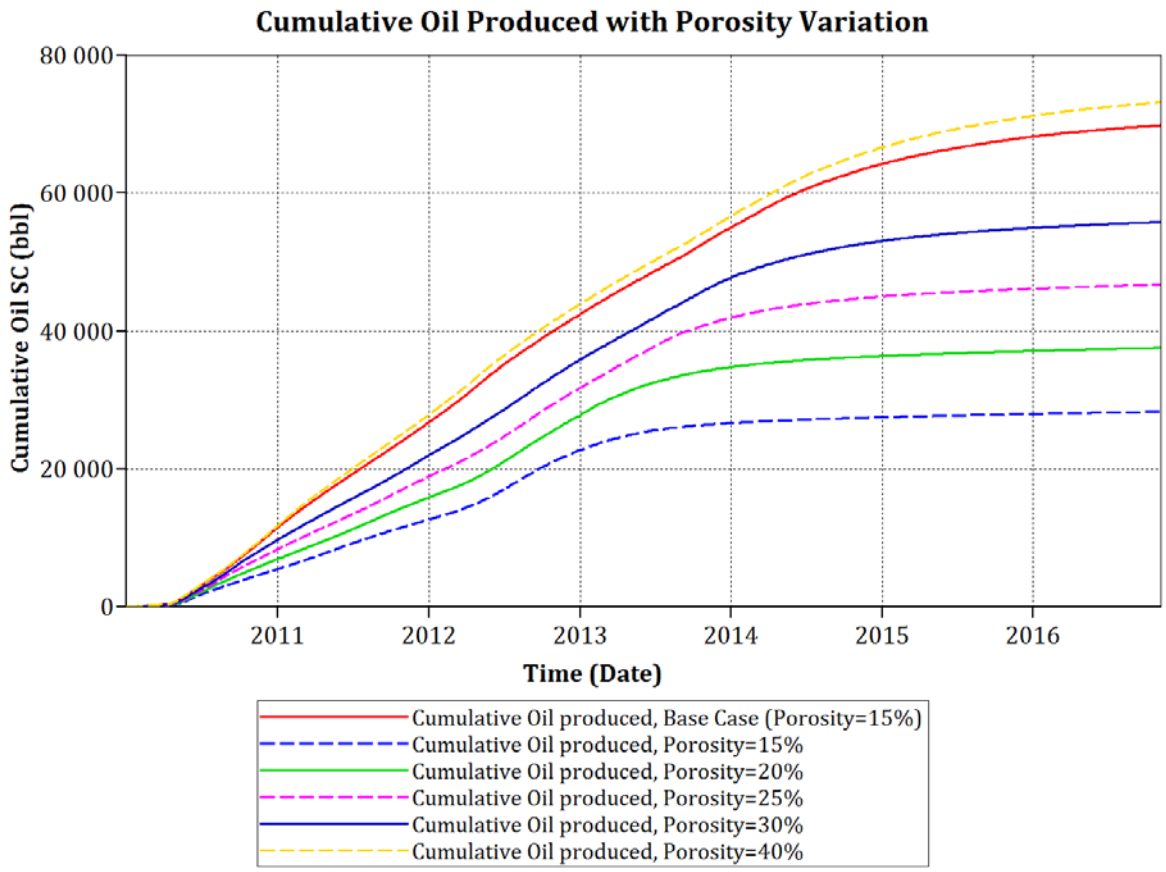

Figure 32: Cumulative oil produced with porosity variation

Figure 33 depicts the oil recovery factor with porosity variation. In general, the case with the highest porosity (40 %) yields the lowest RF and the case with lowest porosity (15%) yields the highest RF during the production period. Yet, the difference in RF between the two cases at the end of the production period is 2.4%. Thus, all tested scenarios lie in between a range of 74.8 % and 77.3 %.

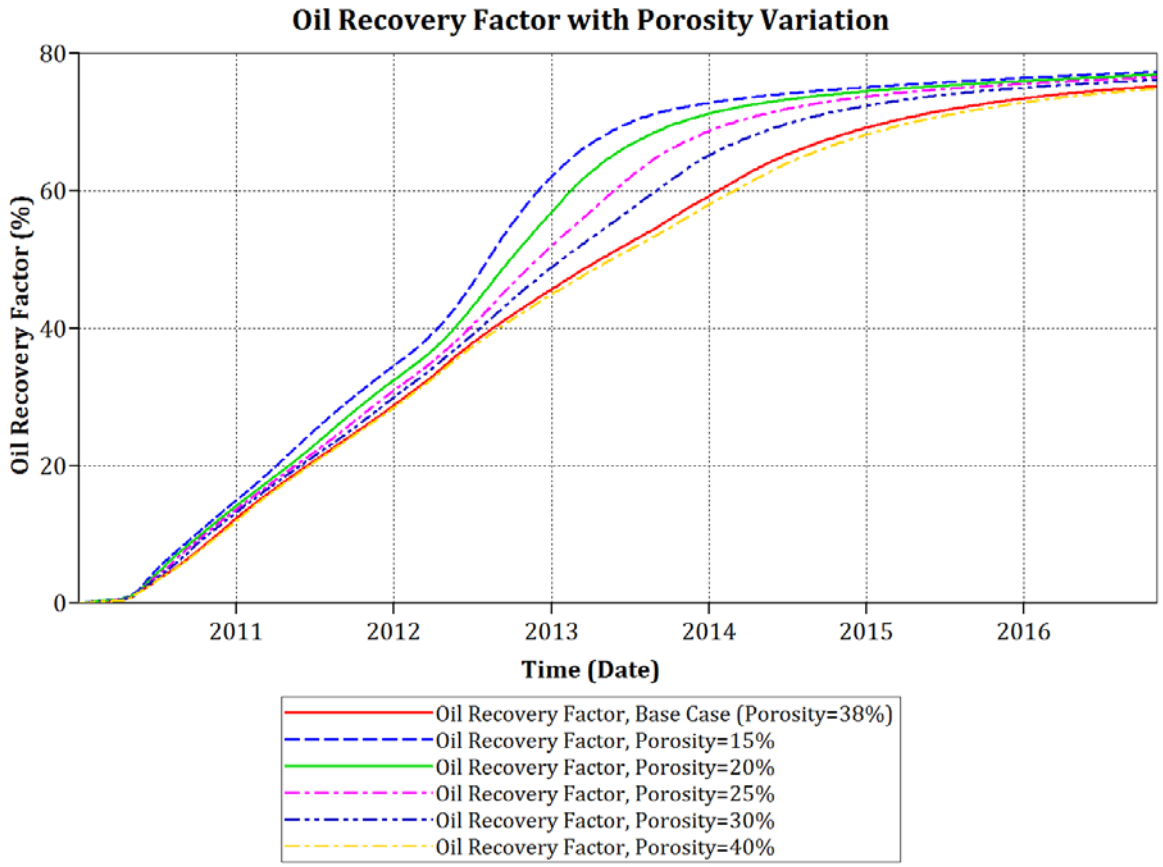

Figure 33: Oil recovery factor with porosity variation

Figure 34 shows the resulting cumulative steam oil ratio when different porosities are applied. The results are consistent as an increase in porosity leads to lower CSOR. Subsequently, the lowest tested porosity (15%) yields the highest CSOR at end of production at 17 bbl/bbl whereas the highest tested porosity (40%) yields the lowest CSOR at end of production at 6.5 bbl/bbl. All other results lie in between those values.

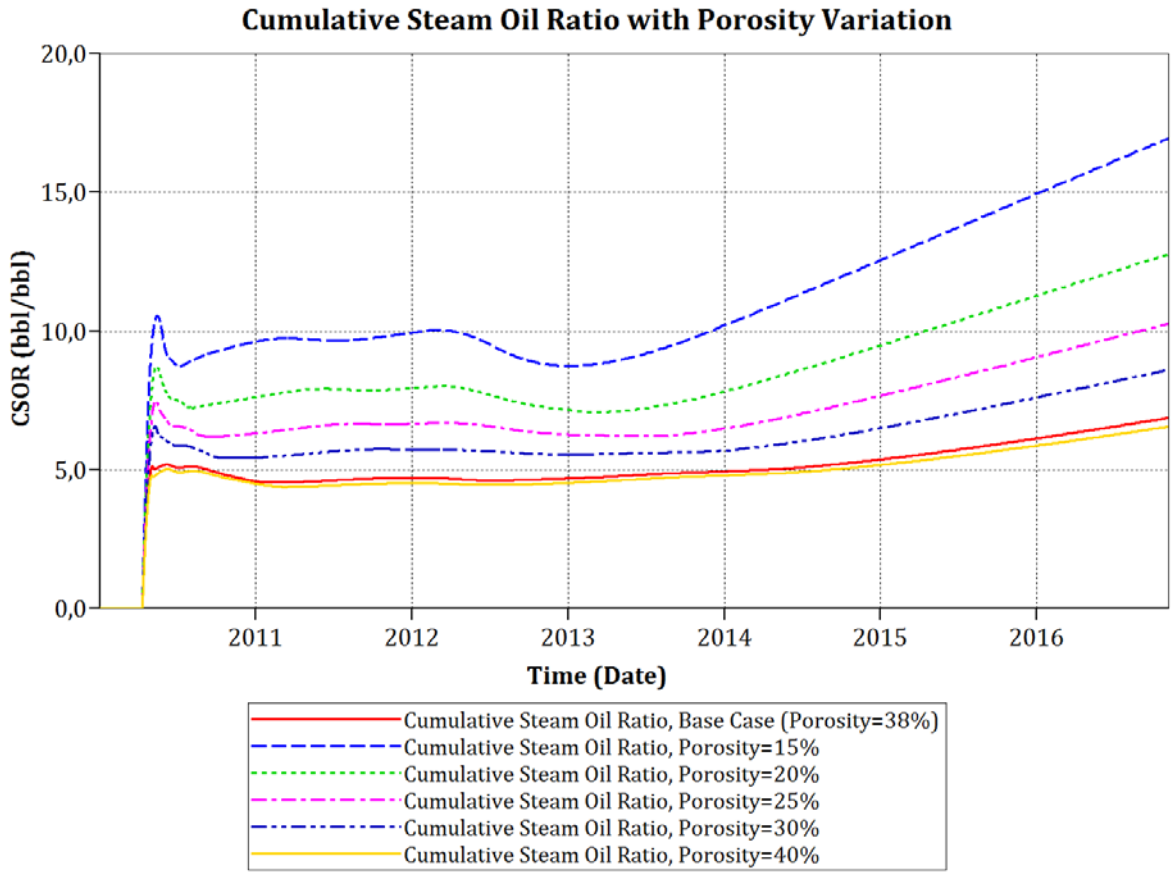

Figure 34: Cumulative steam oil ratio with porosity variation

Figure 35 depicts the resulting oil rates with respect to porosity variation. Only a selection of results has been included in this section to improve the clarity of the results. All results are depicted in Figure 54, Appendix B.4. The results are rather consistent as there is a general trend showing that a higher porosity will yield a higher oil rate. However, due to the different IOIP that occurs as a result of different porosity, it is not of interest to analyse the area under the curves as higher porosity yields higher IOIP and thus more oil will be produced and the oil rate will increase accordingly.

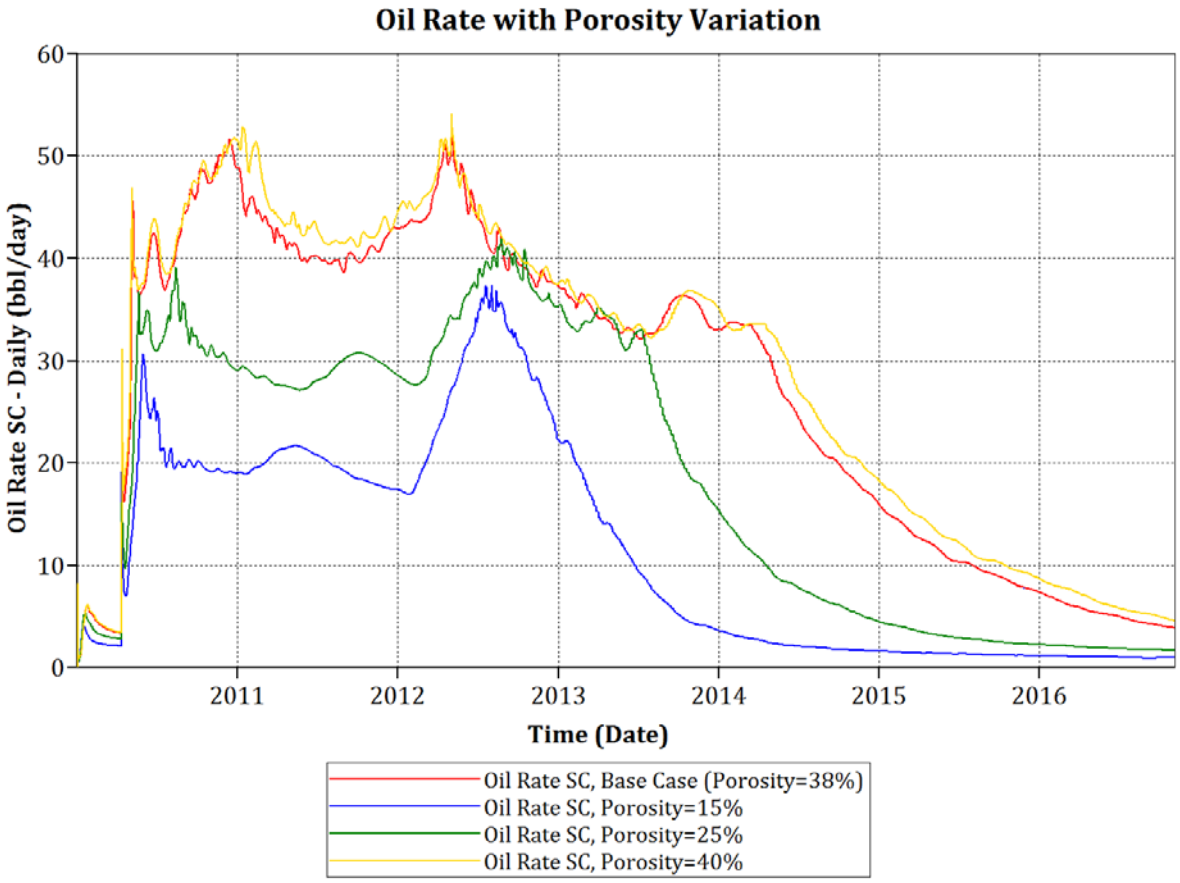

Figure 35: Oil rate with respect to porosity variation

6.8 Injection rate

Figure 36 shows the resulting oil recovery factors obtained when the injection rate was altered. The lower injection rate initially had a lower RF than the other two cases; however the end RF at year 2016 was the same as for the base case, namely 75%. The higher injection rate initially yielded the highest RF, however the end RF for this scenario proved to be 72.5%.

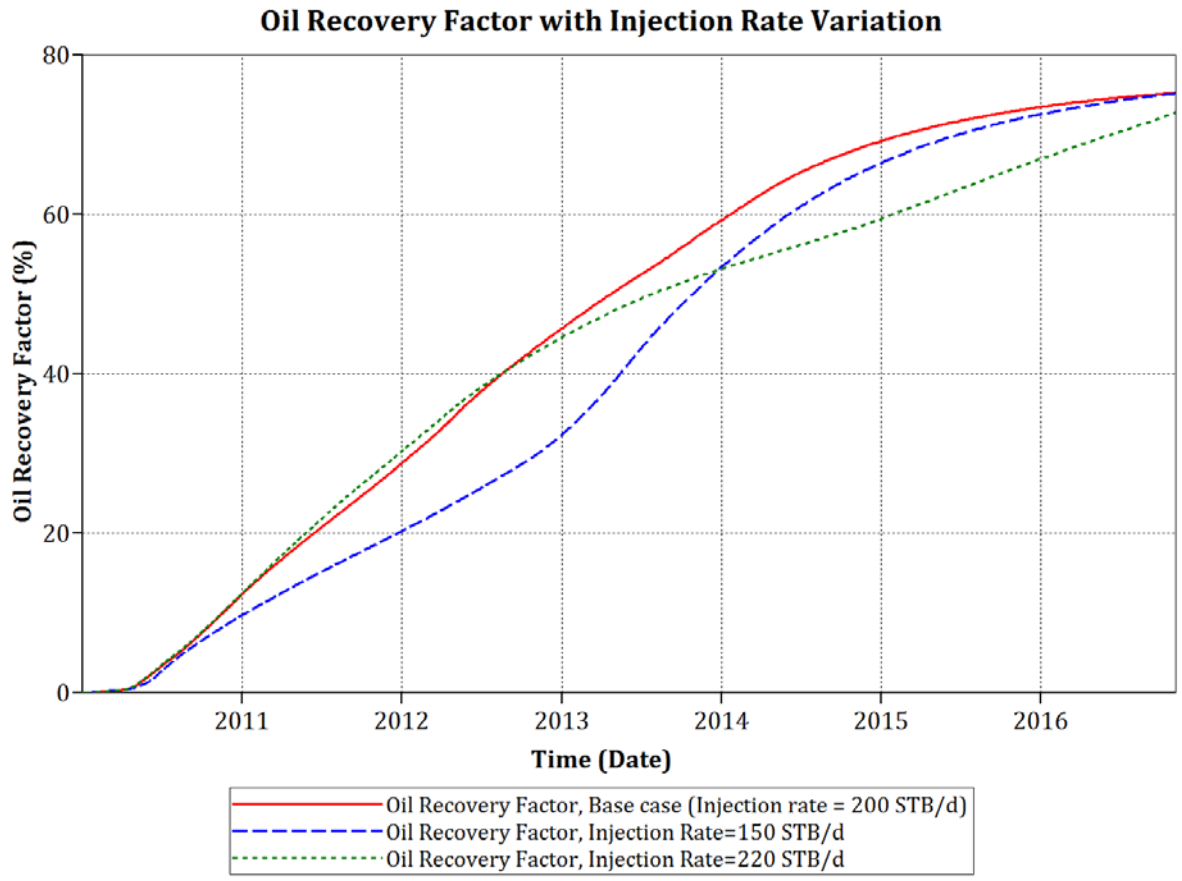

Figure 36: Oil recovery factor with injection rate variation

Figure 37 displays the resulting CSOR obtained when varying the injection rate. For the base case and for an injection rate of 220 STB/d, the general trend is evident throughout production; higher injection rate yields higher CSOR. However, for an injection rate of 150 STB/d the trend is not consistent, it has two periods where it is higher than the two other scenarios; at start of production and from the end of 2011 until mid-2012. However it yields the lowest end CSOR (5 bbl/bbl) compared to those obtained by the base case and the highest tested case which yielded an CSOR of 6.9 bbl/bbl and 7.8 bbl/bbl, respectively.

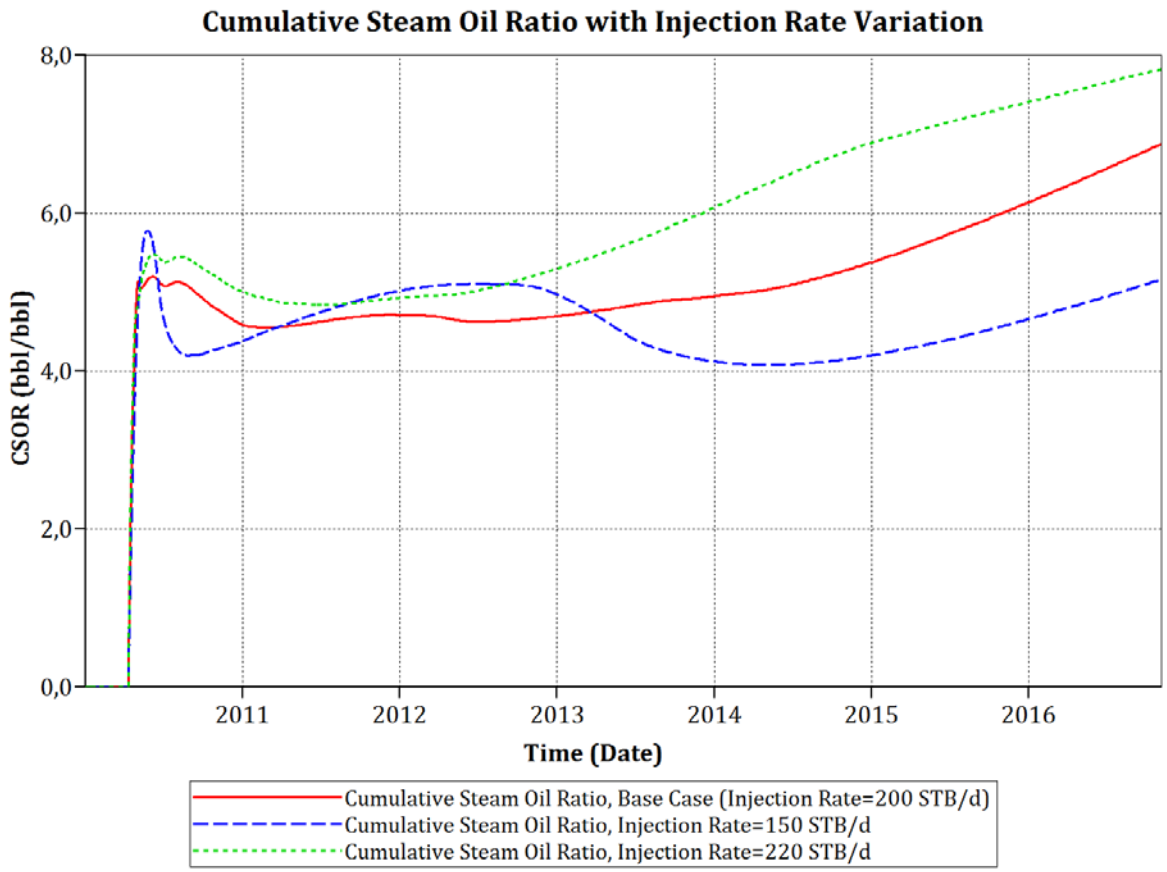

Figure 37: Cumulative steam oil ratio with injection rate variation

Figure 38 displays the resulting oil rates when the injection rate is varied. The highest tested case (injection rate = 220 bbl/d) somewhat follows the trend of the base case. Yet, it should be noticed that the oil rate in this case is lower than the base case from 2012 to the end of 2014. However, the oil rate increases towards end of simulation and possess the highest oil rate at end of year 2016 (18 bbl/d). The lowest tested case, has two periods when it is higher than that of the other cases, namely at start of production and from end 2012 to start of 2015. The highest peak production rate is possessed by the scenario with an injection rate of 150 bbl/d, and occurs in mid-2013 achieving a rate of 66 bbl/d. However, the end rate for this case is 5.7 bbl/d, but still higher than the end rate of the base case which is 3.9 bbl/d.

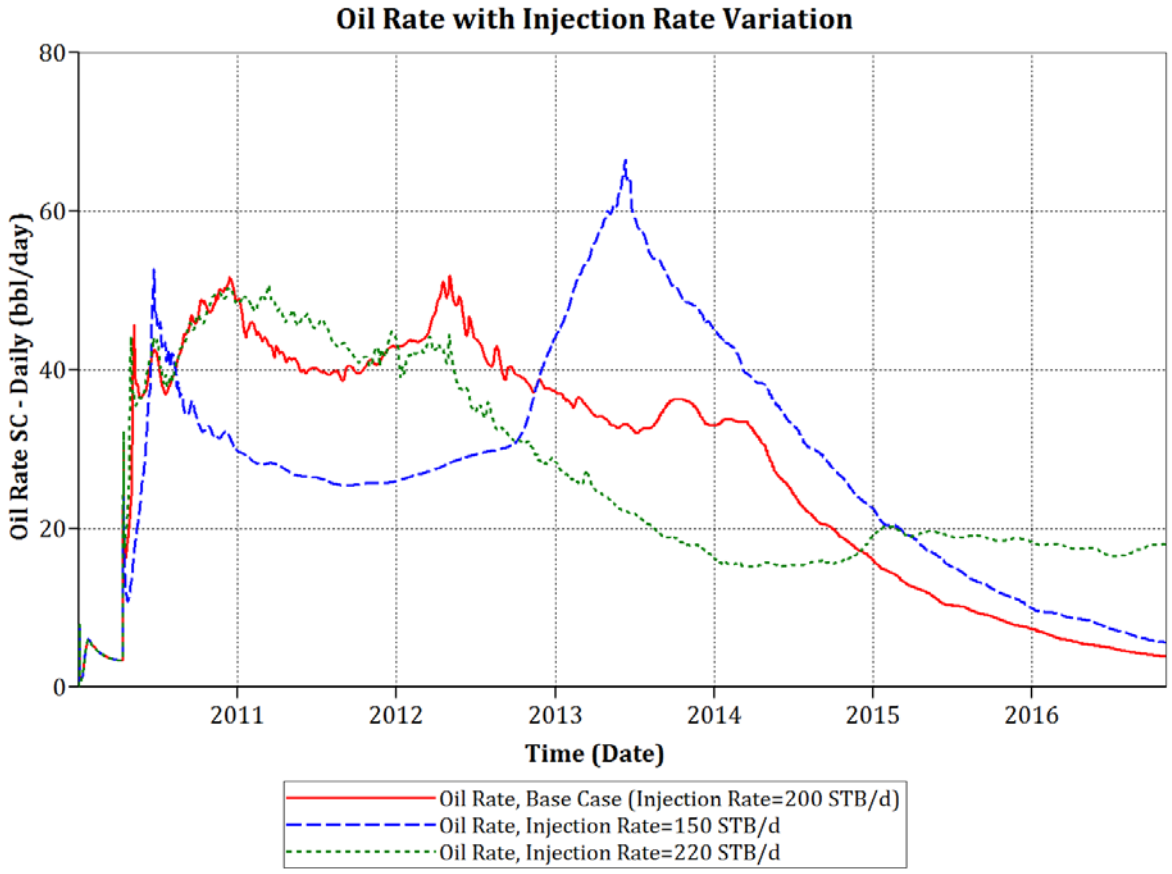

Figure 38: Oil rate with injection rate variation

6.9 Preheating period

Figure 39 shows the oil recovery factors with different preheating periods. It can be observed that all simulated cases have a consistent increase in RF. In general the preheating period of 50 days, yields a higher RF throughout the production period compared to that of the other tested cases. Also, the case simulated with the longest preheating period has a lower RF compared to that of the other cases throughout production. For instance in early 2013, the difference in RF between the highest preheating time (200 days) and the lowest preheating time (50 days) is 5 %. However, the end RF for all cases yields approximately 75%.

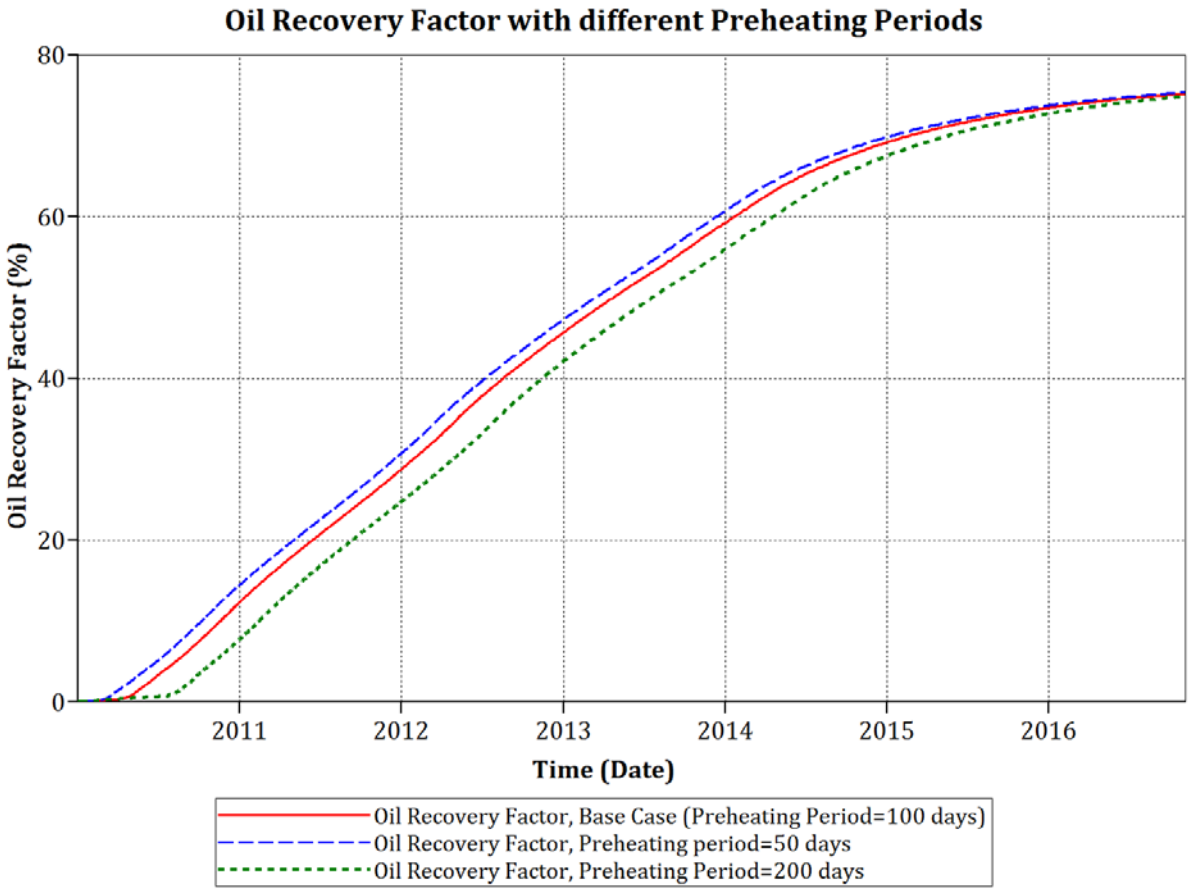

Figure 39: Oil recovery factor with different preheating periods

Figure 40 displays the resulting CSOR for different preheating periods. Both varied scenarios follow the trend of the base case. However, halving the preheating period of the base case increases the CSOR, whereas doubling the preheating time of the base case results in lower CSOR. When examining start of production time the peak CSOR for preheating period of 50 days is 6 bbl/d whereas the peak CSOR for preheating period of 200 days is 4.5 bbl/bbl. The end CSOR yields 7 bbl/bbl and 6.6 bbl/bbl for preheating periods of 50 and 200 days respectively. For comparison, the end CSOR of the base case is 6.8 bbl/bbl.

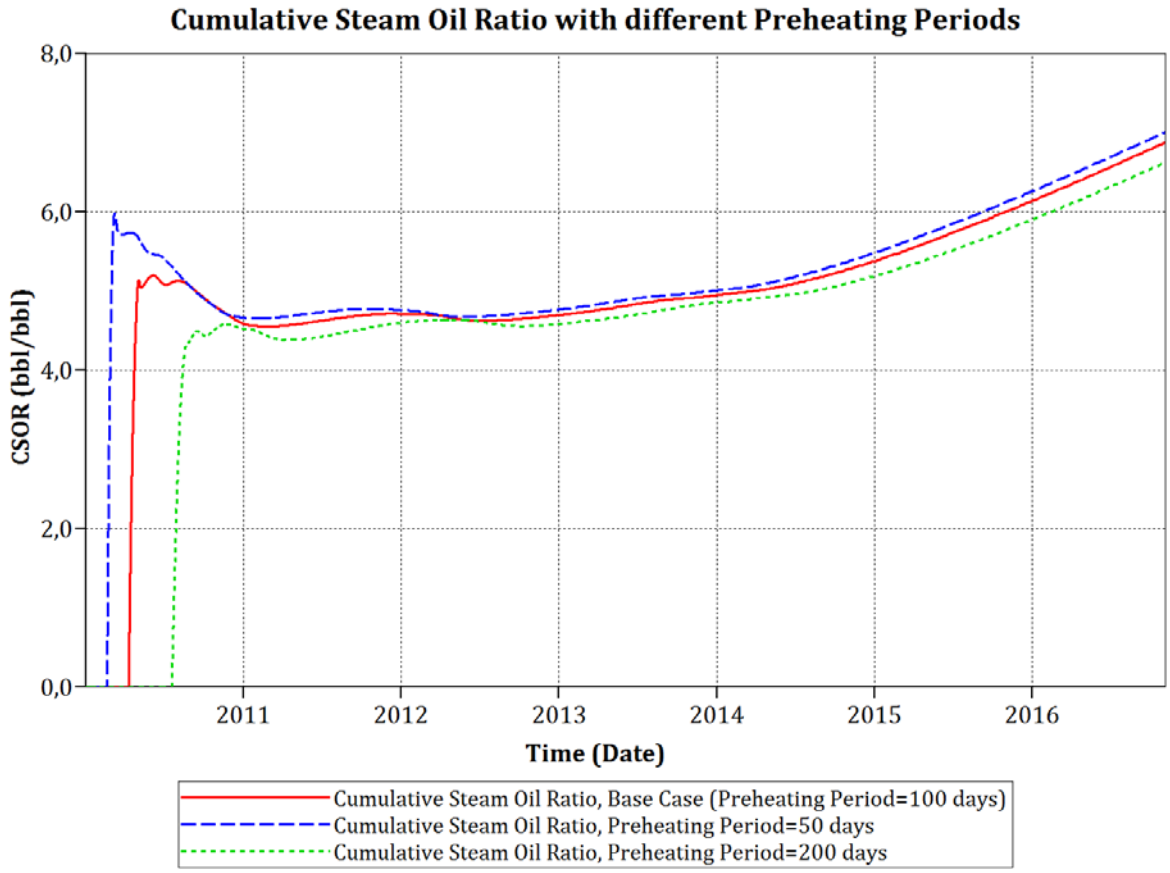

Figure 40: Cumulative steam oil ratio with different preheating periods

Figure 41 depicts the oil rate with different preheating periods. Both simulated cases follow the same trend as the base case. In 2010 a preheating period of 200 days has the lowest rates but increases during 2011 and keeps the highest rate of the three cases towards end of production. However, it is evident that all simulated cases follow the same rate of decline from the start of 2014 and yields an end rate in the range of approximately 3.7-4.5 bbl/d

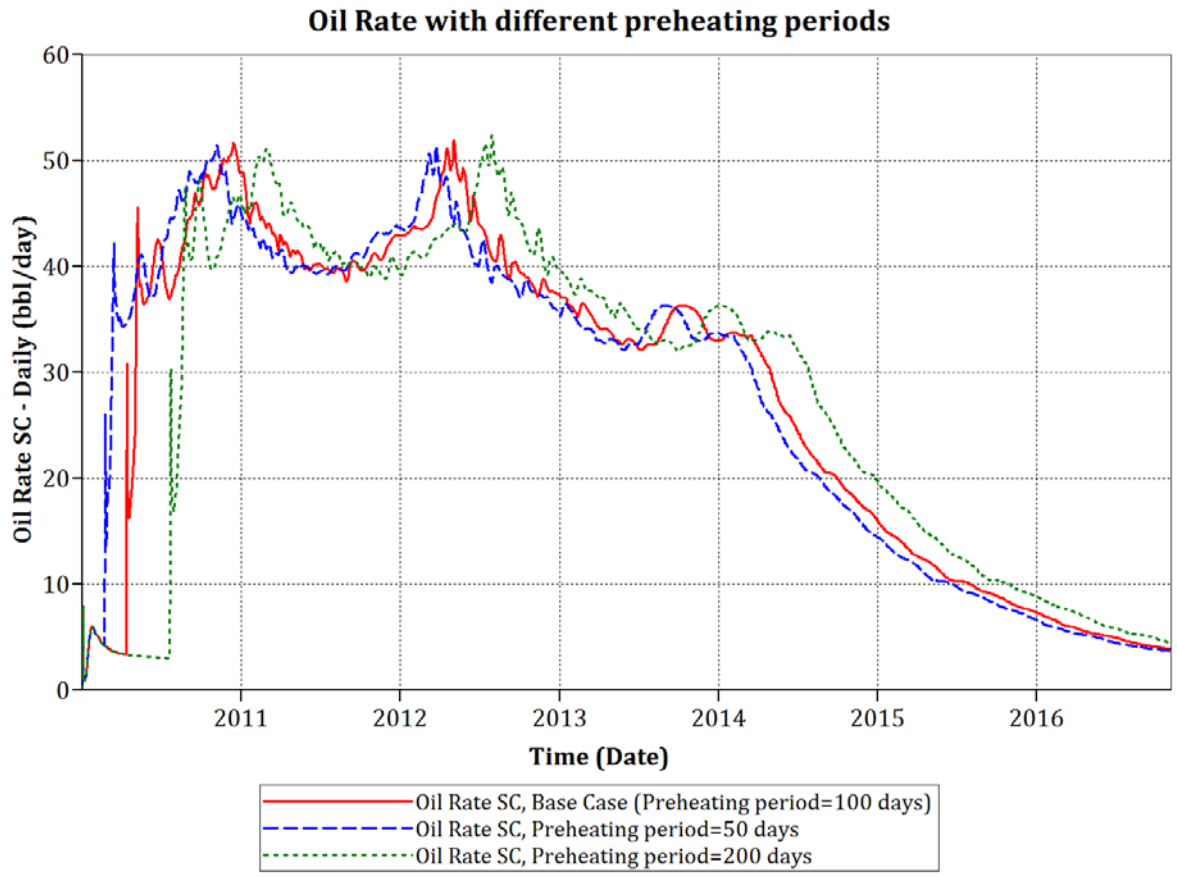

Figure 41: Oil Rate with different preheating periods

7 Discussion

General

It is important to conduct a sensitivity analysis for all reservoir parameters in order to determine the economic feasibility and the production prospects of a given field. Due to the complexity of core extraction from bitumen and heavy oil reservoirs, the sensitivity analysis is even more important than for that of conventional reservoirs. The implication of immobile oil makes it difficult to extract a core that represents the scope of the fundamental reservoir parameters. Thus, a comprehensive sensitivity analysis may give valuable insight in which parameters that will have the largest effect on the output variables. It may also indicate the economic feasibility as testing a wide range of values for each parameters, may yield both a conservative and optimistic view of possible production value.

Reservoir simulation in general is a very helpful tool in deciding on the appropriate production approach. Yet, as Carlson (2003) argues; by experience it has become obvious that many reservoir engineering estimates, plans and schemes have fundamental flaws. The author continues to argue that this may be due to fallible initial assumptions.

Base case

The model created was a *homogenous* model. However, as mentioned earlier the Athabasca field is extremely heterogeneous, and therefore the results obtained will deviate, to some extent, from *reality*. Thus one may argue that this model does not correspond to actual data. Huc (2011) argues that the presence of significant heterogeneities is a detrimental factor with respect to SAGD. As Deutsch (2010) states; the heterogeneities are variable within different depositional environments. Moreover, Huc (2011) explains that process efficiency may be limited by barriers in the steam chamber. As there seems to be no published studies on the minimum size of heterogeneities above which SAGD is no longer economically feasible, he proposes that numerical modeling on a case-by-case basis is required to investigate the real effect of the presence of heterogeneities. The recovery factors in general will be lower for a realistic case than the results presented in the present thesis. Moreover, the aim of this thesis

is to evaluate the effects of variation in the different parameters and thus a simplified homogeneous model will be sufficient and timesaving.

The model does not take heat loss to the surrounding environment outside the simulated region into account. Therefore, no heat leaves the reservoir grid. The steam accumulates in the model and consequently the whole reservoir is heated. In a real case the heat would spread laterally and transfer to the surroundings. A larger region should have been simulated in order to investigate the effect of this. However, this was not in the scope of the present thesis.

The base case involves one SAGD well pair, it can be discussed if several well pairs in a larger field should be simulated. However, the grid refinement results (which will be thoroughly discussed at a later stage) shows that it is not preferable to use a larger grid than that of the base case due to the upper limitation of grid blocks allowed by the available computer capacity.

The time period of simulation is set to 2500 days. This corresponds to approximately 6 years and may seem like a short period of time compared to the lifespan of a conventional well. The estimated ultimate recovery factor for the base case was 75%. Huc (2011) states, by SAGD implementation one may yield a RF of up to 70 % of IOIP in bitumen reservoirs. Thus the recovered oil from the base case corresponds to the RF expected from SAGD implementation in bitumen reservoirs. Based on this one may deduce that more simulation time is not required.

One may argue *why* the lifespan of a SAGD well-pair is so short. A possible reason is that the volume of oil recoverable by one SAGD well pair may be smaller than the volume of oil recoverable by that of a conventional well. In addition as Huc (2010) argues, the use of horizontal wells in SAGD generally attains larger production rates. The lower volume of in place oil combined with high oil rates may result in rapid reservoir depletion. Another interesting aspect is wettability, which may add an additional explanation to the rapid depletion time. The Athabasca reservoir is known to be strongly water-wet. A water-wet reservoir will result in a higher primary recovery compared to an oil wet reservoir. It is also understood that the same amount of oil can be recovered from both oil-wet and water-wet reservoirs, but the oil-wet reservoirs require more depletion time. However in the case of SAGD it is difficult to assess whether it has the same advantage as a conventional water-wet

reservoir as limited experimental research has been conducted on the wettability of heavy oil and bitumen reservoirs.

With a steam quality of 90 %, the CSOR of the base case was estimated to be approximately 4 bbl/bbl during production and yielded an end CSOR of 6.8 bbl/bbl. These results are to some extent contradicted by literature as Huc (2011) states that with a steam quality of 80 %, the CSOR may be lower than 2 bbl/bbl.

Viscosity

The sensitivity analysis performed with respect to viscosity resulted in limited discrepancy when examining RF, CSOR and oil rate. However, they do indicate that the correlation describing the viscosity-temperature relationship for bitumen created by Khan, Mehrotra & Svrcek (1984) is sufficient to estimate the viscosity of Athabasca bitumen. The viscosity decreases dramatically with a temperature increase. As expected, it can be concluded that the RF increases as a result of temperature increase and viscosity decrease. The reason for the small discrepancies visible in Figure 14-Figure 16 lie in the fact that all the tested cases where based on the same correlations with different sample data. Thus the viscosities where somewhat similar.

The effect of pressure on the viscosity of gas-free Athabasca bitumen is not taken into account in the viscosity correlations. Several viscosity-temperature relationships of bitumen have been presented in literature but they all seem to be conducted at atmospheric pressures (Mehrotra & Svrcek, 1986). Thus the obtained viscosities have not been correlated with respect to the actual reservoir pressure. The pressure dependent relationship with respect to viscosity is a rather complicated matter. Figure 42 illustrates a typical pressure dependency of oil viscosity for standard black oil. Though, this might not be directly applicable to bitumen, it illustrates the non-linear behavior of the viscosity with respect to

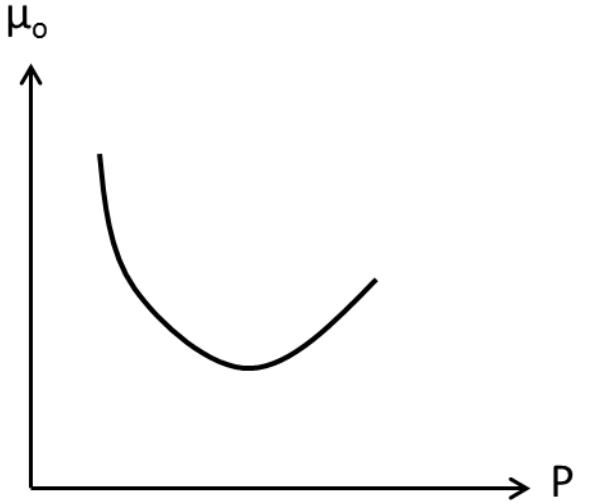

Figure 42: Typical pressure dependency of standard black oil viscosity.

pressure. Mehrotra & Svrcek (1986) conducted a study where a correlation created by Khan, Mehrotra & Svrcek (1984) was modified to include the effect of pressure on the viscosity of the bitumen. It was deduced that compression of bitumen results in a *significant* increase in bitumen viscosity. Thus it is advisable to include the effect of pressure when deducing bitumen viscosity effects. However, in general the viscosity variations with respect to temperature is much larger compared to the variations with respect to pressure.

Grid refinement

Figure 17 displays the recovery factors obtained when examining the effects of a three-dimensional grid. As can be seen from the graph, all the cases are rather similar for the first two years. However, for the continuous years discrepancies are observed. Yet, as can be seen in Figure 45, Appendix B.1, all cases reach equal RF at end of production except for the base case.

In general, the numerical uncertainty is reduced with smaller grid blocks as more grid blocks will create less numerical dispersion and thus the discretization of the equations becomes more accurate. Based on this one may argue that $j = 6$ yields the most accurate result.

However, despite the fact that there is a slight difference in RF in the base case compared to the other cases, the differences probably lie *within* model uncertainty. In addition, the one dimensional model provides a conservative prediction of recovery in relation to economical aspect which is preferable to the other way around when deciding the economic value of a certain SAGD performance. Carlson (2003) argues that most SAGD simulations are run with 2D cross-sectional models as considerably more computation time is required with thermal models than with black oil models.

In the present work it was concluded that a 2D model is sufficient for assessing the effects of SAGD implementation in the Athabasca field, as the discrepancy between the 2D model and the 3D model was very limited (3% RF at end of production) and the latter required significantly more simulation time.

Permeability

The heterogeneity of the Athabasca field presents a challenge when calibrating permeability data for input in flow simulation (Deutsch, 2010). This underlines the importance of testing a

wide range of permeabilities. Moreover Deutsch (2010) argues that especially the vertical permeability is of high importance. The vertical permeability effects amongst others the rise of steam through the formation, the drainage rate of oil and condensed water, and the possible escape of steam to overlying formations.

As Huc (2011) states, one limiting factor of SAGD is the need for high permeability, i.e. larger than 1500 mD. The main reason is that high permeability is required for steam chamber development. The base case permeabilities (kh=7000 mD and kv=2100 mD) are well above the suggested minimum for SAGD implementation. Moreover, the permeability tested for here lie within and below the range of permeabilities (6-12 D) in the Athabasca field defined in Tavalli & Harding (2011).

The present study investigated altering the horizontal and vertical permeability separately and varying both of them simultaneously. In general, the results show a consistent increase in RF, decrease in CSOR, and increase in oil rate with increasing permeability. However, while this trend was profound for the lower permeabilities, it almost diminished for the higher permeabilities. This indicates that for the higher permeabilities in the tested range, other parameters than permeability limit the flow.

It can also be noticed that the relationship between the CSOR and the oil rate is consistent as peaks in the oil rate correspond to the trend in CSOR. The oil rate is controlled by a minimum bottom hole pressure of 250 psi and a maximum liquid production rate of 250 bbl/day. When examining Figure 22: Oil rate with variation in horizontal permeability, it is observed that all simulated cases reaches the same number of peaks except for the lowest tested case (k_h=1750 mD). This may be due to the aspects in controlling the oil rate. When examining the case of k_h=1750 mD closer, it becomes evident that it never reaches the maximum liquid production rate, neither does it have the decline that the other cases possess. It is only controlled by the minimum bottom-hole pressure resulting in a rather stable rate. However, even though it might possess the highest rate at end of production (2016), Figure 20 shows that it yields a rather low recovery in SAGD perspective and may not be economical.

It is inevitable to discuss the effect of vertical permeability without discussing the occurrence of shale layers. Deutsch (2010) argues that a significant amount of shale is present which most certainly reduces the effect of vertical permeability. As proposed by Tavallali & Harding (2011), the McMurray formation is separated by different shaly layers which are up to 2

meters thick. Moreover, they argue that these shales are mostly bioturbated and do not block vertical communication through the net pay. This contradict the views presented by Deutsch(2010). Speight (2009) argues that in spite the presence of shale layers, SAGD may result in 60-70 % recovery even in reservoirs were many shale streaks are present. This is in correspondence of the RF obtained in this analysis with respect to vertical permeability variation as all tested permeabilities ranged an end RF of approximately 60-80 %.The effect of shale layers where not tested in this thesis, however, as Tavalli & Harding (2011) and Speight (2009) proposes, the effect of shale layers, up to a certain thickness, will not affect the vertical permeability significantly, thus one may conclude that the simulation results presented in the current thesis are somewhat valid, for the Athabasca field, despite the occurrence of shale layers.

Injection well location

Placement of the injection well is a rather significant matter in relation to SAGD. From Figure 29: Oil recovery factor with layer of injection, it can be deduced that injecting steam close to the well yields low RF. However, as can be seen from Figure 51, Appendix B.3, where all simulated cases with respect to injection layer variation is displayed, injecting in layer 13 and onwards towards the top layer yields approximately the same RF of 75 %. Thus, it can be concluded that based solely on the amount of oil recovered, the injection well may be placed in all layers except for layer 14.

From Figure 30: Cumulative steam oil ratio with layer of injection, it is evident that placing the injection well close to the production well (i.e. injecting in layer 13 and 14), results in high CSOR during production time. All cases except for injection in layer 14 yield the same CSOR at end of production. However, considering the case of injection in layer 1 one may observe a peak CSOR (of 12 bbl/bbl) immediately after production start. The possible reason for this may be deduced from the *effect* of preheating period for the various cases. The preheating period was kept constant for all simulated cases in order to observe the effect of injection well placement.

From Figure 43 it can be deduced that communication between the injection well and production well occurs during the preheating period in spite of layer of injection, which is essential for a successful SAGD operation.

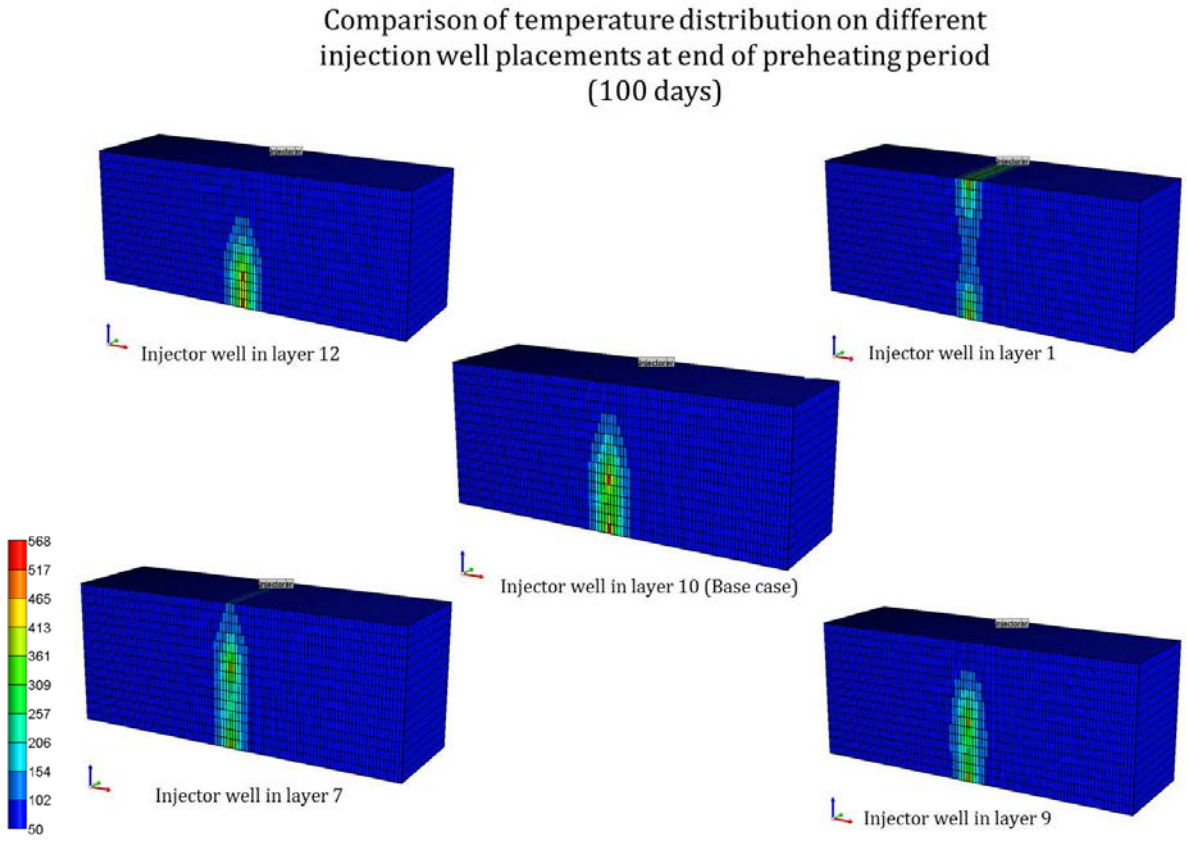

Figure 43: Comparison of temperature distribution (°F) on different injection well placements at end of preheating period (100 days)

However, it can be observed that placing the injector in layer 1 results in limited communication between the injection and production well. This agrees with Figure 31: Oil rate with layer of injection, where it is seen that injection in layer 1 results in very low initial production rate (the rate is initially zero). This is due limited oil mobility in the region near the production well caused by minor heating. However the production rate increases significantly during the start of production period compared to the other cases, possibly due to that communication eventually occurs at this stage. This corresponds to the results obtained when examining the CSOR. Having such a low production compared to the steam injected, yields a very high CSOR. However, this does not affect the overall recovery of oil as this is similar to that of the other cases.

Placing the injection well in layer 13 and 14 results in a minor area of steam contact, thus drainage occurs from a smaller area compared to the other cases. This in turn leads to low oil rate. However at a later stage of the production period the oil rates increase above the other

cases. This is probably due to the longer time required before the steam reaches the top of the reservoir and starts to move laterally. When the reservoir is depleted the oil saturation (S_o) decreases and consequently the oil rate decreases, as can be seen for the other cases. As less oil is produced initially when placing the injector in layer 13 and 14, S_o is somewhat maintained and the oil rate increases towards end of production as the entire reservoir is eventually heated.

The results obtained correspond with literature. Carlson (2003) argues that with larger vertical well spacing, more time is required to create communication between the injector and producer. Further he argues that vertical well spacing is an issue of timing and rates. Seemingly one may conclude that vertical well spacing has limited effect on cumulative oil production, but creates discrepancies with respect to oil rate vs. time. However, some contradictions in literature are present with respect to proposed vertical distance. As Speight (2009) argues, the vertical distance between the injector and producer should be between 5-7 meters. Thus, this corresponds to injection in layer 7 and 9 in the present analysis.

It is deduced that several scenarios are favorable with respect to layer of injection. Based on RF it can be concluded that placement of injection well in general has limited significance. A possible reason could be that the amount of heat created by the amount of steam injected for this period of time, is sufficient to cover the whole reservoir. Therefore, the whole reservoir is depleted and the placement of injection well has very little or even no significance

As the CSOR determines to a great extent whether or not a project is economically feasible, this rating will have the highest weighting. Even though injection in layer 1 *in general* yields a low CSOR, the peak increase at start of production might not make it economically feasible in this time period. There are limited discrepancies at the beginning of the production in CSOR between the cases except for layer 13 and 14. Accordingly, it can be concluded that the vertical spacing between the injection well and production well should be between 3,5 and 7, 5 meters.

Porosity

Figure 32: Cumulative oil produced with porosity variation, shows a consistent increase in cumulative oil produced with increasing permeability. As expected, a higher porosity will yield a higher IOIP and thus the amount of produced oil will be larger in the case of higher

porosities. Figure 33: Oil recovery factor with porosity variation, shows a consistent decrease in RF with increase in porosity. This is probably due to the amount of oil recovered compared to the amount of IOIP being lower in the higher porosity cases. Seemingly, the steam is not able to transport the oil out of the pores due to lower steam velocities compared to the cases with smaller pore volumes. However, it should be emphasized that only limited discrepancies exist in RF between the cases. Thus, a higher porosity is beneficial as it leads to an increased amount of cumulative oil produced.

Figure 34: Cumulative steam oil ratio with porosity variation indicates a consistent increase in CSOR as the porosity decreases. The reason is that the same amount of steam is injected in all the cases whereas the IOIP is lower for the decreased porosities. Consequently, a lower amount of oil is produced in the cases with lower porosities and subsequently the CSOR is higher.

Injection rate

Figure 36: Oil recovery factor with injection rate variation**,** shows that there are limited discrepancies in end RF (only 3 % difference between the three simulated cases). However, larger discrepancies may be observed during the production period.

Figure 37: Cumulative steam oil ratio with injection rate variation shows that a higher injection rate yields higher CSOR. The highest injecting rate at 220 STB/d yields an end CSOR of 7.8 bbl/bbl. Yet, the lowest tested injection rate at 150 STB/d yields an end CSOR of 5 bbl/bbl and is thus more preferable in terms of thermal efficiency. The high initial CSOR obtained by an injection rate of 150 STB/d may be explained by examining Figure 38: Oil rate with injection rate variation, as it is evident that it has ha very *low* initial oil production rate compared to the other cases. However, it increases rapidly and in general holds a very high oil rate resulting in an end RF equal to the base case, 75 %.

As a lower CSOR is highly weighted when evaluating a SAGD operation it can be deduced from this sensitivity analysis, that a lower injection rate may be preferred. This will result in a lower CSOR and higher RF.

Preheating period

A sufficient preheating time is required in order to obtain communication between the injector and the producer. From Figure 44 below, it may be observed that a preheating period of 50 days and a preheating period of 100 days both heat approximately the same area. The preheating period of 200 days heats a larger area of the reservoir.

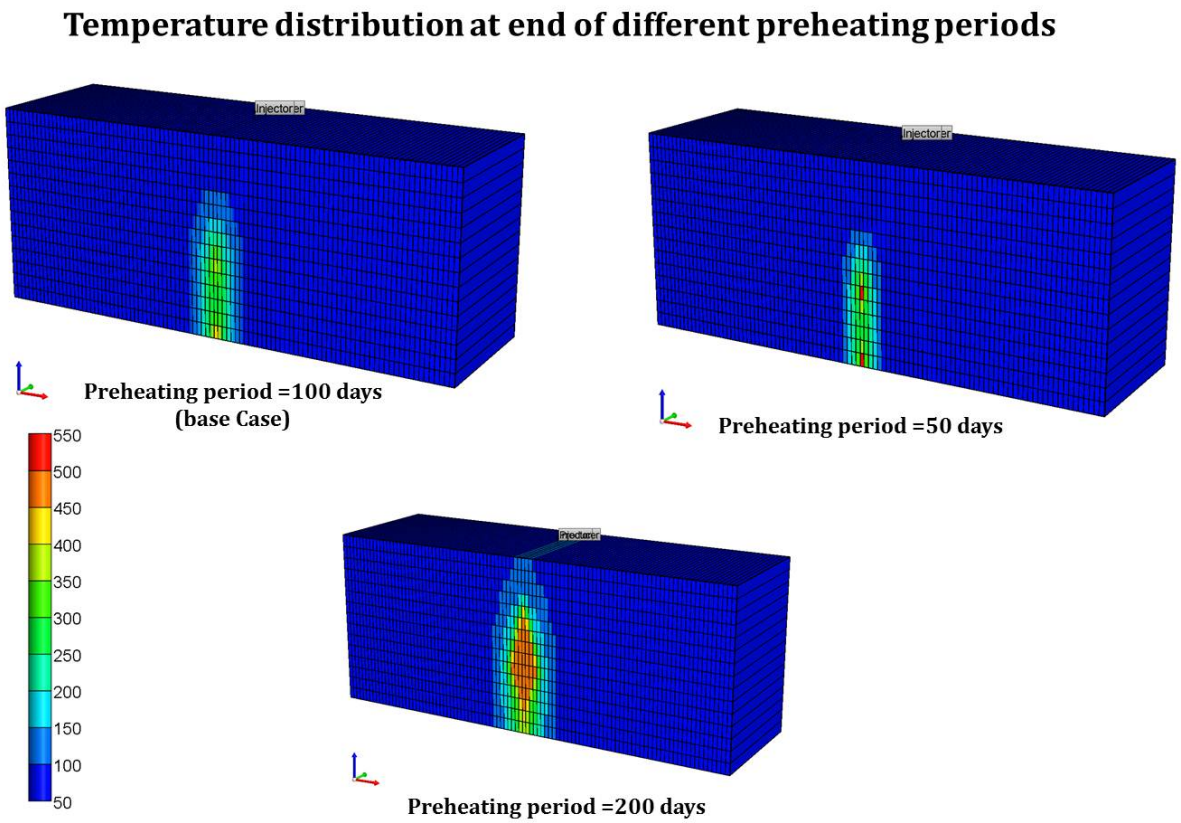

Figure 44: Temperature distribution (°F) at end of different preheating periods

From Figure 39: Oil recovery factor with different preheating periods, it is evident that various lengths of preheating periods do not create discrepancies in end RF. A preheating period of 50, 100, and 200 days; yielded equal end RF of 75 %. However, discrepancies did exist during the production time as a preheating period of 50 days in general had the highest RF. This can be explained by the fact that production was started later for the longer preheating periods. Thus one may deduce that the effect of preheating a larger area of a reservoir prior to production proved to be insignificant with the present simulation set up. It

may be concluded that the length of preheating time tested for, has limited effect on ultimate oil recovery for these cases.

Figure 40: Cumulative steam oil ratio with different preheating periods shows that a preheating period of 50 days yielded a higher end CSOR compared to the other simulated cases. The difference in CSOR between the highest and lowest case is 1 bbl/bbl at end of production. Accordingly, based on the simulation results the longer preheating time (200 days) is preferred with respect to CSOR. However, in economic terms, the cost of heating versus the cost of steam must be evaluated, but has not been included in the scope of the present work.

8 Conclusion

Reservoir simulations are used in order to forecast production for the Athabasca field with SAGD. Due to the complexity of core extraction in heavy oil and bitumen reservoirs a comprehensive sensitivity analysis is significant in reservoir simulations of such fields. A homogenous model will in general yield higher recovery factors than the realistic case. However, in spite of the complexity of a bitumen reservoir, a homogeneous model was utilized in the present work due to limited time and computer capacity.

Several linear viscosity-temperature correlations deduced from sample data were investigated. As expected, the simulation cases with the correlations estimating the highest viscosity, yielded a lower RF. Yet, discrepancies were limited as the sample data used for the correlations held limited viscosity differences. A limitation to the present model was that it did not consider pressure effects.

Investigations of having more than one grid cell in the third dimension were carried out. In general, more grid cells provided more accurate results due to less numerical dispersion. However, as all results apparently lied within the simulator uncertainty, the 2D model was found sufficient. The 2D model was less time-consuming and provided a more conservative prediction of recovery which is preferable to the other way around when deciding the economic value.

Increasing horizontal and vertical permeabilities resulted, in general, in a significant increase in oil recovery and lower CSOR. However, increasing the permeability beyond a certain limit only induced limited increase in RF and minor decrease in CSOR. Accordingly, in these cases, other parameters than the permeability was the limiting factor on the production. Different vertical well spacing proved to have limited effect on ultimate oil recovery provided that the injection well was not placed in the immediate surroundings of the production well. However, based on CSOR, it is proposed that the vertical spacing between the injection well and the production well for SAGD implementation in the Athabasca field should be between 3.5 and 7.5 meters.

Evidently a higher porosity resulted in larger amount of cumulative oil produced, as the IOIP is larger. More surprisingly (although the differences were minor), the RF showed a consistent

decrease with increase in porosity. As the steam injection rate is constant, a higher pore volume yields lower steam velocity. This will decrease friction between steam and oil and might be a reason to why RF is decreasing with increasing porosity.

An injection rate of 150 bbl/day resulted in low CSOR and relatively high RF; compared to that of higher injection rates (200 bbl/day and 220 bbl/day). Thus, based on this sensitivity analysis, the lower injection rate was preferred.

Recommendations

It is recommended to develop a model which accounts for heat loss to surroundings as this is significant effect which was not accounted for in this simulation study. In addition to understand the effect of vertical permeability thoroughly it would have been of interest to test the production rates when shale barriers are present. It would also be of interest to test for a lower and for a higher permeability ratio to see effects. As adding a chemical additive to the steam prior to injecting it is a very up and coming topic with respect to SAGD it would be interesting to see the effect of this.

Nomenclature

μ	Viscosity (cp)
μ_g	Viscosity of gas (cp)
μ_o	Viscosity of oil (cp)
μ_w	Viscosity of water (cp)
Φ	Porosity
λ	Mobility
CSOR	Cummulative Steam Oil Ratio (bbl/bbl)
IOIP	Initial oil in place (Sm^3 or bbl)
k_h	Effective permeability, mD
k_h	Horizontal permeability, mD
k_v	Vertical permeability, mD
k_{rw}	Relative permeability to water
k_{ro}	Relative permeability to oil
M	Mobility ratio
OOIP	Original oil in place (Sm^3 or bbl)
RF	Recovery factor (%)
SAGD	Steam Assisted Gravity Drainage
SC	Standard conditions (1 atm, 15 °C)
S_g	Gas saturation

S_l Liquid saturation

S_o Oil saturation

STB Stock tank barrels

S_w Water saturation

T Temperature (°C, °F or K)

Bibliography

Ashrafi, M., Souraki, Y., Veraas, T. J., Karimaie, H., & Torsæter, O. (2011). Experimental Investigation and Numerical Simulation of Steam Flooding in Heterogeneous Porous Media Containing Heavy Oil. *SPE Asia Pacific Oil and Gas Conference and Exhibition.* Jakarta, Indonesia: Society of Petroleum Engineers.

Attanasi, E., & Meyer, R. (2007). *Natural Bitumen and Extra- Heavy Oil*. Retrieved March 13, 2012, from World Energy Council: http://energy.cr.usgs.gov/oilgas/addoilgas/WEC07NBEHO.pdf

Broadhead, R. F. (2011, April 18). *New Mexico Bureau of Geology & Mineral Resources.* Retrieved October 18, 2011, from Petroleum Geology: An introduction: http://geoinfo.nmt.edu/faq/energy/petroleum/Petroleum_geology_intro.pdf

Carlson, M. (2003). *Practical Reservoir Simulation.* Tulsa: PennWell Corporation.

Chow, L. (1993). Numerical Simulation of Heavy Oil Recovery by The Steam-Assisted Gravity Drainage Process.

Collins, H. (1976). Log-Core Correlations in the Athabasca Oil Sands. *Journal of Petroleum Technology*, 1157-1168.

Curtis, C., Kopper, R., Decoster, E., Guzmán-Garcia, A., Huggins, C., Knauer, L., et al. (2002, October 1). *Oilfield Review.* Retrieved November 18, 2011, from Sclumberger: http://www.slb.com/~/media/Files/resources/oilfield_review/ors02/aut02/p30_51.ashx

Dake, L. (1978). *Fundamentals of Reservoir Engineering.* Oxford: Elsevier.

Das, S. (2007). Application of Thermal Recovery Processes in Heavy Oil Carbonate Reservoirs. *The 15th SPE Middle East Oil & Gas Show and Conference.* Bahrain: Society of Petroleum Engineers.

Deutsch, C. (2010). Estimation of Vertical Permeability in the McMurray Formation. *Journal of Canadian Petroleum Technology*, 10-18.

Doscher, T., & Ghassemi, F. (1983). Limitations on the oil/steam ratio for truly viscous crudes. *SPE California Regional Meeting.* Ventura: Society of Petroleum Engineers.

Dusseault, M. B. (1980). Sample disturbance in Athabasca oil sand. *The Journal of Canadian Petroleum*, 85-92.

Farouq Ali, S. (1974). Heavy Oil Recovery - Principles, Practicality, Potential, and Problems. Billings, Mont: American Institute of Mining, Metallurgical, and Petroleum Engineers, Inc.

Gates, I. D. (2010). Solvent-aided Steam-Assisted Gravity Drainage in thin oil sand reservoirs. *Journal of Petroleum Science and Engineering*, 138-146.

Godderij, R., Gumrah, F., Palmgren, C., & Bruining, J. (1995). An investigation of the vertical sweep efficiency of steam drive in a layered reservoir. *New Developments in Improved Oil Recovery, 84*, 261-273.

Huc, A.-Y. (2011). *Heavy Crude Oils, From Geology to Upgrading, An Overview.* Paris: IFP energies nouvelles, Publications.

Khan, M. I., & Islam, M. (2007). *The Petroleum Engineering Handbook: Sustainable Operations.* Houston, Texas: Gulf Publishing Company.

Khan, M., Mehrotra, A., & Svrcek, W. (1984). Viscosity models for gas-free Athabasca bitumen. *The Journal of Canadian Petroleum Technology*, 47-53.

Lake, L. W. (1989). *Enhanced Oil Recovery.* Austin: Prentice-Hall, Inc.

Marianayagam, K. (2011, December). Heavy Oil Recovery with Steam Injection.

McCormack, M. (2001). Mapping of the McMurray Formation for SAGD. *Journal of Canadian Petroleum Technoogy*, 21-28.

Mehrotra, A. K., & Svrcek, W. Y. (1986). Viscosity of Compressed Athabasca Bitumen. *The Canadian Journal of Chemical Engineering*, 844-847.

Meyer, R. F., & Attanasi, E. D. (2003, October 6). *U.S. Department of the Interior.* Retrieved November 16, 2011, from U.S. Geological Survey: http://pubs.usgs.gov/fs/fs070-03/fs070-03.html

Nasr, T., & Ayodele, O. (2005). Thermal Techniques for the Recovery of Heavy Oil and Bitumen. Kuala Lumpur: Society of Petroleum Engineers.

Owen, N. A., Inderwildi, O. R., & King, D. A. (2010). The status of conventional world oil reserves-Hype or cause for concern. *Energy Policy, 38*, 4743-4749.

Pinzewski, V. (2011). Course handouts in Reservoir Engineering B - PTRL3001. University of New South Wales.

Pollkar, M., Farouq Ali, S., & Puttagunta, V. (1990). High-Temperature Relative Permeabilities for Athabasca Oil Sands. *SPE Reservoir Engineering*, 25-32.

R. Beall, K. S. (2011). Peregrino: An Integrated Solution for Heavy Oil Production and Allocation. *Brasil Offshore Conference and Exhibition* (p. 17). Macaé, Brazil: Society of Petroleum Engineers .

Sasaki, K., Akibayashi, S., Yazawa, N., Doan, Q., & Farouq Ali, S. (2001). Numerical and Exmerimental Modelling of the Steam Assisted Gravity Drainage (SAGD) Process. *Journal of Canadian Petroleum Technology*, 44-50.

Schlumberger. (2011). *Oilfield Glossary*. Retrieved 2011, from Schlumberger: http://www.glossary.oilfield.slb.com/search.cfm

Shell International Petroleum Company Limited. (1983). *The Petroleum Handbook.* Amsterdam: Elsevier Science Publishers B.V.

Shin, H., & Polikar, M. (n.d.). Review of Reservoir Parameters to Optimize SAGD and Fast SAGD Operating Conditions. *Canadian International Petroleum Conference.* Calgary: Canadian institute of Mining, Metallurgy & Petroleum.

Souraki, Y., Ashrafi, M., Karimaie, H., & Torsaeter, O. (2012). Experimental Analyses of Athabasca Bitumen Properties and Field Scale Numerical Simulation Study of Effective Parameters on SAGD Performance. *Submitted for publication.*

Souraki, Y., Ashrafi, M., Karimaie, H., & Torsæter, O. (2011). Experimental Investigation and Numerical Simulation of Steam Flooding in Heavy Oil Fractured Reservoir. *SPE Western North American Regional meeting.* Anchorage, Alaska: Society of Petroleum Engineers.

Speight, J. G. (2009). *Enhanced recovery methods for heavy oil and tar sands.* Texas: Gulf Publishing company.

Srivastava, P., Debord, J., Sadetsky, V., Stefan, B., & Orr, B. (2010). Laboratory Evaluation of a Chemical Additive to Increase Production in Steam Assisted Gravity Drainage (SAGD). *SPE Improved Oil Recovery Symposium.* Oklahoma: Society of Petroleum Engineers.

Tavallali, M., & Harding, T. (2011). Evaluation of New Well configurations for SAGD in Athabasca McMurray Formation. *SPE EUROPEC/EAGE Annual Conference and Exhibition.* Vienna: Society of Petroleum Engineers.

Woodhouse, R. (1976). Athabasca tar sand reservoir properties derived from cores and logs. *SPWLA Seventeen annual logging symposium.*

Appendix A: Additional tables

Appendix A.1: Simulation matrix

Table 15: Summary of simulations performed

Sim no.	Variable	Grid	Kh (mD)	Kv(mD)	Injection well loc.	Porosity	Injection rate (STB/d)	Preheating period (days)	Viscosity coefficient C1	Viscosity coefficient C2
-	**Base case**	**101:1:15**	**7000**	**2100**	**Layer 10**	**0,38**	**200**	**100**	**-**	**-**
1	Viscosity	101:1:15	7000	2100	Layer 10	0,38	200	100	-3,7336	23,8162
2	Viscosity	101:1:15	7000	2100	Layer 10	0,38	200	100	-3,6272	23,2200
3	Viscosity	101:1:15	7000	2100	Layer 10	0,38	200	100	-3,6254	23,1641
4	Grid, j	101:2:15	7000	2100	Layer 10	0,38	200	100	-	-
5	Grid, j	101:3:15	7000	2100	Layer 10	0,38	200	100	-	-
6	Grid, j	101:4:15	7000	2100	Layer 10	0,38	200	100	-	-
7	Grid, j	101:5:15	7000	2100	Layer 10	0,38	200	100	-	-
8	Grid, j	101:6:15	7000	2100	Layer 10	0,38	200	100	-	-
9	Perm. (H)	101:1:15	1750	2100	Layer 10	0,38	200	100	-	-
10	Perm. (H)	101:1:15	3500	2100	Layer 10	0,38	200	100	-	-
11	Perm. (H)	101:1:15	4000	2100	Layer 10	0,38	200	100	-	-
12	Perm. (H)	101:1:15	5000	2100	Layer 10	0,38	200	100	-	-
13	Perm. (H)	101:1:15	6000	2100	Layer 10	0,38	200	100	-	-
14	Perm. (H)	101:1:15	8000	2100	Layer 10	0,38	200	100	-	-
15	Perm. (H)	101:1:15	9000	2100	Layer 10	0,38	200	100	-	-
16	Perm. (V)	101:1:15	7000	1050	Layer 10	0,38	200	100	-	-
17	Perm. (V)	101:1:15	7000	525	Layer 10	0,38	200	100	-	-
18	Perm. (V)	101:1:15	7000	3000	Layer 10	0,38	200	100	-	-
19	Perm. (V)	101:1:15	7000	3300	Layer 10	0,38	200	100	-	-
20	Perm. (H & V)	101:1:15	1750	525	Layer 10	0,38	200	100	-	-
21	Perm. (H & V)	101:1:15	7800	2900	Layer 10	0,38	200	100	-	-
22	Perm. (H & V)	101:1:15	5000	4000	Layer 10	0,38	200	100	-	-
23	Inj. well loc.	101:1:15	7000	2100	Layer 1	0,38	200	100	-	-
24	Inj. well loc.	101:1:15	7000	2100	Layer 7	0,38	200	100	-	-
25	Inj. well loc.	101:1:15	7000	2100	Layer 9	0,38	200	100	-	-
26	Inj. well loc.	101:1:15	7000	2100	Layer 11	0,38	200	100	-	-
27	Inj. well loc.	101:1:15	7000	2100	Layer 12	0,38	200	100	-	-
28	Inj. well loc.	101:1:15	4000	2100	Layer 13	0,38	200	100	-	-
29	Inj. well loc.	101:1:15	5000	2100	Layer 14	0,38	200	100	-	-
30	Porosity	101:1:15	6000	2100	Layer 10	0,15	200	100	-	-
31	Porosity	101:1:15	8000	2100	Layer 10	0,20	200	100	-	-
32	Porosity	101:1:15	7000	2100	Layer 10	0,25	200	100	-	-
33	Porosity	101:1:15	7000	2100	Layer 10	0,30	200	100	-	-
34	Porosity	101:1:15	7000	2100	Layer 10	0,40	200	100	-	-
35	Inj. rate	101:1:15	7000	2100	Layer 10	0,38	150	100	-	-
36	Inj. rate	101:1:15	7000	2100	Layer 11	0,38	220	100	-	-
37	Pre-heat period	101:1:15	7000	2100	Layer 14	0,38	200	50	-	-
38	Pre-heat period	101:1:15	7000	3300	Layer 10	0,38	200	200	-	-

Appendix A.2: Viscosity

Table 16: Simulation variables when testing for viscosity

			Base case	Sim no. 1 (Sample no. 3)			Sim no. 2 (sample no. 1)			Sim no 3. (Average C1 and C2 of all four samples)		
T (F)	T(°C)	T(K)	μ (cp)	C1	C2	μ (cp)	C1	C2	μ (cp)	C1	C2	μ (cp)
50	10	283,15	1000000	-3,7336	23,8162	5030549,21	-3,62722	23,22	5386360,85	-3,6254475	23,1641	2687575,60
69,08	20,6	293,75	316000	-3,7336	23,8162	695558,49	-3,62722	23,22	778387,77	-3,6254475	23,1641	423946,24
85,82	29,9	303,05	92980	-3,7336	23,8162	158679,34	-3,62722	23,22	182570,89	-3,6254475	23,1641	106177,65
104	40	313,15	25395	-3,7336	23,8162	39936,67	-3,62722	23,22	46938,54	-3,6254475	23,1641	29025,71
120,2	49	322,15	9958	-3,7336	23,8162	13786,39	-3,62722	23,22	16415,42	-3,6254475	23,1641	10643,79
140	60	333,15	3839	-3,7336	23,8162	4484,83	-3,62722	23,22	5394,14	-3,6254475	23,1641	3677,50
158	70	343,15	1800	-3,7336	23,8162	1862,01	-3,62722	23,22	2250,65	-3,6254475	23,1641	1595,99
176	80	353,15	903	-3,7336	23,8162	865,83	-3,62722	23,22	1048,58	-3,6254475	23,1641	769,56
194	90	363,15	502	-3,7336	23,8162	443,22	-3,62722	23,22	536,60	-3,6254475	23,1641	405,84
212	100	373,15	251	-3,7336	23,8162	246,24	-3,62722	23,22	297,52	-3,6254475	23,1641	231,06
230	110	383,15	166	-3,7336	23,8162	146,73	-3,62722	23,22	176,71	-3,6254475	23,1641	140,48
248	120	393,15	101	-3,7336	23,8162	92,86	-3,62722	23,22	111,37	-3,6254475	23,1641	90,39
266	130	403,15	70	-3,7336	23,8162	61,90	-3,62722	23,22	73,88	-3,6254475	23,1641	61,07
284	140	413,15	50	-3,7336	23,8162	43,16	-3,62722	23,22	51,24	-3,6254475	23,1641	43,06
302	150	423,15	36	-3,7336	23,8162	31,29	-3,62722	23,22	36,95	-3,6254475	23,1641	31,50
320	160	433,15	27	-3,7336	23,8162	23,47	-3,62722	23,22	27,56	-3,6254475	23,1641	23,81
338	170	443,15	21	-3,7336	23,8162	18,14	-3,62722	23,22	21,17	-3,6254475	23,1641	18,51
356	180	453,15	16	-3,7336	23,8162	14,39	-3,62722	23,22	16,70	-3,6254475	23,1641	14,75
374	190	463,15	13	-3,7336	23,8162	11,68	-3,62722	23,22	13,48	-3,6254475	23,1641	12,02
392	200	473,15	11	-3,7336	23,8162	9,67	-3,62722	23,22	11,10	-3,6254475	23,1641	9,99
410	210	483,15	9,45	-3,7336	23,8162	8,16	-3,62722	23,22	9,31	-3,6254475	23,1641	8,44
428	220	493,15	7,9	-3,7336	23,8162	6,99	-3,62722	23,22	7,94	-3,6254475	23,1641	7,25
446	230	503,15	6,75	-3,7336	23,8162	6,07	-3,62722	23,22	6,86	-3,6254475	23,1641	6,31
464	240	513,15	5,64	-3,7336	23,8162	5,34	-3,62722	23,22	6,01	-3,6254475	23,1641	5,56
482	250	523,15	5	-3,7336	23,8162	4,76	-3,62722	23,22	5,32	-3,6254475	23,1641	4,95
500	260	533,15	4,63	-3,7336	23,8162	4,28	-3,62722	23,22	4,76	-3,6254475	23,1641	4,45
518	270	543,15	4,17	-3,7336	23,8162	3,88	-3,62722	23,22	4,30	-3,6254475	23,1641	4,04
536	280	553,15	3,75	-3,7336	23,8162	3,55	-3,62722	23,22	3,92	-3,6254475	23,1641	3,69
554	290	563,15	3,45	-3,7336	23,8162	3,27	-3,62722	23,22	3,60	-3,6254475	23,1641	3,40
570	298,9	572,0389	3,202	-3,7336	23,8162	3,06	-3,62722	23,22	3,35	-3,6254475	23,1641	3,18
662	350	623,15	2,5	-3,7336	23,8162	2,25	-3,62722	23,22	2,43	-3,6254475	23,1641	2,33
752	400	673,15	2	-3,7336	23,8162	1,84	-3,62722	23,22	1,95	-3,6254475	23,1641	1,90
842	450	723,15	1,7	-3,7336	23,8162	1,59	-3,62722	23,22	1,68	-3,6254475	23,1641	1,64
932	500	773,15	1,3	-3,7336	23,8162	1,44	-3,62722	23,22	1,50	-3,6254475	23,1641	1,47
1112	600	873,15	1	-3,7336	23,8162	1,26	-3,62722	23,22	1,30	-3,6254475	23,1641	1,28

	C1	C2
Sample no.1	-3,62722	23,22
Sample no.2	-3,57379	22,8379
Sample no.3	-3,7336	23,8162
Sample no.4	-3,56718	22,7823
Average	**-3,62545**	**23,1641**

Appendix A.3: Relative permeability data

Water-oil Relative Permeabilities		
Sw	Krw	Krow
0,2	0	0,7
0,25	0,0006	0,525
0,3	0,0013	0,3955
0,35	0,0024	0,2905
0,4	0,0035	0,2135
0,45	0,006	0,1575
0,5	0,009	0,1155
0,55	0,014	0,0784
0,6	0,02	0,0476
0,65	0,03	0,0231
0,7	0,05	0,0001
1	1	0

Liquid-gas relative permeabilities		
Sl	Krg	Krog
0,2	0,85	0
0,25	0,731	0
0,3	0,6205	0,0105
0,35	0,527	0,0238
0,4	0,4446	0,0392
0,45	0,3723	0,0616
0,5	0,3128	0,0882
0,55	0,2618	0,119
0,6	0,2168	0,154
0,65	0,1675	0,1925
0,7	0,1301	0,238
0,75	0,0961	0,2926
0,8	0,0663	0,3514
0,85	0,0383	0,4172
0,9	0,0085	0,4984
0,95	0	0,5894
1	0	0,7

Appendix B: Additional figures

Appendix B.1: Grid refinement

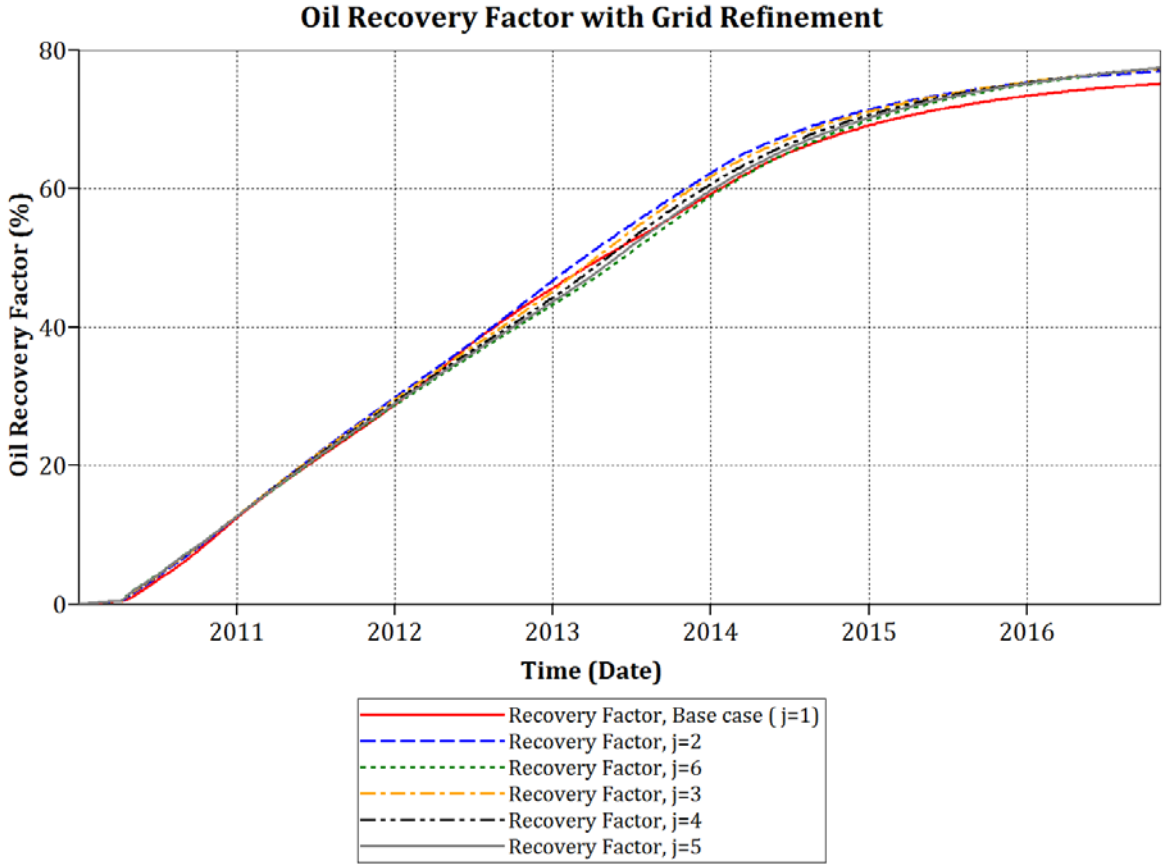

Figure 45: Oil recovery factor with grid refinement

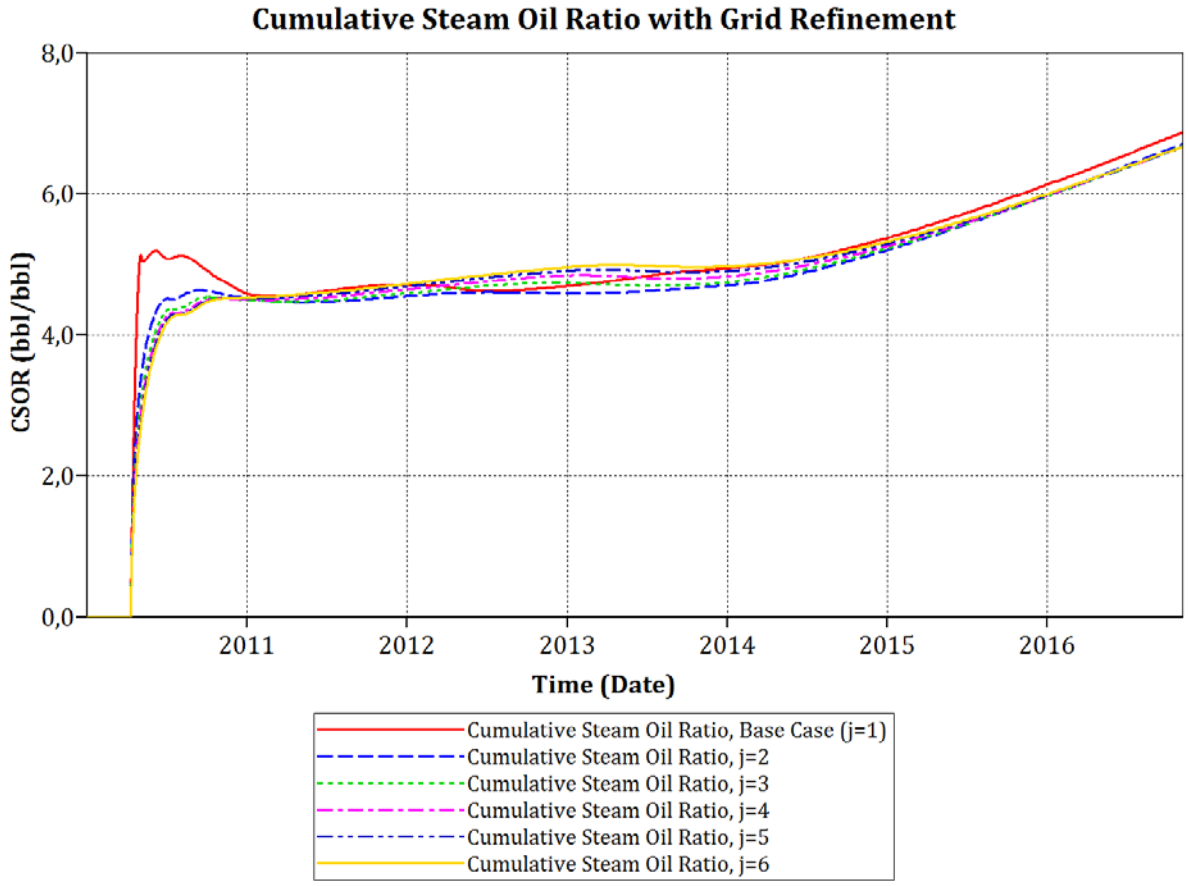

Figure 46: Cumulative steam oil ratio with grid refinement

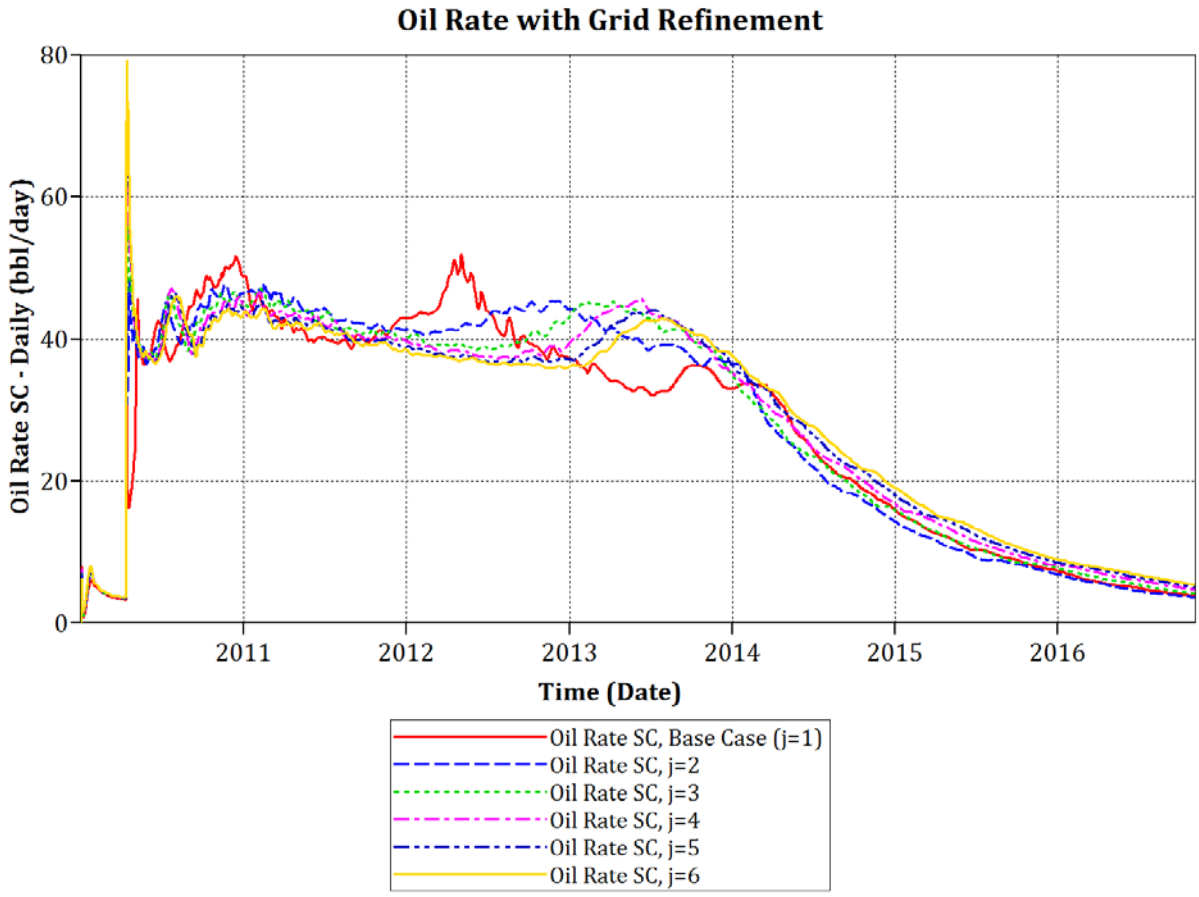

Figure 47: Oil rate with grid refinement

Appendix B.2: Variation in horizontal permeability

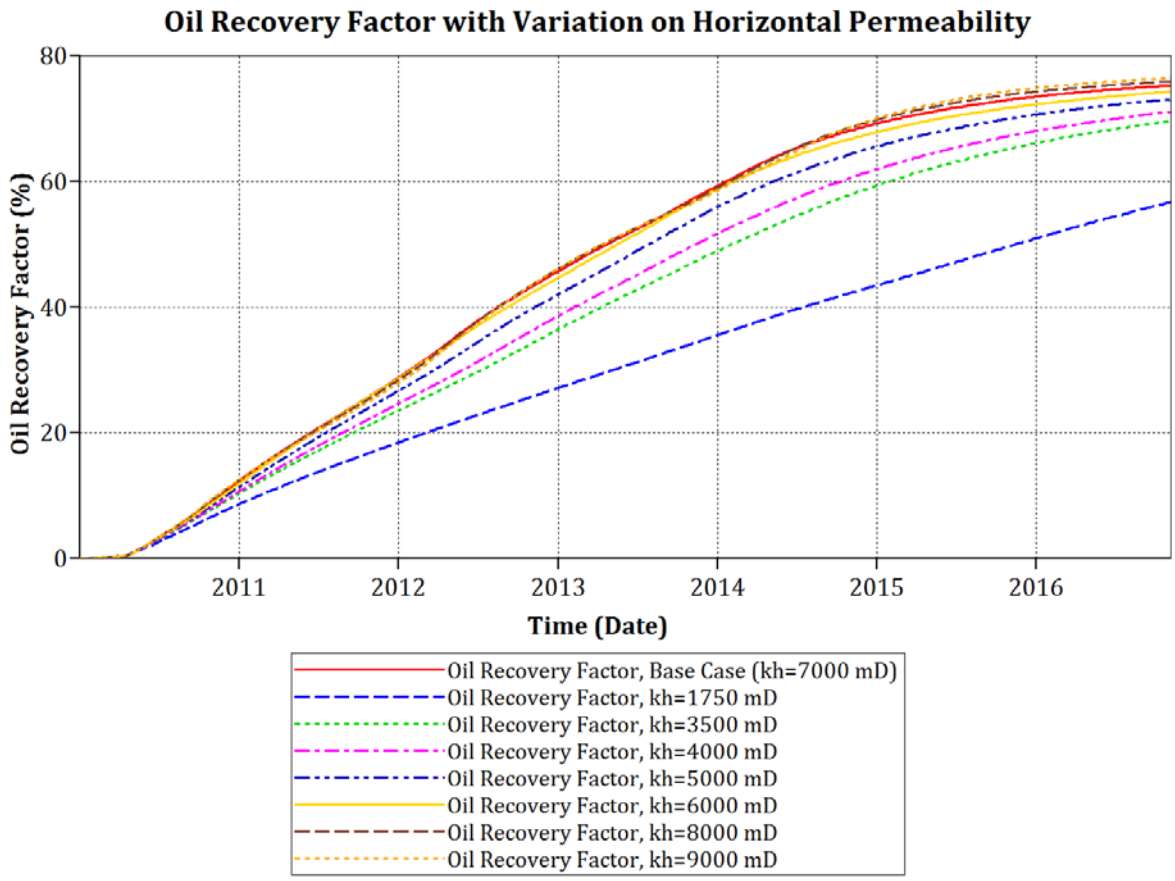

Figure 48: Oil recovery factor with variation in horizontal permeability

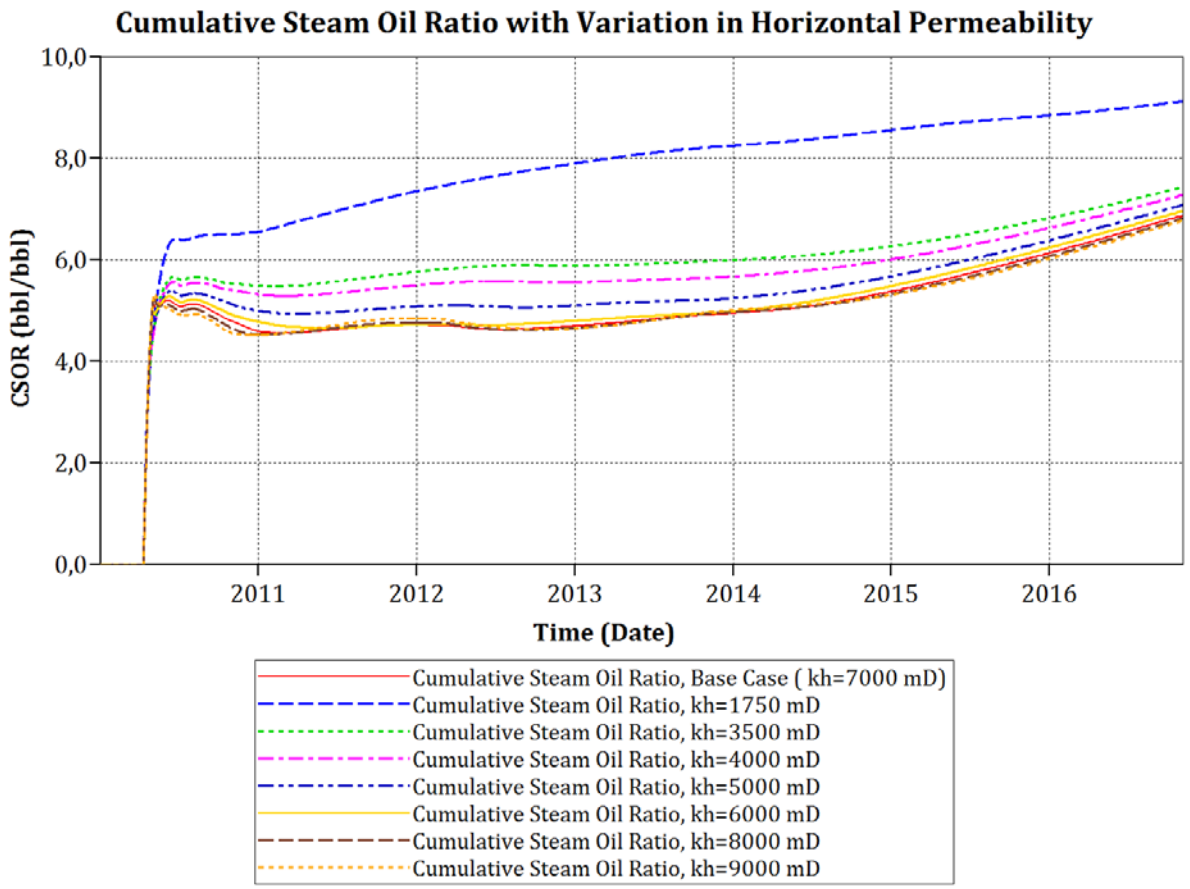

Figure 49: Cumulative Steam oil ratio with variation in horizontal permeability

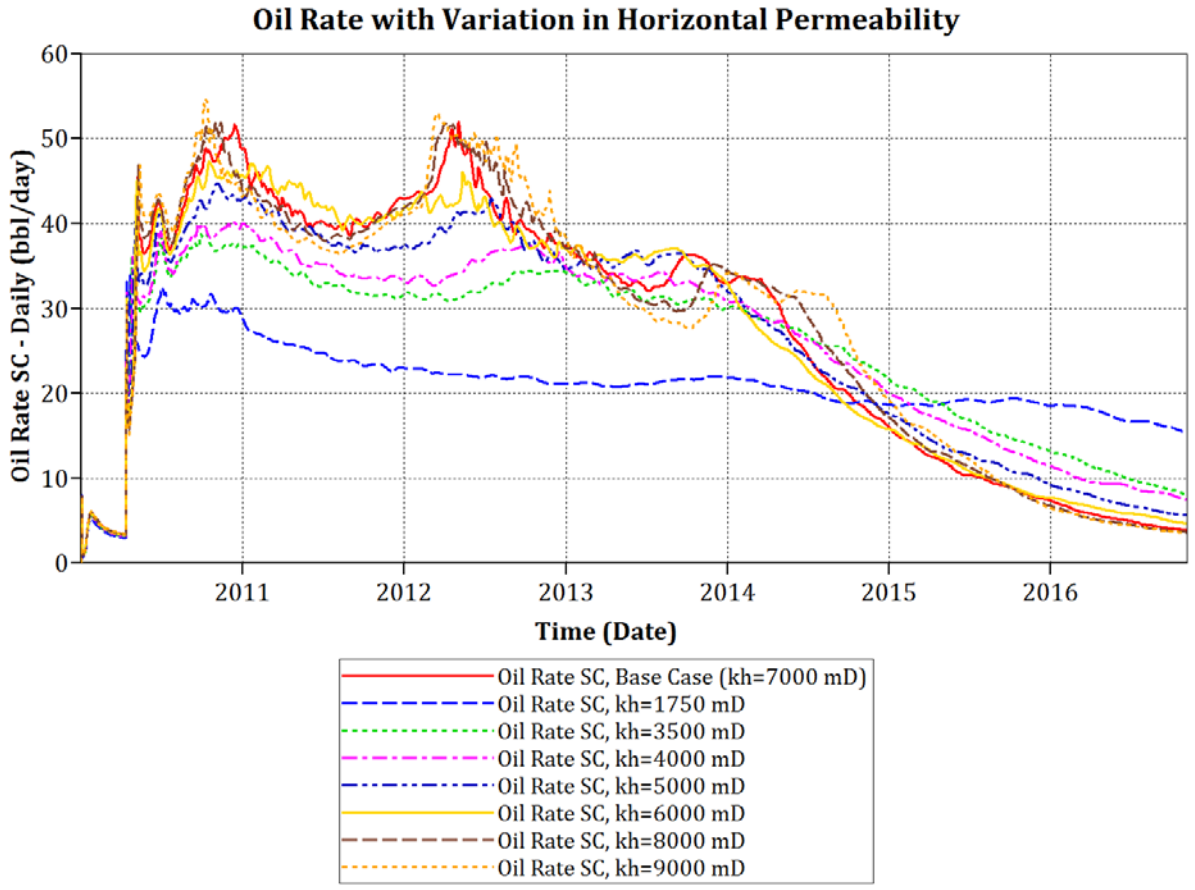

Figure 50: Oil rate with variation in horizontal permeability

Appendix B.3: Injection well placement

Table 17: Determination of injection well placement

Injection layer	Production layer	Layers between inj. and prod.	Distance (feet)	Distance in (meters)
1	15	14	42	12,72
2	15	13	39	11,81
3	15	12	36	10,90
4	15	11	33	9,99
5	15	10	30	9,08
6	15	9	27	8,18
7	15	8	24	7,27
8	15	7	21	6,36
9	15	6	18	5,45
10	15	5	15	4,54
11	15	4	12	3,63
12	15	3	9	2,73
13	15	2	6	1,82
14	15	1	3	0,91
15	15	0	0	0,00

The marked area is within the range suggested by Speight (2009)

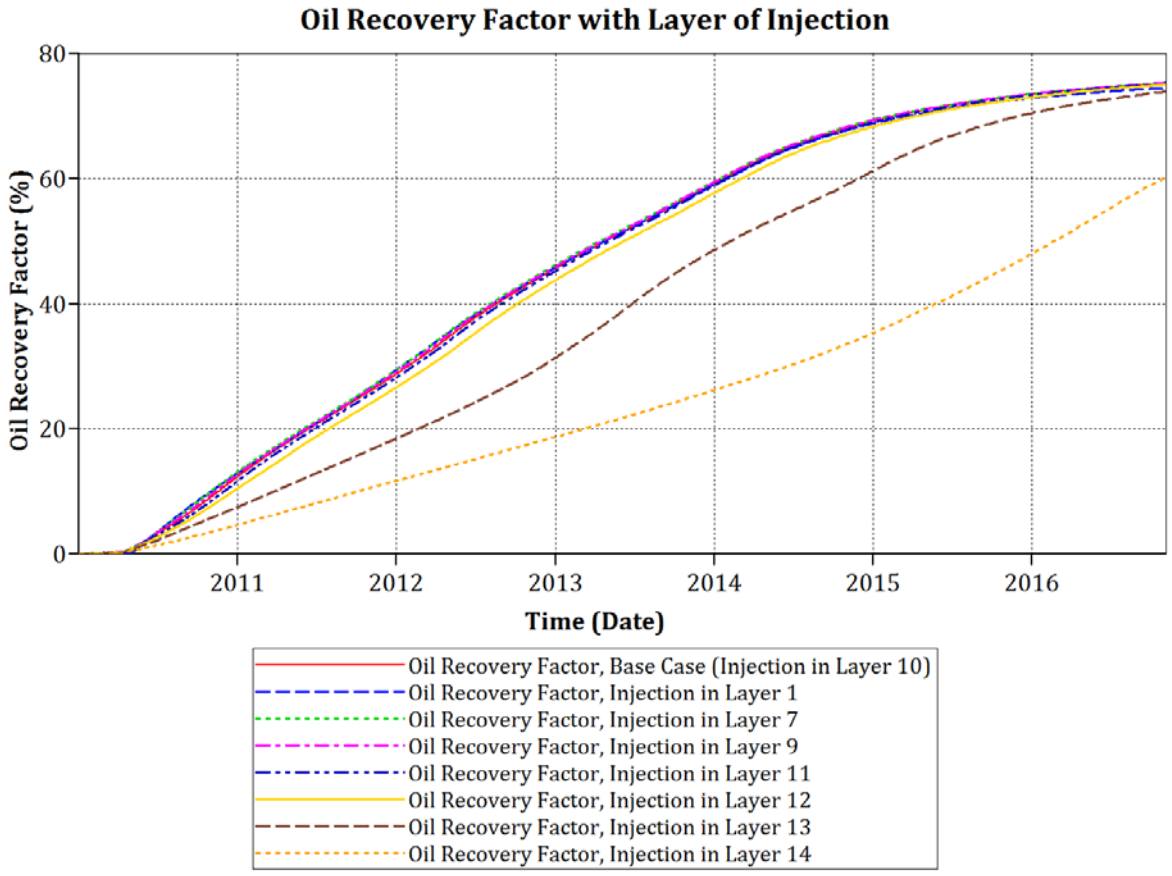

Figure 51: Oil recovery factor with layer of injection

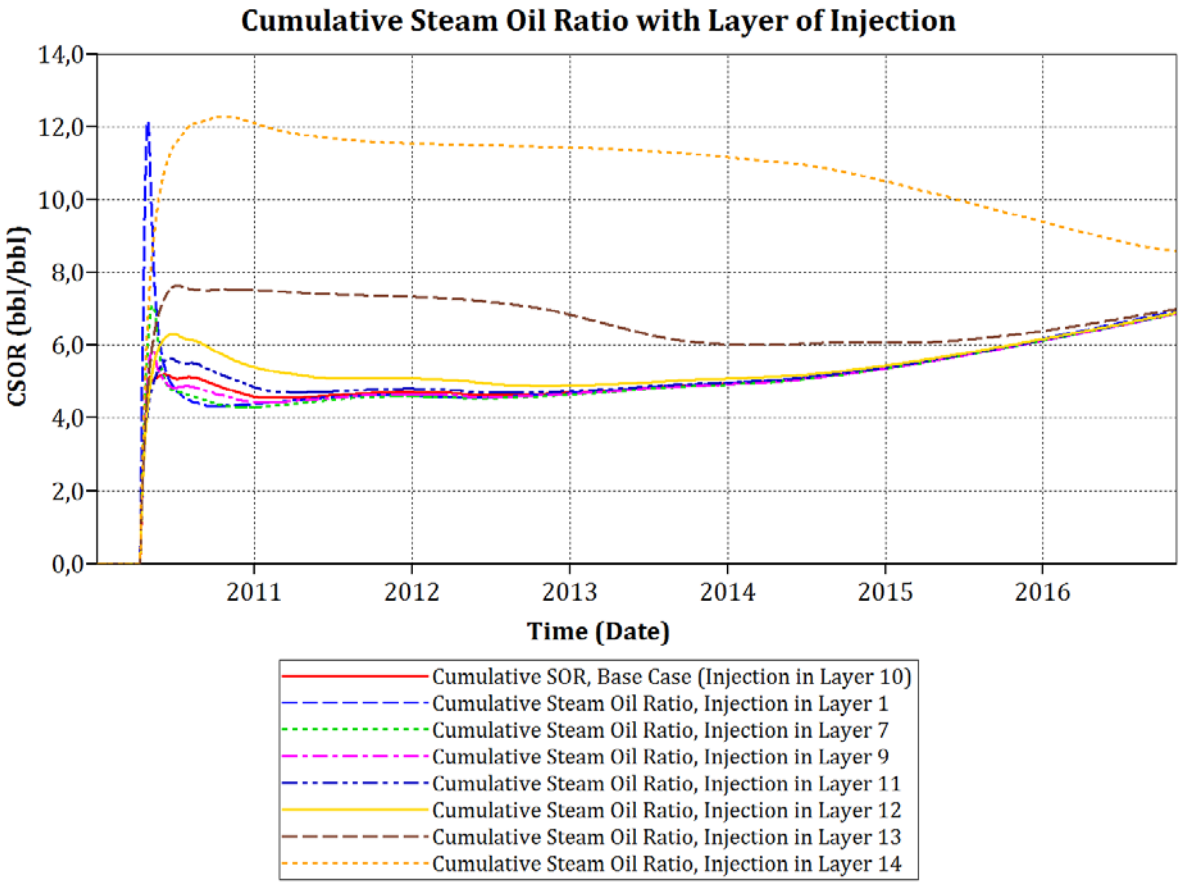

Figure 52: Cumulative steam oil ratio with layer of injection

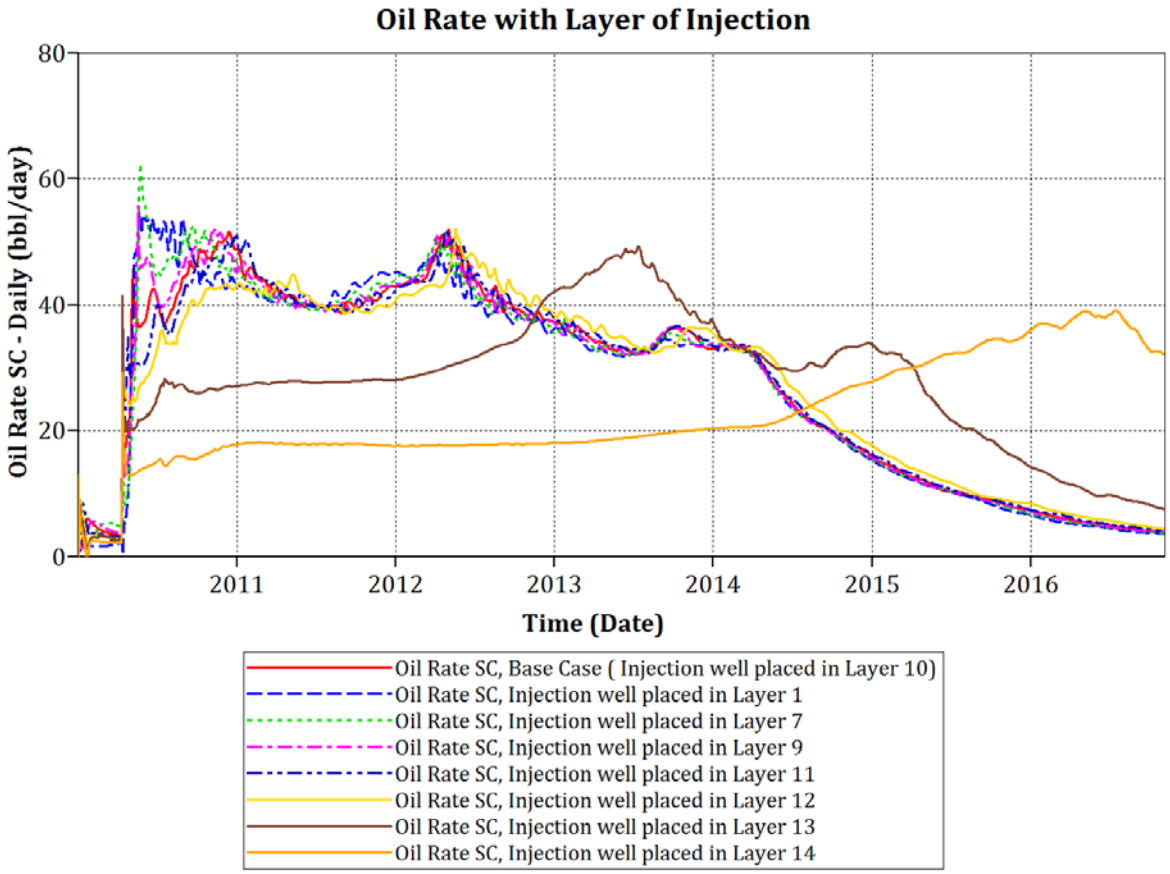

Figure 53: Oil rate with layer of injection

Appendix B.4: Porosity

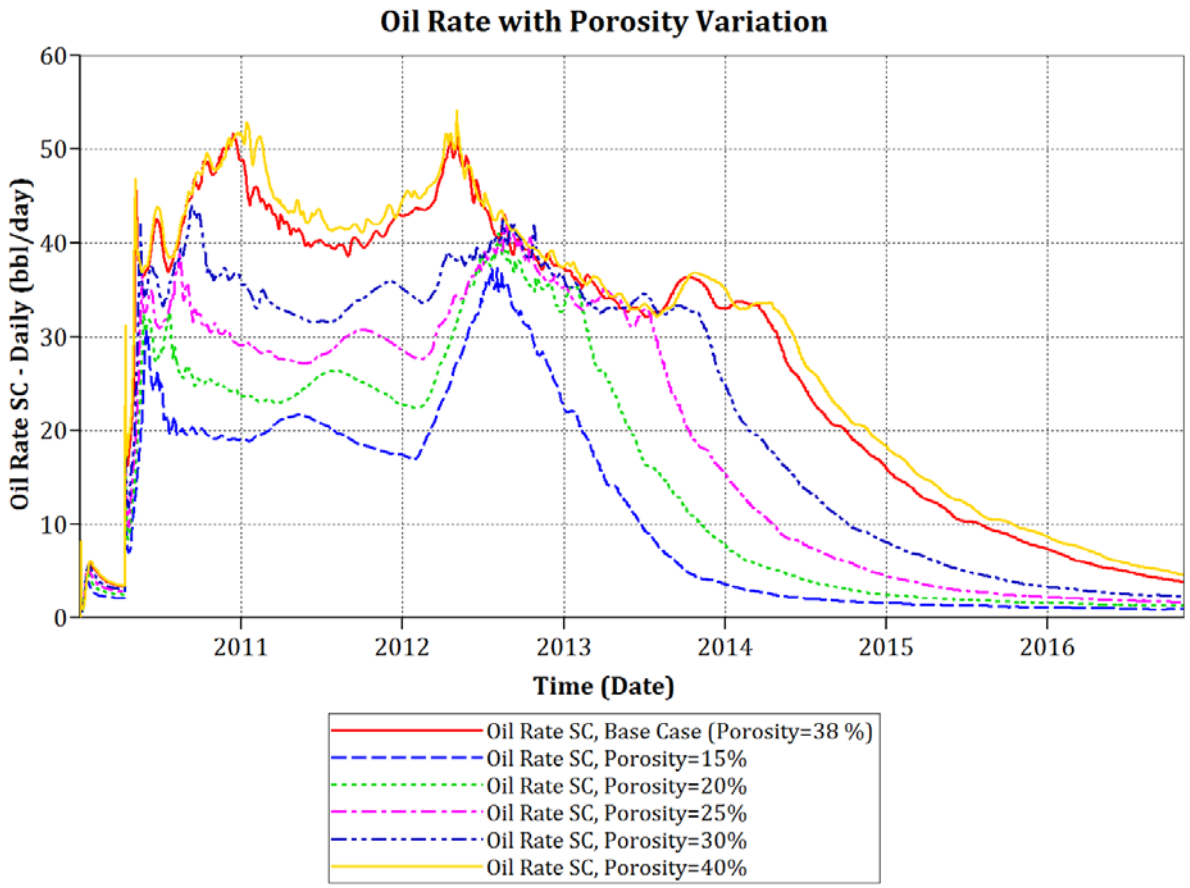

Figure 54: Oil rate with porosity variation

Appendix C: Base case data file

```
RANGECHECK OFF

**   ========== Description ==========================

** Simulation of SAGD Process

** 2D - Cartesian

** Horizontal Injector Well

** Horizontal Producer Well

**   ========== INPUT/OUTPUT CONTROL ==================

*interrupt *stop

*TITLE1 'Athabasca-Type Reservoir'

*TITLE2 'tan0.dat - SAGD Operation'

*TITLE3 'Homogeneous Reservoir Properties'

*INUNIT *FIELD

*OUTPRN *WELL *ALL

*OUTPRN GRID IFT KRG KRO KRW PCOG POREVOL PRES SG SO SW TEMP VISO

*OUTPRN *ITER *NEWTON

*WPRN *GRID 200

*WPRN *ITER 200

*PRNTORIEN 2 0

*WPRN *SECTOR 100

*WSRF *SECTOR 100

OUTSRF SPECIAL MATBAL  WELL 'DEAD OIL'

               MATBAL  WELL 'H2O'

OUTSRF GRID CCHLOSS FLUIDH MASDENO MASDENW MOLDENO PRES QUALBLK SG SO SW TEMP

            THCONDUCT VISO

**   ============ GRID AND RESERVOIR DEFINITION ====================
```

```
*GRID *CART 101 1 15

*KDIR *DOWN

*DI *IVAR 50*3.3 1*2.8 50*3.3   ** Foot

*DJ *CON 100              ** Foot

*DK *CON 3                ** Foot

*DEPTH 1 1 1 1000          **Reservoir Depth

**$ Property: NULL Blocks  Max: 1  Min: 1

**$  0 = null block, 1 = active block

NULL CON            1

*POR *CON 0.38

*PERMI *CON 7000          ** mDarcy

*PERMJ *CON 7000          ** mDarcy

*PERMK *CON 2100          ** mDarcy

**$ Property: Pinchout Array  Max: 1  Min: 1

**$  0 = pinched block, 1 = active block

PINCHOUTARRAY CON            1

*END-GRID

** ========= Reference Pressure for The Rock Compressibility ==============

*PRPOR 14.6

*ROCKTYPE 1

*CPOR 5E-4

*ROCKCP 35

*THCONR 106

*THCONW 8.6

*THCONO 1.8

*THCONG 1.2

** Heat Loss to Overburden and Underburden
```

```
*HLOSSPROP *OVERBUR 35.07 24.01 *UNDERBUR 35.07 24.01

*HLOSST 50              ** Initial Temperature of Overburden/Underburden (degree F)

*HLOSSTDIFF 10          ** Limit of T difference for Heat Loss calculations (degree
F)

*THTYPE *CON 1

** ============= FLUID DEFINITIONS ==================================

** 'DEAD OIL' is used here as a Bitumen

*MODEL 9 9 2 1

*COMPNAME      'H2O'   'DEAD OIL'   'C6H14'   'C5H12'    'C4H10'    'CH4'
'C2H6'    'C3H8'     'CO2'

**             ------  -----------   -------   --------   --------   ------   ------
-    -------   -------

*CMM            0         650        86.178    72.151     58.124    16.043    30.07
44.097    44.01

*PCRIT          0         147       430.617    489.357    551.143   667.174
708.364    612.93    1069.8

*TCRIT          0        1155       453.65     385.61     305.69    -116.59   90.05
205.97    87.89

*MASSDEN        0       63.7165

*CP             0       2.8E-6

*CT1            0       1E-4


*VISCTABLE

** ========      TEMP (DEGREE F)

**             -------------------------

                50.0      0   1000000

                69.08     0    316000

                85.82     0     92980

              104      0     25395
```

120.2	0	9958
140	0	3839
158	0	1800
176	0	903
194	0	502
212	0	251
230	0	166
248	0	101
266	0	70
284	0	50
302	0	36
320	0	27
338	0	21
356	0	16
374	0	13
392	0	11
410	0	9.45
428	0	7.9
446	0	6.75
464	0	5.64
482	0	5
500	0	4.63
518	0	4.17
536	0	3.75
554	0	3.45
570.	0	3.202
662	0	2.50

```
              752       0      2.00
              842       0      1.70
              932       0      1.30
              1112      0       1.0


*PRSR     14.7       ** Reference Pressure, corresponding to the density
*TEMR     60         ** Reference Temperature, corresponding to the density
*PSURF    14.7       ** Pressure at Surface
*TSURF    60         ** Temperature at Surface
** ================== ROCK-FLUID PROPERTIES ==================================
*ROCKFLUID
*RPT 1     ** STONE2 default
*SWT       ** Water-Oil Relative Permeabilities
**       Sw           Krw        Krow
**     ------      --------    --------
        0.2          0           0.70
        0.25         0.0006      0.525
        0.3          0.0013      0.3955
        0.35         0.0024      0.2905
        0.4          0.0035      0.2135
        0.45         0.006       0.1575
        0.5          0.009       0.1155
        0.55         0.014       0.0784
        0.6          0.02        0.0476
        0.65         0.03        0.0231
        0.7          0.05        0.0001
        1.0          1.0         0
```

```
*SLT        **NOSWC     **  Liquid-Gas Relative Permeabilities
**       Sl           Krg        Krog
**     ------      --------    --------
        0.2          0.85         0
        0.25         0.731        0
        0.3          0.6205       0.0105
        0.35         0.527        0.0238
        0.4          0.4446       0.0392
        0.45         0.3723       0.0616
        0.5          0.3128       0.0882
        0.55         0.2618       0.119
        0.6          0.2168       0.154
        0.65         0.1675       0.1925
        0.7          0.1301       0.238
        0.75         0.0961       0.2926
        0.8          0.0663       0.3514
        0.85         0.0383       0.4172
        0.9          0.0085       0.4984
        0.95         0.0          0.5894
        1.0          0.0          0.7
*SWR  0.20
*SORW 0.10
*KRTYPE  *CON 1    **Entire Grid
** ============== INITIAL CONDITIONS ==================================
*INITIAL
VERTICAL OFF
INITREGION 1
```

```
*PRES CON 300
*SW *CON 0.20
*SO *CON 0.80
*TEMP *CON 50             **Initial Reservoir Temperature 50 degree F
** ============== NUMERICAL CONTROL ==============================
*NUMERICAL
*DTMAX 5
*NEWTONCYC 8
*NORM    *PRESS 16   *SATUR 0.2   *TEMP 10  *Y 0.2  *X 0.2
*MINPRES 1.0
*CONVERGE PRESS 1
*MATBALTOL 0.00001
*PIVOT *ON
*RUN
** ============ RECURRENT DATA ================================
*DATE 2010 01 01
*DTWELL 1E-5
*WELL 'Injector'
INJECTOR MOBWEIGHT IMPLICIT 'Injector'
INCOMP  WATER  1.  0.
TINJW  420.
QUAL  0.9
OPERATE  MAX  STW  200.  CONT REPEAT
PERF  WI  'Injector'
**$ UBA      wi     Status  Connection
    51 1 10  3256.  OPEN    FLOW-FROM  'SURFACE'
**OPERATE  MAX  BHP  330.  CONT REPEAT
```

```
**$          rad  geofac  wfrac  skin
WELL  'Producer'
PRODUCER 'Producer'
OPERATE  MIN  BHP  250.  CONT
OPERATE  MAX  STL  250.  CONT
**$          rad  geofac  wfrac  skin
PERF  WI  'Producer'
**$ UBA      wi     Status  Connection
    51 1 15  3256.  OPEN    FLOW-TO  'SURFACE'


*SHUTIN 'Injector'
*UHTR *IJK 51 1:1 10 347320
*TMPSET *IJK 51 1:1 10 500
*UHTR *IJK 51 1:1 15 347320
*TMPSET *IJK 51 1:1 15 500
*TIME 1
*TIME 5
*TIME 10
*TIME 15
*TIME 30
*TIME 100
*UHTR *IJK 51 1:1 10 0  ** SHUTOFF Heating in injector
*UHTR *IJK 51 1:1 15 0  ** SHUTOFF Heating in producer
*OPEN 'Injector'
*TIME 105
*TIME 110
*TIME 120
```

```
*TIME 150

*TIME 200

*TIME 400

*TIME 500

*TIME 1000

*TIME 2000

*TIME 2500

**TIME 4000

*STOP
```